Journal of the American Heart Association

ORIGINAL RESEARCH

S-Nitrosoglutathione Reductase Deficiency Causes Aberrant Placental S-Nitrosylation and Preeclampsia

Shathiyah Kulandavelu, PhD; Raul A. Dulce, PhD; Christopher I. Murray, PhD; Michael A. Bellio, PhD; Julia Fritsch, PhD; Rosemeire Kanashiro-Takeuchi, DVM, PhD; Himanshu Arora, PhD; Ellena Paulino, PhD; Daniel Soetkamp, PhD; Wayne Balkan, PhD; Jenny E. Van Eyk, PhD; Joshua M. Hare, MD

BACKGROUND: Preeclampsia, a leading cause of maternal and fetal mortality and morbidity, is characterized by an increase in S-nitrosylated proteins and reactive oxygen species, suggesting a pathophysiologic role for dysregulation in nitrosylation and nitrosative stress.

METHODS AND RESULTS: Here, we show that mice lacking S-nitrosoglutathione reductase (*GSNOR*$^{-/-}$), a denitrosylase regulating protein S-nitrosylation, exhibit a preeclampsia phenotype, including hypertension, proteinuria, renal pathology, cardiac concentric hypertrophy, decreased placental vascularization, and fetal growth retardation. Reactive oxygen species, NO, and peroxynitrite levels are elevated. Importantly, mass spectrometry reveals elevated placental S-nitrosylated amino acid residues in *GSNOR*$^{-/-}$ mice. Ascorbate reverses the phenotype except for fetal weight, reduces the difference in the S-nitrosoproteome, and identifies a unique set of S-nitrosylated proteins in *GSNOR*$^{-/-}$ mice. Importantly, human preeclamptic placentas exhibit decreased GSNOR activity and increased nitrosative stress.

CONCLUSIONS: Therefore, deficiency of GSNOR creates dysregulation of placental S-nitrosylation and preeclampsia in mice, which can be rescued by ascorbate. Coupled with similar findings in human placentas, these findings offer valuable insights and therapeutic implications for preeclampsia.

Key Words: mouse model ■ NO ■ preeclampsia ■ pregnancy ■ S-nitrosylation

Preeclampsia is a life-threatening disorder of pregnancy, characterized by new-onset hypertension, proteinuria, abnormal maternal cardiovascular and renal adaptations, poor placental vascularization, and fetal growth restriction. Preeclampsia affects up to 10% of pregnancies and is a leading cause of maternal and fetal/neonatal mortality and morbidity worldwide,[1,2] and maternal mortality rates have been steadily rising over the past 30 years in large part attributable to cardiovascular complications.[3,4] The pathogenesis of preeclampsia is incompletely understood, but emerging data support a role for impaired protein S-nitrosylation, nitration, and increased reactive oxidative stress (ROS), contributing to alterations in NO bioavailability and nitroso-redox imbalance.[5–10] A paradoxical finding in preeclampsia is the elevation in circulating S-nitrosylated albumin in human pregnancy[6,7] because elevated S-nitrosylated albumin would traditionally be considered a vasorelaxant and an antioxidant.[11] Furthermore, cellular S-nitrosylation level is elevated despite factors that are assumed to abrogate the formation of nitroso-thiols, including oxidative stress and defects in NO bioavailability.[7,12] These findings raise 2 alternative pathogenic possibilities: Either

Correspondence to: Joshua M. Hare, MD, Interdisciplinary Stem Cell Institute, Biomedical Research Building, Room 909, 1501 NW 10th Avenue, Miami, FL 33136. E-mail: jhare@med.miami.edu

Preprint posted on BioRxiv June 21, 2021. doi: https://doi.org/10.1101/2020.07.01.183012.

Supplemental Material for this article is available at https://www.ahajournals.org/doi/suppl/10.1161/JAHA.121.024008

For Sources of Funding and Disclosures, see page 17.

JAHA is available at: www.ahajournals.org/journal/jaha

CLINICAL PERSPECTIVE

What Is New?

- Preeclampsia is a major unmet need in maternal fetal medicine engendering substantial mortality and morbidity in both mothers and infants.
- While nitroso-redox imbalance is an implicated pathogenetic process, the full extent to which it plays a role in preeclampsia has remained controversial; in this study, we demonstrated that mice lacking the gene for S-nitrosoglutathione reductase, a denitrosylase that regulates protein S-nitrosylation, recapitulate the majority of preeclampsia maternal and fetal phenotypes.
- Antioxidant treatment rescued preeclampsia phenotypes by reducing dysregulation of nitrosylation and nitrosative stress; importantly, placentas from women with preeclampsia exhibited S-nitrosoglutathione reductase deficiency, suggesting that this enzyme plays a potentially key role in normal human pregnancy.

What Are the Clinical Implications?

- Our findings support the idea that S-nitrosoglutathione reductase is a central regulator of physiologic nitrosylation and is crucial to governing normal pregnancy.
- These findings have important implications for understanding the pathogenesis of preeclampsia, developing novel preeclampsia therapies, and identifying clinically useful biomarkers for this unaddressed need in maternal-fetal medicine.
- Moreover, the S-nitrosoglutathione reductase homozygous knockout mouse represents a valuable animal model for ongoing study of the numerous processes operative in preeclampsia.

Nonstandard Abbreviations and Acronyms

eNOS	endothelial nitric oxide synthase
GSNOR	S-nitrosogluathione reductase
HPDP	N-[6-(biotinamido)hexyl]-3′-(2′-pyridyldithio) propionamide
ROS	reactive oxidative stress
SOD	superoxide dismutase

S-nitrosylation increases to compensate for the increased ROS levels or elevated S-nitrosylation directly reflects abnormal regulation of S-nitrosylation in preeclampsia (nitrosative stress). To differentiate between these 2 possible roles, we studied the impact of the loss of an important denitrosylase, S-nitrosogluathione reductase (*GSNOR*$^{-/-}$), in pregnant mice.

Protein S-nitrosylation participates in numerous pregnancy-related processes including placental trophoblast cell migration, apoptosis, angiogenesis, immunomodulation, and oxygen delivery.[13,14] Protein S-nitrosylation is enhanced in a transnitrosylation reaction using S-nitrosogluathione, which thus acts as a second messenger to transduce NO bioactivity.[15] This process is tightly regulated by GSNOR, which selectively metabolizes S-nitrosogluathione, thereby depleting the levels of S-nitrosylated proteins in equilibrium with S-nitrosogluathione. Ascorbate, with its dual roles as an antioxidant and a reductant, is required for the release of biologically active NO from these nitrosylated thiols. Although *GSNOR*$^{-/-}$ mice have increased numbers of S-nitrosylated proteins,[16,17] which can in some circumstances lead to favorable outcomes (eg, recovery from myocardial infarction),[18] deficiency of this enzyme can also disrupt physiological nitrosylation-denitrosylation dynamic cycles, leading to unfavorable outcomes (eg, increase in oxidative stress).[17,19–21] Thus, to assess the role of S-nitrosylation and GSNOR in pregnancy outcome, we examined multiple organ systems, including the heart, kidney, and placenta, and the offspring during pregnancy in *GSNOR*$^{-/-}$ mice. Initially, we anticipated that *GSNOR*$^{-/-}$ mice would exhibit favorable maternal and fetal adaptations to pregnancy and were surprised to discover that pregnant *GSNOR*$^{-/-}$ mice recapitulate many of the features of preeclampsia. As a result, we subsequently tested the predictions that placental nitrosylation would exhibit widespread derangement in the knockout compared with control mice and that ascorbate would restore the intact animal and nitroso-proteome phenotypes toward normal.

METHODS

All data are available in the main text or the supplemental materials.

Study Approval

All animal care was carried out in accordance with approval by the Institutional Animal Care and Use Committee. For the human study, tissue collection was approved by the University of Miami Institutional Review Board, and the patient and family privacy were assured under the conditions of the Health Insurance Portability and Accountability Act. Written informed consent was received from participants before inclusion in the study.

Breeding

C57Bl/6J (wild type [B6]) controls (stock No. 000664) were purchased from Jackson Laboratories (Bar Harbor, ME). GSNOR$^{-/-}$ mice were raised in house. GSNOR$^{-/-}$ mouse line was created from ES clones after 10 consecutive backcrosses with C57Bl/6J.[16]

Females were bred at 3 to 4 months of age and were studied in their first pregnancies. The presence of a sperm plug was defined as day 0.5 of gestation. Experimental time points included before breeding (nonpregnant), and day 17.5 (late gestation, 2 days before normal-term delivery). Fetal, placental, and maternal organ weights were also recorded at time of euthanasia. For breeding, B6 females were bred with B6 males and GSNOR$^{-/-}$ females were bred with GSNOR$^{-/-}$ males.

Blood Pressure Determination

Mice were anesthetized with isoflurane. A 1.4-F micromanometer-tipped catheter (SPR-839; Millar Instruments, Houston, TX) was inserted into the right carotid artery and advanced retrograde into the aorta. All analyses were performed using LabChart Pro 7 software (Millar Instruments).

Urinary Protein Measurements

Urine samples were collected from nonpregnant and pregnant mice (17.5 days of gestation). Urinary protein levels were measured using dipstick. A score of 0 to 3 was given on the basis of the color change on the dipstick following urine analysis. Twenty-four-hour urine was collected using metabolic cages (Tecniplast). Urine samples were analyzed for macroglobulin levels using Coomassie blue staining (Fisher).

Echocardiography

Echocardiographic assessments were performed in anesthetized mice (1% isoflurane in oxygen) using a Vevo-770 micro-ultrasound (VisualSonics, Toronto, Ontario, Canada) equipped with a 30-MHz transducer. Cardiac dimensions including left ventricular end-diastolic diameter, left ventricular end-systolic diameter, and anterior and posterior wall thickness at systole and diastole were recorded from M-mode images; cardiac output and stroke volume were calculated from bidimensional long-axis parasternal views from 3 consecutive cardiac cycles. Doppler waveforms in the umbilical vein and artery were obtained near the placental end of the umbilical cord. Area under the peak velocity–time curve and R-R interval were measured from 3 consecutive cardiac cycles, and the results were averaged. Umbilical venous and arterial diameters were measured from B-mode images. Mean velocity over the cardiac cycle was calculated by dividing the area under the peak velocity–time curve by the R-R interval. A parabolic blood velocity distribution was assumed so that umbilical venous and arterial blood flows were determined by the formula: F=½ ⊓ MV (D/2)2 (where MV=mean peak velocity (cm/s); D=diameter [cm]; F=blood flow [mL/min]).

Cardiomyocyte Isolation

The isolation of cardiomyocytes was performed as previously described.[22] Briefly, hearts were perfused with Ca^{2+}-free bicarbonate buffer containing 120 mmol/L NaCl, 5.4 mmol/L KCl, 1.2 mmol/L $MgSO_4$, 1.2 mmol/L NaH_2PO_4, 5.6 mmol/L glucose, 20 mmol/L $NaHCO_3$, 20 mmol/L 2,3 butanedione monoxime (Sigma-Aldrich, St. Louis, MO), and 5 mmol/L taurine (Sigma-Aldrich), gassed with 95%O_2/5% CO_2, followed by enzymatic digestion with collagenase type II (1 mg/mL) (Worthington, Lakewood, NJ) and protease type XIV (0.1 mg/mL; Sigma-Aldrich). Cardiomyocytes were obtained from digested hearts followed by mechanical disruption, filtration, centrifugation, and resuspension in a Tyrode solution containing 0.125 mmol/L $CaCl_2$ Tyrode buffer containing 144 mmol/L NaCl, 1 mmol/L $MgCl_2$, 10 mmol/L HEPES, 1.2 mmol/L NaH_2PO_4, 5.6 mmol/L glucose, and 5 mmol/L KCl, adjusted to pH 7.4 with NaOH.

ROS by DCF, NO by DAF, Peroxynitrite by DHR 123

ROS, intracellular NO, and peroxynitrite were measured by epifluorescence using 2′,7′-dichlorodihydrofluoresceine (10 μmol/L; Molecular Probes), 4,5-diaminofluorescein (10 mmol/L; Cayman Chemical Co., Ann Arbor, MI) and dihydrorhodamine 123 (DHR 123, 25 mmol/L; Sigma-Aldrich), respectively. These dyes have been well validated.[23,24] Briefly, fresh isolated mouse cardiomyocytes were placed in the chamber of an IonOptix spectrofluorometer and the background fluorescence (F_0) was acquired with an excitation wavelength of 488 nm and emission fluorescence collected at 510±15 nm. Cardiomyocytes were incubated for 40 minutes at room temperature (23 °C) with 2′,7′-dichlorodihydrofluoresceine or 4,5-diaminofluorescein or 20 minutes with DHR 123 and washed by superfusing fresh Tyrode (1.8 mmol/L $CaCl_2$) solution for 10 minutes. Fluorescence (F) was acquired at 37 °C every 1 minute for 10 minutes. Myocytes were stimulated at 1 Hz during the 10-minute experiment. ROS, NO or peroxynitrite levels were expressed as:

$$\Delta F/F_0 = (F - F_0)/F_0$$

Superoxide Dismutase Measurement

Sample preparation: frozen placentas were ground up in a Dounce homogenizer on liquid nitrogen. Then, pulverized tissue was homogenized in ice-cold PBS (10 μL per mg of tissue). The suspension was strained through a 250 μm-pore mesh. Then, samples were assessed for protein content by BCA (Pierce, Thermo Scientific) and diluted 1:10 in PBS for superoxide measurement. Superoxide was assessed by lucigenin-enhanced chemiluminescence.

For superoxide dismutase (SOD) assay, superoxide was assessed with the Superoxide Anion Assay Kit CS1000 (Sigma-Aldrich). Briefly, a superoxide-generator system (xanthine–xanthine oxidase [XO]) was used as a source of superoxide. Xanthine–xanthine oxidase (25 mU/mL final activity) plus 5 µL of [SOD-containing] samples and 94.5 µL of PBS were added to the multiwell plate (in duplicate). Then, the luminol plus the enhancer salutation and xanthine were added. For positive control, a mix of 1 µL of 4 U/µL SOD (Sigma-Aldrich) with 99 µL of PBS was used. As negative control for SOD, the superoxide generation system alone (without the sample) was used.

Luminescence was acquired for 10 minutes every 30 seconds and the integrated luminescence units were used for calculations.

Ascorbate Treatment

Ascorbate (sodium L-ascorbate, 3.3 g/L, Sigma, St. Louis, MO)[25] was given in the drinking water starting from day 0.5 (time of plug detection). The water was changed every 2 days. In isolated cardiomyocytes, ascorbate (0.1 mmol/L, 0.5 mmol/L, or 1 mmol/L) was incubated for 30 minutes before the start of the epifluorescence experiments.

Tissue Preparation and Histology and Immunohistochemistry

At the end of the study, maternal organs (heart, kidney) and placenta were harvested, weighed, and processed for further analysis. Tissues were either flash-frozen in liquid nitrogen for total RNA isolation and protein analysis, while some tissues were fixed with 10% formalin for histology. Slides were stained with hematoxylin and eosin and Masson's trichrome staining for heart and kidney and periodic acid–Schiff staining for kidney. Glomerular size was quantified using Image J (National Institutes of Health).

Scanning Electron Microscopy of the Kidney

Tissue was fixed in 2% glutaraldehyde in 0.05 M phosphate buffer and 100mM sucrose, post-fixed overnight in 1% osmium tetroxide in 0.1 M phosphate buffer, dehydrated through a series of cold graded ethanols, and embedded in a mixture of EM-bed/Araldite (Electron Microscopy Sciences). 1 µm thick sections were stained with Richardson's stain for observation under a light microscope. 100 nmol/L sections were cut on a Leica Ultracut-R ultramicrotome and stained with uranyl acetate and lead citrate. The grids were viewed at 80 kV in a Philips cardiomyocyte-10 transmission electron microscope and images captured by a Gatan ES1000W digital camera. N=2 samples were examined per each group at 17.5 d of gestation.

Isolectin Immunofluorescence for Paraffin-Embedded Tissues and Analysis of Placental Capillary Density

Paraffin-embedded placental sections were deparaffinized and rehydrated by immersion in xylene followed by a graded series of ethanol. Antigen retrieval was performed by a heat-induced method with citrate buffer (Dako, Carpinteria, CA). The slides were then blocked for 1 hour in 10% normal donkey serum to reduce background. Sections were then incubated with DyLight 594-GSL I-isolectin B4 (Vector Laboratories, Burlingame, CA) primary antibody for 1 hour. at 37 °C. After washing with PBS, nuclei were counterstained with DAPI (Invitrogen, Carlsbad, CA). A stereological grid consisting of crosses was superimposed on images of placental sections stained with isolectin. The relative capillary density in the tissue was calculated on each section by dividing the number of crosses falling on capillary structure by the total number of points falling on the sampling area using Image J. For each placenta, 4 sections were analyzed.

Human Placental Tissue Collection

Placentas were collected immediately after delivery from normotensive (N=8) and preeclamptic (N=6) pregnancies at Jackson Memorial Hospital and Jackson North (Miami, FL). Tissue collection was approved by the University of Miami Institutional Review Board, and patient and family privacy were assured under conditions of the Health Insurance Portability and Accountability Act. Written informed consent was received from participants before inclusion in the study. Placental tissue was isolated by sterile dissection. The tissue was washed with cold PBS to remove blood from the intervillous spaces and then snap frozen in liquid nitrogen for storage at −80 °C. The demographic data are summarized in Table 2. Preeclampsia was defined as maternal systolic blood pressure at least 140 mm Hg or higher or diastolic blood pressure at least 90 mm Hg or higher and 1 additional factor such as proteinuria, impaired liver function, or thrombocytopenia was also observed.

GSNOR Activity in the Mouse Heart and Mouse and Human Placenta

Heart and placental homogenate (100 µg/mL) were incubated with Tris-HCl (2 mmol/L, pH 8.0), EDTA (0.5 mmol/L) and NADH (200 µmol/L). The reaction was started by adding S-nitrosogluathione (400 µmol/L) and activity was measured as S-nitrosogluathione–dependent NADH consumption at absorbance of

340 nm for 5 minutes in the mouse tissue and area under the curve for 8 minutes in the human placenta.

Protein Immunoanalysis

Samples were electrophoresed using a NuPAGE 10% Bis-Tris gel (Invitrogen) and transferred to polyvinylidene membranes (Bio-Rad Laboratories). Immunoblot detection was performed for vascular endothelial growth factor (VEGF) (ab46154, 1:1000; Abcam, Cambridge, MA), VEGFR2 (55B11, 1:1000; Cell Signaling, Danvers, MA), eNOS (1:1000; BD Bioscience, BD Bioscience, San Jose, CA) in mouse tissue, GSNOR in (1:1000, 11051-1-AP, Proteintech, Rosemont, IL) in human tissues, B-actin (4957S, 1:1000, Cell Signaling, Danvers, MA), GAPDH (G8795, 1:1000, Sigma, St Louis, MO) and subsequent reaction with a goat anti-rabbit horseradish peroxidase–conjugated antibody (1:1000; Cell Signaling). Then, membranes were developed by enhanced chemiluminescence (Super Signal West Pico, Thermo Scientific, Hampton, NH) and analyzed by the QuantityOne software (Bio-Rad, Hercules, CA).

VEGF Nitrosylation

To assess S-nitrosylation, biotin-switch assay was used following methods described. Hearts were homogenized in HEN buffer (250 mmol/L Hepes (pH 7.7), 1 mmol/L EDTA, and 0.1 mmol/L neocuproine). Free cysteine (Cys) residues were blocked with S-methyl methanethiosulfonate and labeled with N-[6-(biotinamido)hexyl]-3′-(2′-pyridyldithio) propionamide (HPDP-biotin) with or without sodium ascorbate. Biotinylated VEGF was individually immunoprecipitated with protein G-Sepharose beads, electrophoretically resolved, and immunoblotted with anti-biotin antibody. Blotted membranes were re-probed with related antibody for detection of protein load.

RNA Preparation and Quantitative Real-Time Polymerase Chain Reaction

Total RNA was extracted from tissues using the TRIzol method, and then reverse transcribed to complementary DNA using High-Capacity cDNA Reverse Transcription Kits (Applied Biosystems, Foster City, CA) according to the manufacturer's protocol. The quantitative reverse transcriptase polymerase chain reaction for indicated genes was performed in TaqMan Universal PCR Master Mix (Applied Biosystems). Quantitation of mRNAs was performed using Applied Biosystems TaqMan Gene Expression Assays according to the manufacturer's protocol. Samples were analyzed using the BIORAD sequence detection system. All polymerase chain reactions were performed in triplicate, and the specificity of the reaction was determined by melting curve analysis at the dissociation stage. The relative quantitative method was used for the quantitative analysis. The calibrator was the averaged ΔCt from the untreated cells. The endogenous control was GAPDH.

Mass Spectrometry Sample Preparation

All blocking and labeling steps were performed protected from light. Frozen placentas were individual minced in 0.9 mL of cold homogenization buffer (PEN: PBS pH 8.0, 1mM ETDA, 0.1 mmol/L Neocupine; supplemented with 20 mmol/L n-ethylmaleimide). The tissue was then disrupted in 1ml mixer mill (Mixer Mill MM 400, retsch.com) for 5 minutes and then subjected to probe sonication. Samples were adjusted to 2.5% SDS and clarified by centrifugation for 5 minutes at 2000*g*. The resulting supernatant was incubated for 10 minutes at 50 °C to completing the blocking step. The unreacted n-ethylmaleimide was removed using a Zeba spin column (Thermo Fisher Scientific, Waltham, MA) equilibrated with PEN buffer supplemented with 0.5% SDS. Each sample was divided and labeled with either 1 mmol/L biotin-HPDP (Thermo Fisher Scientific) or 0.3 mmol/L iodoTMT^6 (Thermo Fisher Scientific) in the presence of 5 mmol/L sodium ascorbate. As a labeling control, five pooled samples consisting of one replicate from each of the biological samples were prepared and reacted with each label in the absence of ascorbate. Samples were incubated for 1 hour. (HPDP) or 2 hour. (iodoTMT^6) at 37 °C. Excess label was removed from the HPDP-treated samples by adding 2 volumes of cold acetone and incubating for 20 minutes at –20 °C. Precipitated protein was pelleted by centrifugation and washed with 2 additional volumes of cold acetone. The pellets were resuspended 200 µL of PBS containing 1% (w/v) SDS aided by sonication. The excess iodoTMT^6 label was removed by adding 5 volumes of cold acetone and precipitating as above. Samples were resuspended in 600 µL of PBS containing 1% (w/v) SDS aided by sonication. IodoTMT^6 samples were then further reduced and alkylated using DTT and iodacetamide. Residual reagents were removed by Zeba spin column equilibrated with PBS. The protein concentration of each labeled sample was determined by BCA assay.

For HPDP-labeled samples, 500 µg was digested overnight using 0.02 µg trypsin/µg of protein (Promega). iodoTMT^6 labeled samples were combined according to the label's isotope. Five-plexes were prepared containing 350 µg of each of the different biological samples and the pooled control. An additional set of 6-plexes was prepared containing 250 µg of each biological replicates and a pooled control. The mixtures were digested overnight with 0.02 µg trypsin/µg of protein. Digestions were halted with 0.25 mmol/L PMSF. The resulting peptides were captured using either

streptavidin (HPDP) or TMT affinity resin (iodoTMT^6). Peptides were enriched, washed, and eluted according to the manufacture's protocol or as described here (PMID: 21036925). In the case of HPDP, eluted peptides were further alkylated with iodoacetamide.

Mass Spectrometry Analysis

The resulting peptides were desalted using Oasis HLB µ-elution plates (Waters, Milford, MA). Samples were eluted with 300 µL of 50% ACN, 0.1% FA dried in speedvac, then resuspended in 0.1% FA for liquid chromatography–tandem mass spectrometry analysis. Liquid chromatography–tandem mass spectrometry analysis was performed using an Ultimate 3000 nano LC (Thermo Scientific) connected to an Orbitrap LUMOS mass spectrometer (Thermo Scientific) equipped with an EasySpray ion source. Peptides were loaded onto a PepMap RSLC C18 column (2 µm, 100 Å, 75 µm i.d. ×250 mm, Thermo Scientific) using a flow rate of 300 nL/min for 15 minutes at 1% B (mobile phase A was 0.1% formic acid in water and mobile phase B was 0.1% formic acid in acetonitrile) after which point they were separated with a linear gradient of 2% to 20%B for 90 minutes, 20% to 32%B for 20 minutes, 32% to 95%B for 2 minutes, holding at 95%B for 8 minutes and reequilibrating at 1%B for 5 minutes. Each sample was followed by a blank injection to both clean the column and reequilibrated at 1%B. MS1 scans were acquired at a resolution of 240 000 Hz from mass range 400 to 1600 m/z. For MS1 scans the automatic gain control target was set to 4×10^5 ions with a max fill time of 50 ms. MS2 spectra were acquired using the TopSpeed method with a total cycle time of 3 seconds and an automatic gain control target of 1×10^4 and a max fill time of 100 ms, and an isolation width of 1.6 Da in the quadrapole. Precursor ions were fragmented using higher-energy C-trap dissociation with normalized collision energy of 30% and analyzed using rapid scan rates in the ion trap. Monoisotopic precursor selection was enabled and only MS1 signals exceeding 5000 counts triggered the MS2 scans, with +1 and unassigned charge states not being selected for MS2 analysis. Dynamic exclusion was enabled with a repeat count of 1 and exclusion duration of 15 seconds.

Mass Spectrometry Data Analysis

Raw data were searched using a uniprot reviewed mouse database (09/18) with the X!Tandem (PMID: 14976030) algorithm version 2013.06.15.1 and Comet (PMID:23148064) algorithm version 2014.02 rev.2 search engines with the following parameters: full trypsin cleavage allowing for up to 2 missed cleavages, variable modifications +16 Da on methionine (oxidation), +57 Da, +125 Da and, in the case of IodoTMT6 labeled samples, +329 on cysteine (carbamidomethylation, n-ethylmaleimide, TMT). Mass tolerance of MS1 error of 10 ppm, MS2 error of 1 Da were used. The mass spectrometry proteomics data have been deposited to the ProteomeXchange Consortium via the PRIDE (PMID: 30395289) partner repository with the data set identifier PXD012706 (reviewer account details: Username: reviewer52954@ebi.ac.uk; Password: MkOzBjKi).

Differences in S-nitrosylation modification for HPDP-labeled samples were determined by label-free quantitation using MS1 extracted ion chromatograms in Skyline (version 4.1) using a dot product cutoff 0.8 (PMID: 22454539). Signal for each modified cysteine was summed within a replicate and normalized against the average of the pooled controls for that site. For iodoTMT^6 labeled samples, only peptides with an iprofit score >0.95 were considered. Reporter ion intensities were determined using the Libra module of the trans-proteomic pipeline (PMID: 20101611). Replicates were normalized against the pooled control present in the 5- or 6-plex. For all analysis, replicates need to be at least 1.5-fold greater than control and present in at least 40% of the replicates per group. Bioinformatic analysis was performed using Ingenuity Pathway Analysis (QIAGEN Inc., https://www.qiagenbioinformatics.com/products/ingenuity-pathway-analysis) and using gene ontology annotations in the Uniprot database (uniprot.org).

String v11 software was used to create pathway analysis of the data shown in Figure S3.[26]

Statistical Analysis

The results are expressed as mean±SEM. Differences between groups were examined for statistical significance using Student's *t* test or 1-way or 2-way ANOVA, with Newman-Keuls for multiple comparisons for post hoc analysis where appropriate. Results with $P<0.05$ were considered significant. All analysis were performed using SPSS and Prism Statistical software.

RESULTS

Pregnant *GSNOR*$^{-/-}$ Mice Exhibit Hallmark Features of Preeclampsia, Hypertension, and Proteinuria

Development of hypertension and proteinuria are hallmarks of preeclampsia, and *GSNOR*$^{-/-}$ mice are hypotensive compared with wild-type mice before pregnancy,[16] consistent with GSNOR regulation of endothelium-dependent vasodilation (Figure 1A). At day 17.5 of pregnancy, *GSNOR*$^{-/-}$ mice develop hypertension (Figure 1A, Figure S1) and proteinuria (Figure 1B), characterized by elevated urine macroglobulin levels, associated with renal pathology including enlarged glomeruli, swelling of the endothelial cells and loss of

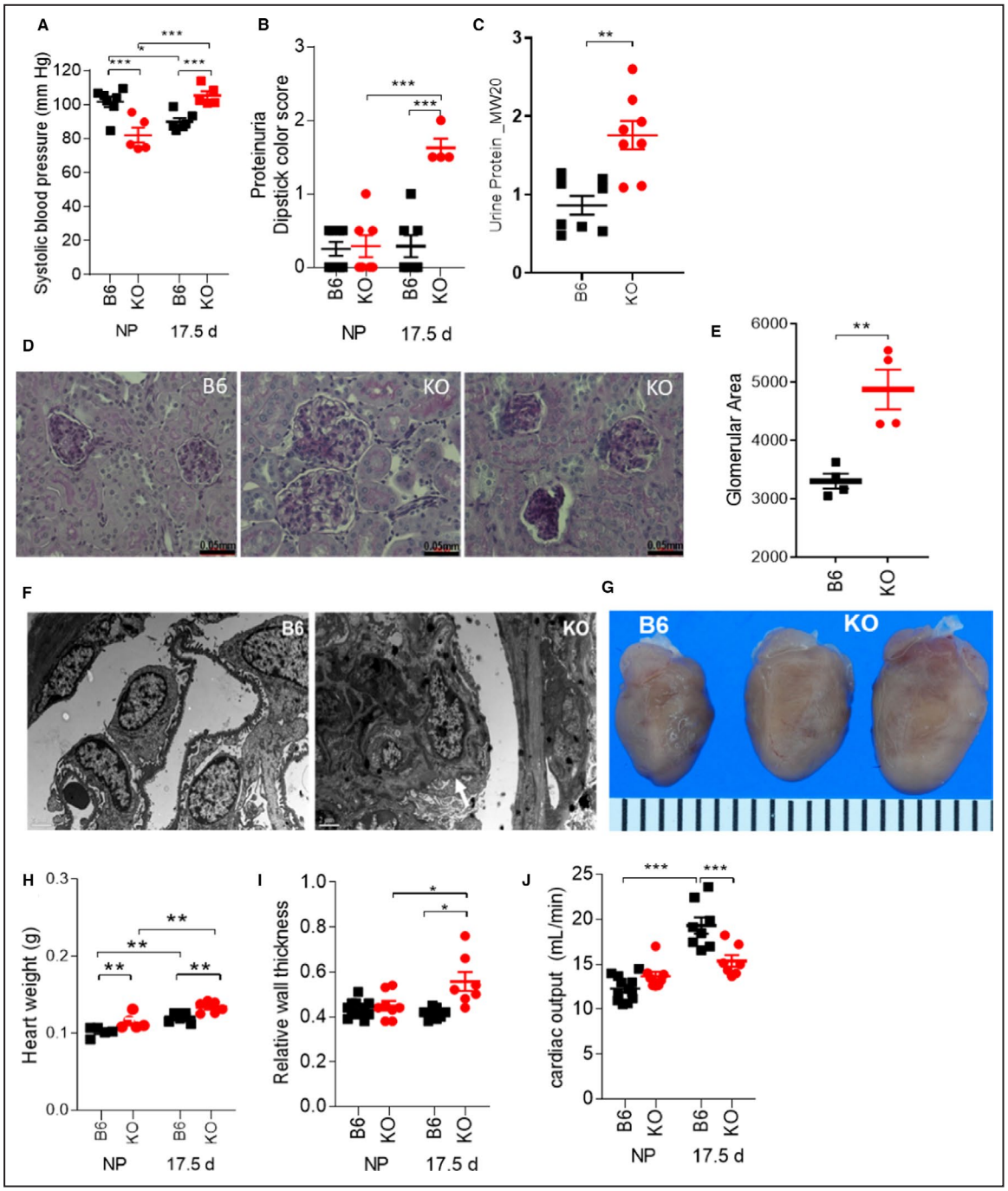

Figure 1. Pregnant *GSNOR*$^{-/-}$ mice exhibit hallmark features of preeclampsia including hypertension, proteinuria, and concentric hypertrophy in the heart.

Nonpregnant and pregnant (17.5 d) (N=4–12 mothers per group) C57Bl/6J (B6) and *GSNOR*$^{-/-}$ (KO) mice were examined. At late gestation, knockout (KO) mothers exhibited (**A**) hypertension, (**B**) proteinuria, and elevated (**C**) urine macroglobulin levels. **D**, **E**, Kidney sections at late gestation stained with periodic acid–Schiff showed enlarged glomeruli and focal and sclerosis with collapsed glomerular capillaries. **F**, Electron microscopy on renal tissues showed that GSNOR$^{-/-}$kidneys exhibited glomerular endotheliosis comprised of endothelial cell swelling, along with loss in fenestration and corrugation of the glomerular basement membrane (N=2 was examined per group). **G**, **H**, Heart weight and (**I**) relative wall thickness were significantly bigger in KO mice as compared with controls, indicating the presence of concentric hypertrophy. **J**, The normal increase in cardiac output was absent in KO mice at late gestation. For systolic blood pressure, proteinuria, heart weight, relative wall thickness, and cardiac output, a 2-way ANOVA with Newman-Keuls for post hoc analysis was performed. For the other variables, Student's *t* test was performed. Results are shown as mean±SEM. ***P<0.001, **P<0.01, *P<0.05. B6 indicates C57Bl/6J mice; KO, *GSNOR*$^{-/-}$ mice; and NP, non-pregnant.

fenestration and corrugation of the glomerular basement membrane (Figures 1C through 1F), changes that recapitulate human preeclampsia.[27,28]

GSNOR$^{-/-}$ Hearts Exhibit Concentric Hypertrophy During Pregnancy

We next studied cardiac responses to pregnancy in the *GSNOR*$^{-/-}$ mouse. The heart responds to sustained hypertension by an increase in wall thickness leading to concentric hypertrophy, and concentric hypertrophy independently predicts adverse outcome in preeclamptic pregnancies.[29] At late gestation, left ventricular end-diastolic dimension was lower, whereas the anterior wall at diastole (Table 1) was thicker, contributing to higher relative wall thicknesses in pregnant *GSNOR*$^{-/-}$ mice as compared with controls (Figures 1G through 1I, Table 1). Using isolated cardiomyocytes we observed that width was greater in *GSNOR*$^{-/-}$ mice, whereas length was not different between the 2 strains at late gestation (Table 1). These factors likely contributed to the enlarged *GSNOR*$^{-/-}$ hearts at late gestation, even when normalized to tibia length (Figure 1G and 1H, Table 1). Furthermore, the normal physiologic increases in maternal cardiac output and stroke volume were completely abrogated at late gestation in *GSNOR*$^{-/-}$ mice (Figure 1J, Table 1), consistent with the phenotype of lower cardiac output and stroke volume in preeclamptic patients with concentric heart geometry.[29] Heart rate remained unchanged between groups (Table 1). These data suggest that S-nitrosylation homeostasis plays an important role in limiting pathological hypertrophy.[30]

GSNOR$^{-/-}$ Mice Exhibited Placental Insufficiency During Pregnancy

Placental insufficiency (fetal weight to placental weight ratio) is believed to contribute directly to the development of preeclampsia. The placentas of preeclamptic pregnancies often exhibit fetoplacental hypovascularity and decreased fetoplacental perfusion,[31] both of which decrease transfer of oxygen and nutrients to the placenta, thereby limiting fetal growth. Fetal litter size was significantly lower in *GSNOR*$^{-/-}$ mice at 17.5 d of gestation (Figure 2A). Fetal body weights were significantly lower in *GSNOR*$^{-/-}$ mice at 17.5 d of gestation (Figure 2B). To evaluate the role of GSNOR on placental vascularization and fetoplacental perfusion, we examined the placentas at late gestation. GSNOR activity was present in the control placentas, and as anticipated was absent in the knockout mice (Figure 2C). Placental weight (Figure 2D) and umbilical arterial blood flow (Figure S2) were not significantly different between the 2 strains. However, placental efficiency and umbilical venous blood flow were significantly lower in *GSNOR*$^{-/-}$ placentas as compared with controls at late gestation (Figures 2E, Figure S2). In addition, placental vascularization was decreased in *GSNOR*$^{-/-}$ placentas (Figures 2F and 2G). These findings suggest that GSNOR plays an essential role in placental development and function during pregnancy.

VEGF Pathway Was Blunted in *GSNOR*$^{-/-}$ Placentas at Late Gestation

We next examined the VEGF pathway as a potential mechanism for the impaired placental vascularization as VEGFR2 levels are decreased in human preeclamptic pregnancies.[32] Whereas VEGF protein abundance in the placentas was not different between the 2 strains at late gestation (Figure 2H), nitrosylation of VEGF protein was significantly lower in *GSNOR*$^{-/-}$ placentas (Figures 2H and 2I). VEGF binds to its receptor VEGFR2 and signals through the endothelial nitric oxide synthase (eNOS) pathway.[33] Similar to human preeclampsia,[10,32] we found that total VEGFR2 ($P<0.05$) and eNOS ($P<0.01$) protein quantities were lower in the *GSNOR*$^{-/-}$ placentas as compared with controls (Figures 2J and 2K). Thus, alterations in VEGF signaling may represent a contributory mechanism for impaired placental development in GSNOR$^{-/-}$ mice.

GSNOR$^{-/-}$ Mice Exhibit Nitroso-Redox Imbalance and Nitrosative Stress During Pregnancy

Aberrant ROS and NO signaling has been implicated in the pathogenesis of preeclampsia.[34,35] To address this issue, we measured the cellular ROS levels in *GSNOR*$^{-/-}$ mice. Before pregnancy, cellular ROS generation was higher in cardiomyocytes isolated from *GSNOR*$^{-/-}$ mice as compared with control mice (Figure 3A), yet ROS levels were not significantly different between the 2 groups (Figure 3B), suggesting increased involvement of antioxidant scavengers. During pregnancy, ROS generation and levels were significantly higher in *GSNOR*$^{-/-}$ cardiomyocyte as compared with controls (Figures 3A and 3B) confirming the presence of oxidative stress. Increased oxidative stress can lead to alterations in NO/S-nitrosylation signaling; therefore, we next measured NO levels. As expected, there was a significant increase in NO levels in isolated cardiomyocytes of control mice during pregnancy (Figure 3C). This increase likely plays a critical role in vasodilation leading to the normal adaptations to pregnancy. NO levels were also significantly higher in cardiomyocytes isolated from pregnant as compared with nonpregnant *GSNOR*$^{-/-}$ mice. With the presence of elevated ROS and NO/S-nitrosylation levels in *GSNOR*$^{-/-}$ mice, we predicted an increase production of the potent prooxidant peroxynitrite. Before pregnancy, peroxynitrite levels were significantly higher in *GSNOR*$^{-/-}$ cardiomyocytes as compared with controls (Figure 3D). This

Table 1. KO Mice Exhibited Concentric Hypertrophy and Abnormal Maternal Cardiovascular Adaptation to Pregnancy, Which Was Rescued With Ascorbate Treatment

	Nonpregnant		Pregnant		Ascorbate-treated pregnant	
	B6	Knockout	B6	Knockout	B6	Knockout
Maternal body weight, g	20.3±0.36*	20.3±0.70*	35.4±0.56	31.1±1.55†	36.24±0.78	34.2±0.55*
Heart rate, bpm	454±9	497±18	494±14	498±12	484±7	517±14
LV end-diastolic dimension, diastole, mm	3.40±0.04*	3.50±0.05	3.78±0.04	3.52±0.12†	3.67±0.07	4.00±0.09*,†
LV anterior wall thickness, diastole, mm	0.80±0.02	0.82±0.04*	0.91±0.03	1.07±0.07†	0.84±0.03	0.88±0.04*
Relative wall thickness	0.43±0.01	0.45±0.02*	0.41±0.01	0.56±0.04†	0.44±0.01	0.45±0.03*
Myocyte length, μmol/L	138±2*	164±4*,†	158±2	154±2	158±7	150±2
Myocyte width, μmol/L	25.7±0.28	25.1±0.46*	25.2±0.53	29.4±0.67†	25.3±0.34	22.4±0.29*,†
Stroke volume, μL	27.1±0.50*	27.8±1.16	39.2±1.96	30.9±1.27†	34.5±1.54*	40.1±1.60*,†
Heart weight normalized to tibal length, mg	5.88±0.13*	7.09±0.31*,†	7.07±0.10	7.98±0.34†	7.01±0.63	9.98±3.38†

Results are shown as mean±SEM. Two-way ANOVA with Newman-Keuls for post hoc analysis. LV indicates left ventricular.
*$P<0.05$ vs pregnancy (same strain).
†Vs strain difference.

preexisting elevation in peroxynitrite levels suggests that the *GSNOR*$^{-/-}$ mice were less able to respond to the stress of pregnancy. At late gestation, peroxynitrite levels were, indeed, significantly higher in isolated cardiomyocytes of *GSNOR*$^{-/-}$ mice (Figure 3D), suggesting the presence of nitrosative stress. Furthermore, superoxide dismutase (SOD) levels were significantly lower in *GSNOR*$^{-/-}$ placentas as compared with controls, suggesting decreased antioxidant capacities (Figure 3E). NO signaling via S-nitrosylated proteins may exert a protective role against an oxidative environment by competing with other posttranslational modifications and shielding critical cysteine residues from the damaging effects of irreversible oxidation as shown in ischemic preconditioning.[36,37] These findings suggests that S-nitrosylation–based mechanisms that protect physiologic signaling may be impaired in pregnant *GSNOR*$^{-/-}$ mice, contributing to the preeclampsia phenotype. Alternatively, increased levels of NO and ROS can form peroxynitrite, which can irreversibly lead to protein nitration.[8] Protein nitration plays a relevant role in posttranslational modification of protein and increased nitration of proteins has been implicated in human preeclampsia pregnancies.[8] Thus, protein nitration may be another mechanism involved in the development of preeclampsia-like conditions in *GSNOR*$^{-/-}$ animals.

Antioxidant Treatment Rescued the Preeclampsia Phenotype in *GSNOR*$^{-/-}$ Mice During Pregnancy

To test whether antioxidant treatment can rescue the preeclampsia phenotype, we treated animals or isolated cardiomyocytes with ascorbate. In addition to being an antioxidant, ascorbate also functions as a reductant, promoting the release of biologically active NO from nitrosylated thiols, and plasma ascorbate levels are commonly diminished in preeclamptic patients.[38] Importantly, ascorbate treatment rescued the onset of hypertension, proteinuria, and urinary macroglobulin levels (Figures 4A through 4C). The enlarged anterior wall thickness, relative wall thickness and cardiomyocyte width, all indicative of concentric hypertrophy, returned to normal levels in ascorbate treated pregnant *GSNOR*$^{-/-}$ mice (Table 1). Ascorbate also significantly improved cardiac output and stroke volume in *GSNOR*$^{-/-}$ mothers at late gestation, whereas it lowered both parameters in pregnant B6 controls (Figure 4D, Table 1). Ascorbate treatment significantly improved placental vascularization along with placental VEGFR2 and eNOS protein levels (Figures 4G, 4J and 4K). In addition, ascorbate improved umbilical venous blood flow and litter size but did not improve placental efficiency, which may account for the failure of fetal weights to improve at late gestation in the *GSNOR*$^{-/-}$ mice (Figure 4E through 4I, Figure S2). Acute and chronic treatment of ascorbate similarly reduced ROS, NO, and peroxynitrite levels in isolated cardiomyocytes from pregnant *GSNOR*$^{-/-}$ mice (Figure 3A through 3D). Thus, ascorbate may work as a potent scavenger of free radicals as seen in experimental models of hypertension[39,40] and in rat models of nephrotoxicity[41] to balance the nitroso-redox system and in turn rescue the preeclampsia-like phenotype in pregnant *GSNOR*$^{-/-}$ mice.

Mass Spectrometry Revealed Elevated Placental S-Nitrosylated Amino Acid Residues in *GSNOR*$^{-/-}$ Mice

To directly test the prediction that S-nitrosylation is dysregulated in *GSNOR*$^{-/-}$ placentas, we performed

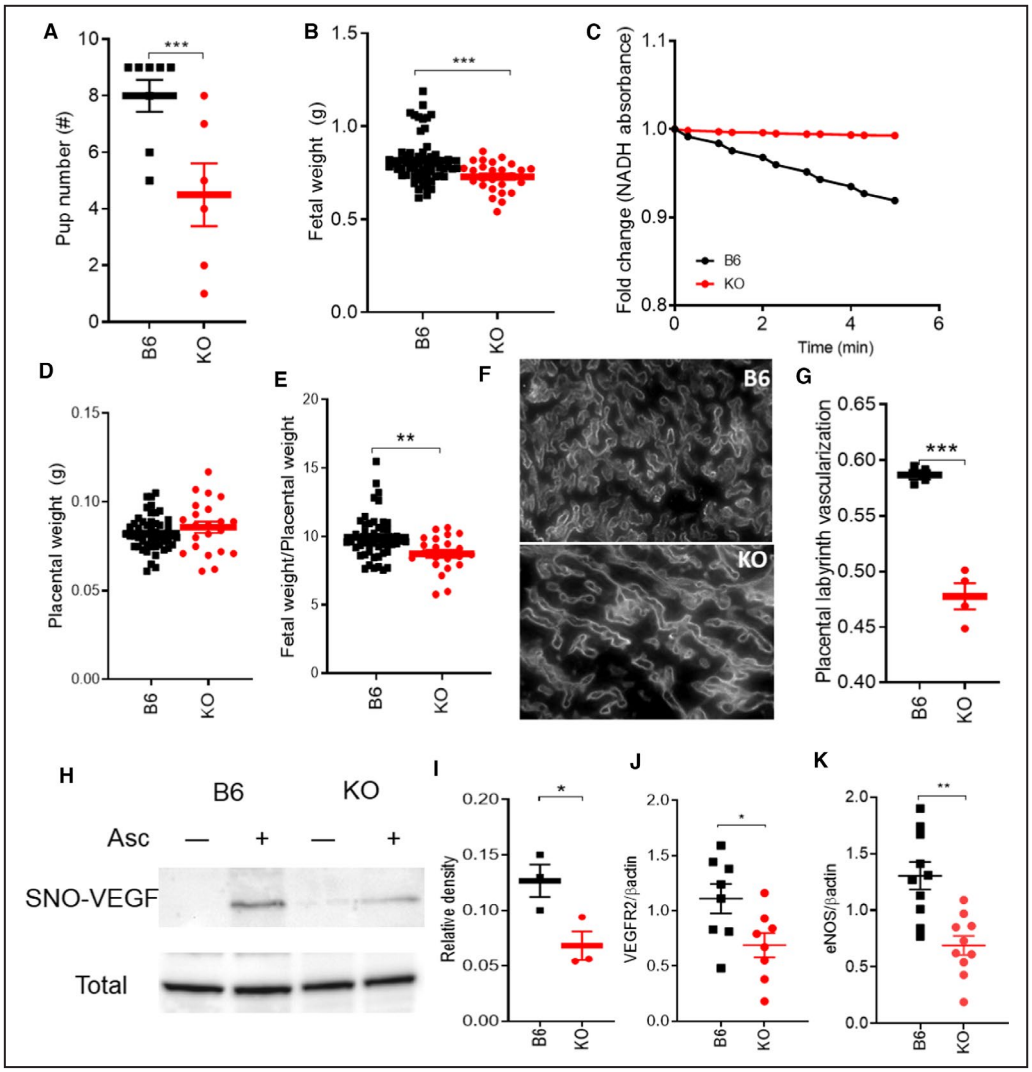

Figure 2. *GSNOR*$^{-/-}$ mice exhibited placental insufficiency during pregnancy and showed alteration of VEGF pathway.

Nonpregnant and pregnant (17.5 d) (N=4–12 mothers per group) C57Bl/6J (B6) and *GSNOR*$^{-/-}$ (knockout [KO]) mice were examined. **A**, Fetal number and (**B**) weight were significantly lower in KO mice. **C**, NADH-dependent GSNOR enzymatic activity was determined in placental tissue at 17.5 days of gestation. GSNOR activity is enriched in B6 placentas, whereas it is completely absent in the KO placentas. **D**, **E**, Placental weight was not significantly different between the 2 strains, whereas placental efficiency was significantly lower in KO mice as compared with control. **F**, **G**, Placental vascularization determined using isolectin immunostaining, was significantly lower in KO as compared with B6 at late gestation. SNO-VEGF was measured using Biotin-switch assay. **H**, Representative blots shown for S-nitrosylated and total VEGF in the placenta. Omission of ascorbate was used as the negative control. **I**, Nitrosylation of VEGF was significantly lower in KO placentas as compared with B6 at late gestation. **J**, **K**, VEGFR2 and eNOS protein levels were determined in the placentas at 17.d of gestation. Both VEGFR2 and eNOS protein levels were significantly lower in in GSNOR$^{-/-}$ placentas as compared with B6 placentas at 17.5 days of gestation. For statistical significance, 2-way ANOVA with Newman-Keuls for post hoc analysis or Student's *t* test were performed. Results are shown as mean±SEM. ***P<0.001, **P<0.01, *P<0.05. B6 indicates C57Bl/6J mice; GSNOR, S-nitrosoglutathione reductase; KO, *GSNOR*$^{-/-}$ mice; and NP, nonpregnant.

mass spectrometry using both thiol reactive biotin–HPDP and cysTMT labeling to maximize coverage.[42] Consistent with our prediction, this analysis revealed a marked increased number of S-nitrosylated residues in *GSNOR*$^{-/-}$ placentas (459 corresponding to 351 proteins) compared with controls (264 S-nitrosylated residues corresponding to 198 proteins) (Figure 5A through 5C, Table S1 through S3). Importantly, placentas from ascorbate-treated mice exhibited an increased net number of S-nitrosylated proteins in both control and *GSNOR*$^{-/-}$ placentas (consistent with the transnitrosylation properties of

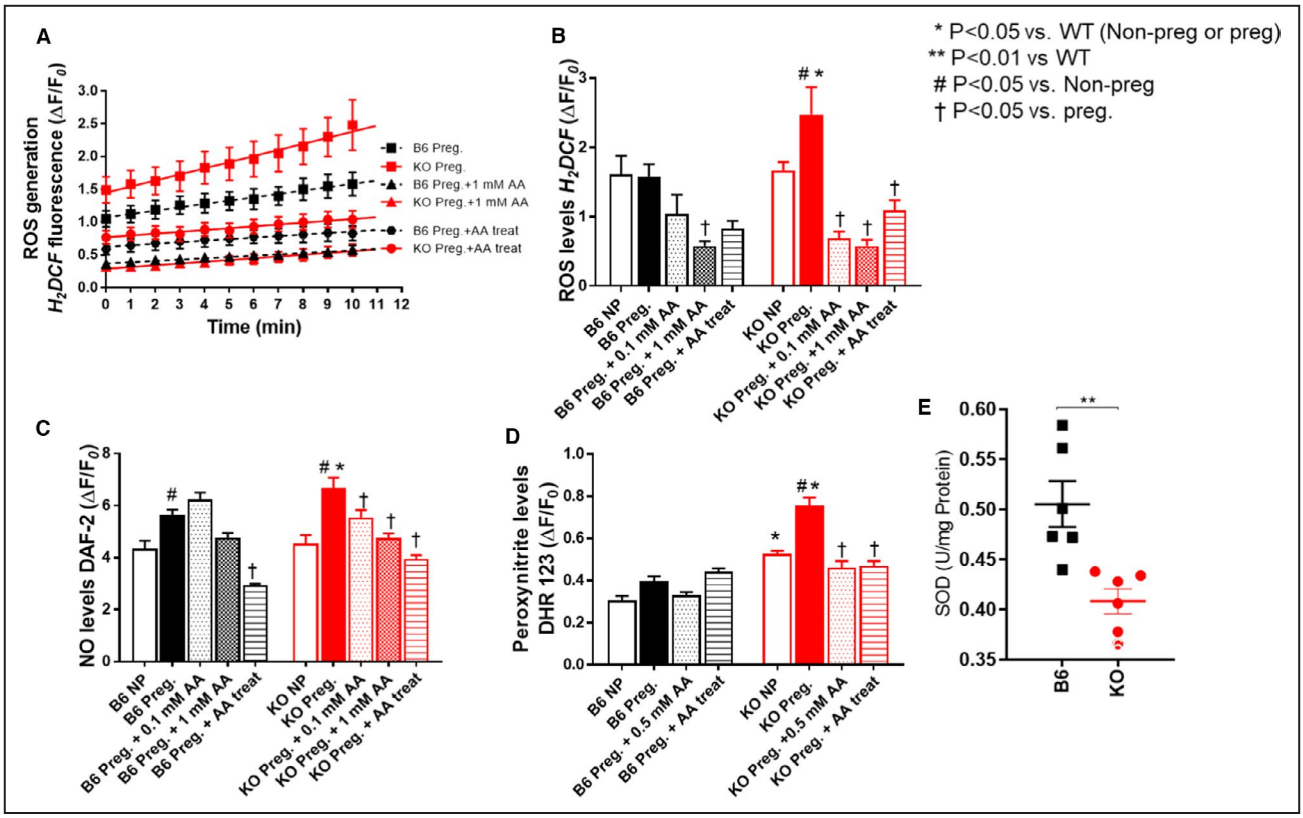

Figure 3. ***GSNOR*$^{-/-}$ mice exhibit nitroso-redox imbalance and nitrosative stress that is rescued with ascorbate treatment.** In nonpregnant (NP) and pregnant (17.5 d) C57Bl/6J (B6) and *GSNOR*$^{-/-}$ (knockout [KO]) mice, reactive oxygen species, NO and peroxynitrite levels were determined in isolated cardiomyocyte using epifluorescence by 2',7'dichlorodihydro-fluoresceine (H2DCF–DA, 10mM), 4,5-diaminofluorescein (DAF-2DA, 10 mmol/L) and dihydrorhodamine 123 (DHR 123, 25 mmol/L), respectively. Ascorbate (AA) studies included both acute (0.1 mmol/L, 0.5 mmol/L, 1 mmol/L) and chronic (AA provided in drinking water from day 0.5) treatments. **A** and **B**, ROS generation and levels, and (**C**) NO and (**D**) peroxynitrite levels were significantly higher in cardiomyocyte isolated from pregnant *GSNOR*$^{-/-}$ mice. This increase was prevented with acute and chronic AA treatment. **E**, Superoxide dismutase (SOD) levels were measured in the placenta using lucigenin-enhanced chemiluminescence. SOD levels were significantly lower in the KO placentas as compared with controls. Results are shown as mean±SEM. N=3–5 animals per experiment. One-way ANOVA with Newman Keuls post hoc test.B6 indicates C57Bl/6J mice; KO, *GSNOR*$^{-/-}$ mice; NP, nonpregnant; and SNO, S-nitrosylated.

chronic ascorbate[43]), but this increase was less in the *GSNOR*$^{-/-}$ mice (Figure 5D) decreasing the difference in number of S-nitrosylated proteins between the 2 groups. Furthermore, we examined subcellular compartmentalization of the total proteins detected in the 4 groups. Similar to our previous study,[44] we found majority of the nitrosylated proteins were located in the cytoplasm and the nucleus (Figure 5E). To gain insights into the most important signaling pathways affected by excess S-nitrosylation, we examined the subset of S-nitrosylated proteins found exclusively in GSNOR versus B6, and which exhibited denitrosylation with ascorbate. Of all the detected peptides, there were 50 S-nitrosylation residues unique to the *GSNOR*$^{-/-}$ placentas, but only 16 residues unique to the B6 placentas (Figures 5C and 5F, Table S1 through S3). All 50 S-nitrosylation residues were reversed by ascorbate (Table S2). From these 50 proteins, 14 have been linked to important roles in processes essential in pregnancy, including angiogenesis, inflammation, cell migration, and apoptosis (Figure 5F), supporting the pathophysiological relevance of these proteins.

GSNOR Activity Is Reduced in Human Preeclampsia Placentas

To examine the potential relevance of this pathway in human preeclampsia, we measured GSNOR mRNA, protein, and activity levels in the placenta of patients with pregnancies complicated with preeclampsia (Figure 6, Table 2). Whereas GSNOR mRNA and protein abundance were similar (data not shown), GSNOR activity was significantly lower in placentas of human pregnancies complicated with preeclampsia compared with placentas from normal pregnancies (Figure 6). Furthermore, affected placentas also had increased nitrosative stress as indicated by increased protein expression of nitrotyrosine and decreased antioxidant capacity as shown by decreased SOD levels (Figure 6). These

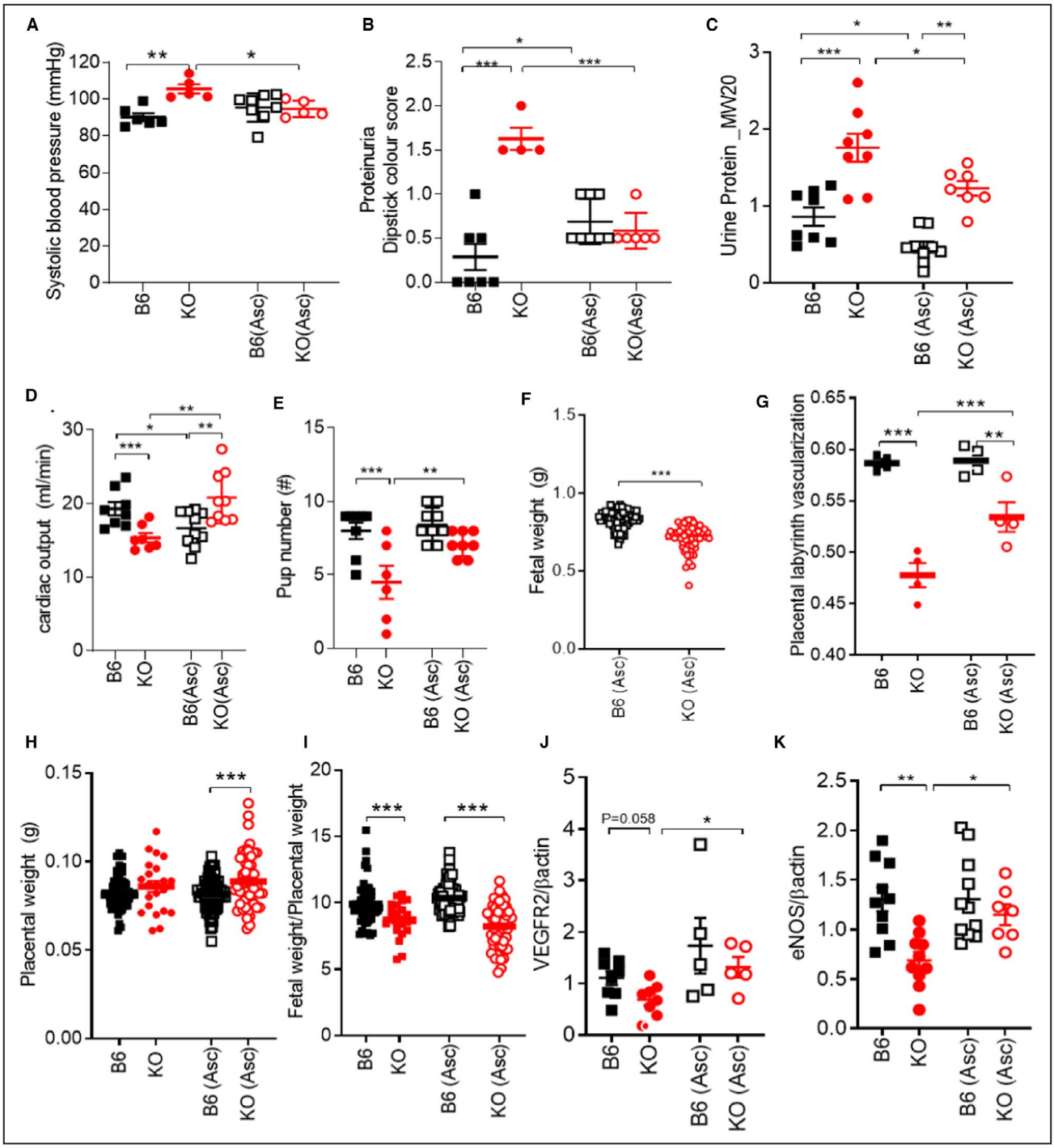

Figure 4. Preeclampsia phenotype in the mother and litter size is rescued with ascorbate.
Late pregnant (17.5 d) C57Bl/6J (B6) and *GSNOR*$^{-/-}$ (knockout [KO]) mice were examined. N=4–10 mothers per group. **A**, Hypertension, (**B**) proteinuria, and (**C**) urine macroglobulin levels were rescued with ascorbate treatment. Ascorbate treatment increased (**D**) cardiac output in knockout (KO) mice at late gestation. **E**, Pup number was improved, whereas (**F**) fetal weight remained significantly lower in KO mice treated with ascorbate. **G**, Impaired placental vascularization was rescued with ascorbate treatment in KO placentas. With ascorbate treatment, (**H**) placental weight was significantly higher in the KO treated animals as compared with B6-treated animals. Whereas (**I**) placental efficiency remained significantly lower in treated KO mice as compared with controls. **J**, **K**, VEGFR2 and endothelial nitric oxide synthase placental protein levels were significantly increased in KO (Asc) treated animals as compared with nontreated KO animals. Results are shown as mean±SEM. ***P<0.001, **P<0.01, *P<0.05. One-way or 2-way ANOVA with Newman Keuls post hoc test and Student's t test were performed. Asc, ascorbate; B6, C57Bl/6J mice; KO, *GSNOR*$^{-/-}$ mice; and VEGF, vascular endothelial growth factor.

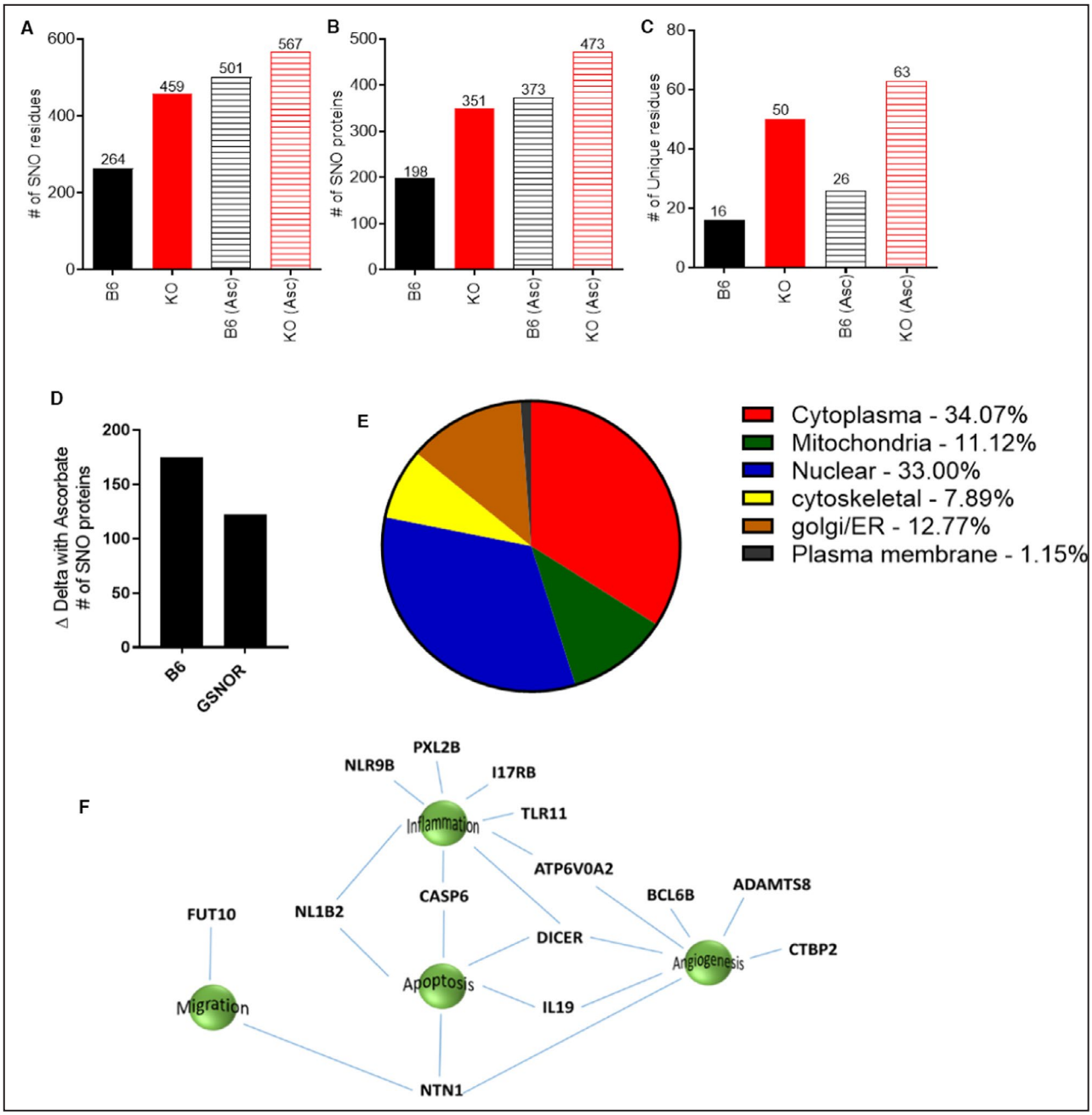

Figure 5. Duel-labeling mass spectrometry revealed an increased number of SNOylated proteins in the placentas from *GSNOR*$^{-/-}$ animals.

A and **B**, An increased number of S-nitrosylated proteins were detected in the placentas of the knockout (KO) animals, and of these there were more unique S-nitrosylated residues (**C**) in *GSNOR*$^{-/-}$ placentas as compared with controls. Ascorbate treatment increased S-nitrosylated proteins in both groups, but this increase was less in the KO group as compared with control (**D**). **E**, The majority of the nitrosylated proteins were detected in the cytoplasm and in the nucleus in the 4 different groups analyzed. **F**, Schematic showing proteins unique in *GSNOR*$^{-/-}$ placentas but absent in the B6 placentas, and B6- and *GSNOR*$^{-/-}$ placentas treated with ascorbate. ADAMTS8 indicates A disintegrin and metalloproteinase with thrombospondin motifs 8; ATP6V0A2, V-type proton ATPase 116 kDa subunit a isoform 2; BCL6B, B-cell CLL/lymphoma 6 member B protein; CASP6, Caspase-6 (CASP-6); CASP6, Caspase-6; CTBP2, C-terminal-binding protein 2; DICER, Endoribonuclease Dicer; FUT10, Alpha-(1,3)-fucosyltransferase 10; IL17RB, IL-17 receptor B; IL-19, interleukin-19; NL1B2, NACHT, LRR and PYD domains-containing protein 1b allele 2; NLR9B, NACHT, LRR and PYD domains-containing protein 9B; NTN1, Netrin-1; PXL2B, Prostamide/prostaglandin F; and TLR11, Toll-like receptor 11.

findings support the physiologic importance of GSNOR in regulating human placental homeostasis and that the *GSNOR*$^{-/-}$ mouse represents a model of preeclampsia.

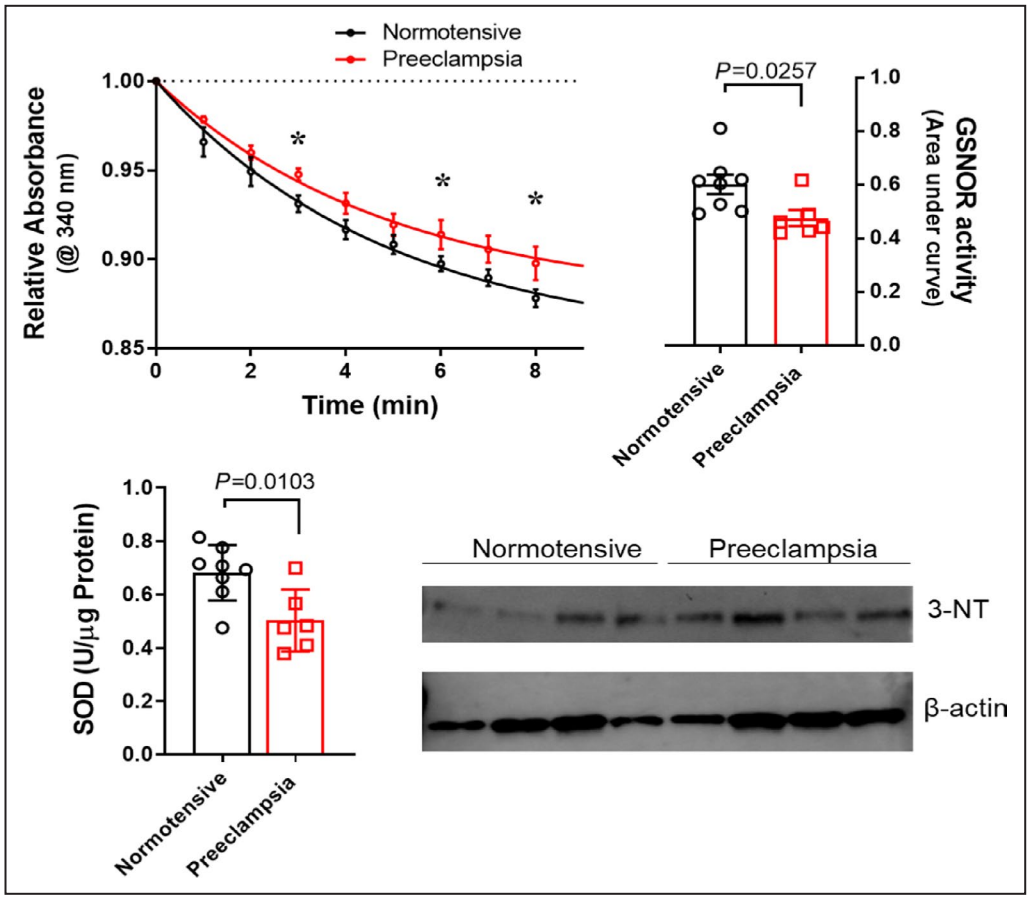

Figure 6. GSNOR activity is reduced and contributes to nitroso-redox balance in the human preeclamptic placenta.
Human preeclamptic placentas exhibited decreased GSNOR activity, decreased antioxidant capacity (determined by superoxide dismutase levels), and increased nitrosative stress (determined by increased protein expression of nitrotyrosine). Significance for relative absorbance of GSNOR activity was determined by 2-way ANOVA with Newman-Keuls post hoc test. For other variables, Student's *t* test was used. Results are shown as mean±SEM. **P*<0.05, N=6–8 mothers. GSNOR indicates S-nitrosoglutathione reductase; and SOD, superoxide dismutase.

DISCUSSION

We have identified that mice lacking S-nitrosoglutathione reductase (GSNOR–/–), a denitrosylase regulating S-nitrosylation, exhibit most of the clinical features of preeclampsia including hypertension, proteinuria, renal pathology, cardiac concentric hypertrophy, decreased placental vascularization and fetal growth restriction. The primary mechanisms involved in this preeclampsia phenotype appears to be nitrosative stress attributable to aberrant S-nitrosylation leading to the presence of nitroso-redox imbalance. In addition, we showed that antioxidant, ascorbate, rescued the nitrosative stress and preeclampsia phenotype in the mother (Figure 7). Our findings demonstrate that the absence of a single gene, GSNOR, alters large numbers of downstream signaling pathway. Ascorbate, which creates a net increase in the number of S-nitrosylated proteins, decreases the differences between the GSNOR$^{-/-}$ and B6 mice. As such, these results suggest that the regulation of the S-nitrosylation–integrated posttranslational modification system may account in large part for the phenotype of preeclampsia in the *GSNOR*$^{-/-}$ mice. Together, these results suggest that this system-wide alteration in S-nitrosylated proteins has a detrimental effect on the function of these pathways and, as such, could be a key mechanism involved in the pathological phenotype seen in multiple organ systems, including the heart, kidney, and placenta, and the offspring of the knockout animals with preeclampsia. Furthermore, our data revealed that GSNOR plays an essential role in normal human pregnancies, as human placentas from pregnancies complicated with preeclampsia showed a significant decrease in GSNOR activity with the presence of nitrosative stress and decrease in antioxidant capacities.

Table 2. Demographic Data of the Pregnant Study Human Subjects Used in the Study

Variables	Normotensive	Preeclampsia	*P* value
	N=8	N=6	
Maternal age, y	33±2	32±3	…
Race or ethnicity			
Non-Hispanic Black	8	5	…
Hispanic	0	1	…
Gestational age, wk	38±1	36±2	…
Mode of delivery			
Vaginal	5	3	…
Cesarean section	3	3	…
Blood pressure, mm Hg			
Systolic	116±6	166±5	<0.001
Diastolic	67±3	89±4	<0.01

Statistical significance between the 2 groups was determined by Student's *t* test; Mean±SEM.

One of the primary clinical features of preeclampsia is an elevation in blood pressure and number of different mechanisms may account for the alterations in blood pressure in *GSNOR*$^{-/-}$ animals. Elevated plasma S-nitrosylation can lead to adverse cardiovascular outcomes in patients with end-stage renal disease, which correlates with elevated blood pressure.[45] Gandley et al[7] postulated that the buffering function of S-nitrosylated albumin was impaired in patients with preeclampsia, where the thiol of albumin acts as a sink for NO, therefore lowering NO bioavailability and thus raising blood pressure. Alternatively, denitrosylation of S-nitrosylated albumin may be regulated by glutathione. In preeclampsia, plasma glutathione levels are low,[46] most likely attributable to oxidative stress, and this decrease may effect NO-dependent vasodilation of red blood cells, as glutathione may facilitate their export of S-nitrosylations.[47] In addition, ROS which is increased in preeclampsia, potentiates protein S-nitrosylation.[48] Therefore, an altered redox state, which influences the thiol/nitrosothiol balance, may convey NO bioactivity, regulating free NO, thereby affecting blood pressure in *GSNOR*$^{-/-}$ mice.

It is well established that VEGF mediates endothelium-dependent vasodilation and angiogenesis, in part via the NO pathway. Furthermore, our laboratory previously showed that mesenchymal stem cells isolated from GSNOR$^{-/-}$ mice exhibited markedly

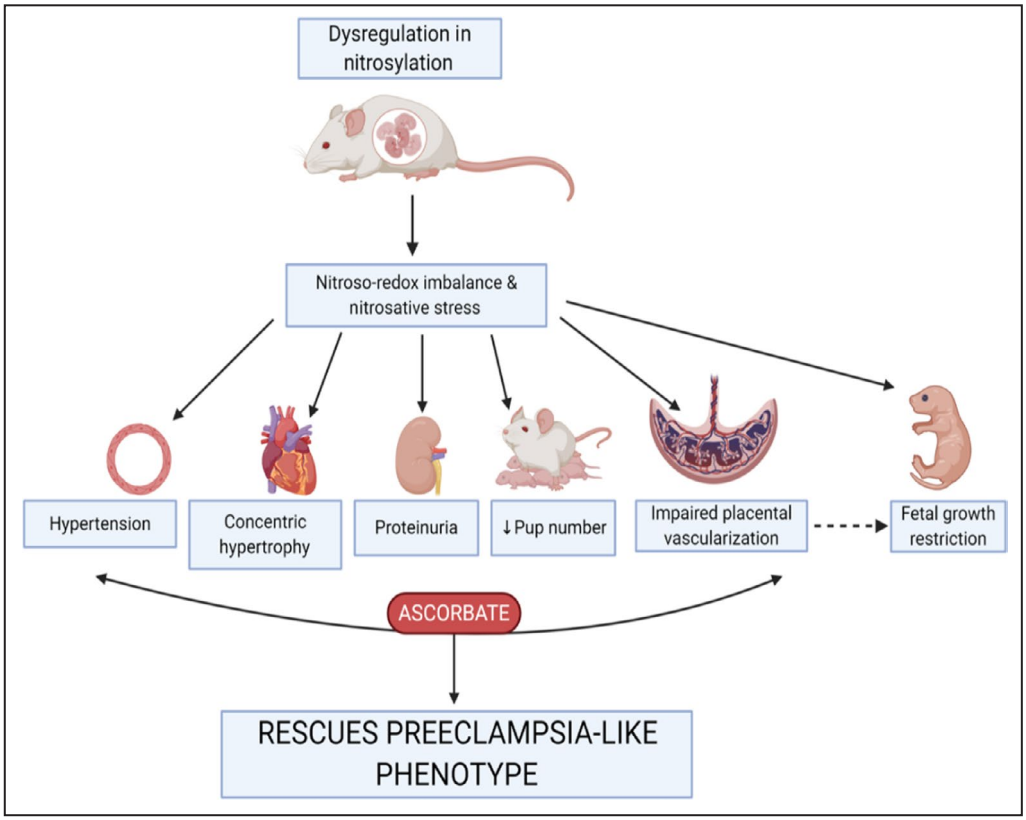

Figure 7. Dysregulation in nitrosylation contributes to nitroso-redox imbalance and nitrosative stress contributing to clinical features of preeclampsia including hypertension, proteinuria, concentric hypertrophy in the heart, decrease placental vascularization, and fetal growth restriction.
Antioxidant treatment rescued the preeclampsia-like phenotype in the mother.

diminished capacity for vasculogenesis,[49] suggesting that GSNOR plays a role in part working through the VEGF/NO pathway. VEGF binds to its receptor VEGFR2 and signals through the eNOS pathway,[33] and a decrease in VEGFR2 and eNOS levels are reported in human preeclamptic pregnancies.[10,32] During preeclampsia, impaired placental vascularization contributes to chronic ischemia and increases oxidative stress causing the placental release of factors such as soluble Flt1 (sFlt1). In turn, sFlt1 acts as a decoy receptor for VEGF,[50] and also antagonizes autocrine VEGF signaling,[51] rendering endothelial cells more sensitive to proinflammatory factors released by the placenta and decreasing the bioavailability of VEGF.[50,51] Accordingly, our current data suggest that the decrease in VEGF nitrosylation could further contribute to the downregulation of VEGF function, decreased eNOS protein levels, in turn affecting both vasodilation and angiogenesis during pregnancy. VEGF has not been previously reported to be nitrosylated, although it bears 4 potential cysteine sites; future experiments will be conducted to identify the exact nitrosylation posttranslational sites.

Several clinical trials have examined the effectiveness of antioxidants (ascorbate) in preventing preeclampsia. Small, randomized placebo-controlled trials showed reduced preeclampsia with ascorbate treatment, whereas all large multicenter randomized trials have yielded disappointing results. These large trials showed that ascorbate did not decrease the risk of preeclampsia in either high-risk (women with type 1 diabetes, nutritionally deficient, poor social economic status) or low-risk populations.[52–54] In turn, increased incidence of low birthweight, gestational hypertension, fetal loss, stillbirth, or premature rupture of membranes have been reported in some trials, but these findings were not confirmed across all studies; therefore, their significance remains uncertain.[52–54] The dosage and/or timing of the antioxidant treatment (8–22 weeks) may have played a role in the unsuccessful outcomes in these large clinical trials. Alternatively, oxidative stress may be relevant to the pathogenesis in only a subgroup of women, with no appreciable benefit of antioxidant therapy for the overall population. Preeclampsia is a multisystemic/multifactorial disease, and based on the heterogeneity of the clinical presentation, there may be different "subtypes" of preeclampsia,[55] which may explain, in part, why many of the clinical trials using ascorbate have yet to show favorable outcomes. Therefore, identifying women showing dysregulation in nitrosylation and/or altered GSNOR activity levels may be the ideal target subpopulation for treatment with ascorbate, permitting a precision medicine approach for future clinical trials.

This study has several limitations. All the features of the murine phenotype may not translate into human pathophysiology given its heterogenous nature and involvement of multiple organ systems. We did not examine some of the clinical features of preeclampsia such as thrombocytopenia, abnormal liver enzymes or abnormal spiral artery remodeling in the placenta. Furthermore, blood pressure was measured in unconscious animals.

Development of effective therapies for preeclampsia is hampered by a failure to understand the causative mechanisms involved and the absence of robust animal models that exhibit essentially all the clinical features of preeclampsia. Therefore, the identification of the GSNOR$^{-/-}$ mice as such a model with the causative role of dysregulation in nitrosylation contributing to nitrosative stress and dysregulation of physiologic posttranslational modification in a large number of signaling pathways as one of the primary mechanisms contributing to this disorder, has important implications for developing novel therapies and identifying clinically useful biomarkers for this difficult to treat maternal-fetal syndrome.

ARTICLE INFORMATION

Received September 16, 2021; accepted November 22, 2021.

Affiliations

Interdisciplinary Stem Cell Institute, University of Miami Miller School of Medicine, Miami, FL (S.K., R.A.D., M.A.B., J.F., R.K., H.A., E.P., W.B., J.M.H.); Department of Pediatrics, University of Miami Miller School of Medicine, Miami, FL (S.K.); Medicine and Heart Institute, Cedars Sinai Medical Center, Los Angeles, CA (C.I.M., D.S., J.E.V.E.); Department of Molecular and Cellular Pharmacology (R.K.); Department of Urology (H.A.) and Division of Cardiology, Department of Medicine, University of Miami Miller School of Medicine, Miami, FL (W.B., J.M.H.)..

Acknowledgments

We acknowledge Vania Almeida and the UM Transmission Electron Microscopy Core, Dr Wen Ding for urine collection and Infant Kidney Project for collection of human placentas.

Dr Kulandevlu conceived, designed, and executed the experiments and wrote the manuscript. Drs Dulce, Bellio, Fritsch, Kanashiro-Takeuchi, Paulino, and Arora performed experiments. Drs Murray, Soetkamp, and Van Eyk performed mass spectrometry experiment and analysis. Dr Balkan assisted in manuscript writing. Dr Hare conceived of and designed experiments, cowrote the manuscript, and provided funding.

Sources of Funding

This study was funded by R01 HL09489 and R01 HL137355 to Dr Hare and by Canadian Institute of Health Research postdoctoral fellowship and American Heart Association Career Development Award (19CDA34660102) to SK. Dr Hare is also supported by National Institutes of Health grants R01 HL134558, R01 HL101110, and 5UM 1HL113460 and by the Starr and Soffer Family Foundations.

Disclosures

Dr Hare reported having a patent for cardiac cell-based therapy. He holds equity in Vestion Inc. and maintains a professional relationship with Vestion Inc. as a consultant and member of the Board of Directors and Scientific Advisory Board. Dr Hare is the chief scientific officer, a compensated consultant and advisory board member for Longeveron, and equity holder in Longeveron. He is also the coinventor of intellectual property licensed to Longeveron. Longeveron LLC and Vestion Inc. did not participate in funding this work. Dr Hare's relationships are disclosed to the University of Miami, and a management plan is in place. The remaining authors have no disclosures to report.

Supplemental Material

Tables S1–S3
Figures S1–S3

REFERENCES

1. Sibai B, Dekker G, Kupferminc M. Pre-eclampsia. *Lancet*. 2005;365:785–799. doi: 10.1016/S0140-6736(05)17987-2
2. Ives CW, Sinkey R, Rajapreyar I, Tita ATN, Oparil S. Preeclampsia-pathophysiology and clinical presentations: JACC state-of-the-art review. *J Am Coll Cardiol*. 2020;76:1690–1702. doi: 10.1016/j.jacc.2020.08.014
3. Creanga AA, Syverson C, Seed K, Callaghan WM. Pregnancy-related mortality in the United States, 2011–2013. *Obstet Gynecol*. 2017;130:366–373. doi: 10.1097/AOG.0000000000002114
4. Molina RL, Pace LE. A renewed focus on maternal health in the United States. *N Engl J Med*. 2017;377:1705–1707. doi: 10.1056/NEJMp1709473
5. Al-Gubory KH, Fowler PA, Garrel C. The roles of cellular reactive oxygen species, oxidative stress and antioxidants in pregnancy outcomes. *Int J Biochem Cell Biol*. 2010;42:1634–1650. doi: 10.1016/j.biocel.2010.06.001
6. Tyurin VA, Liu SX, Tyurina YY, Sussman NB, Hubel CA, Roberts JM, Taylor RN, Kagan VE. Elevated levels of S-nitrosoalbumin in preeclampsia plasma. *Circ Res*. 2001;88:1210–1215. doi: 10.1161/hh1101.092179
7. Gandley RE, Tyurin VA, Huang W, Arroyo A, Daftary A, Harger G, Jiang J, Pitt B, Taylor RN, Hubel CA, et al. S-nitrosoalbumin-mediated relaxation is enhanced by ascorbate and copper: effects in pregnancy and preeclampsia plasma. *Hypertension*. 2005;45:21–27. doi: 10.1161/01.HYP.0000150158.42620.3e
8. Webster RP, Roberts VH, Myatt L. Protein nitration in placenta – functional significance. *Placenta*. 2008;29:985–994. doi: 10.1016/j.placenta.2008.09.003
9. Possomato-Vieira JS, Khalil RA. Mechanisms of endothelial dysfunction in hypertensive pregnancy and preeclampsia. *Adv Pharmacol*. 2016;77:361–431.
10. Osol G, Ko NL, Mandala M. Altered endothelial nitric oxide signaling as a paradigm for maternal vascular maladaptation in preeclampsia. *Curr Hypertens Rep*. 2017;19:82. doi: 10.1007/s11906-017-0774-6
11. Stamler JS, Jaraki O, Osborne J, Simon DI, Keaney J, Vita J, Singel D, Valeri CR, Loscalzo J. Nitric oxide circulates in mammalian plasma primarily as an S-nitroso adduct of serum albumin. *Proc Natl Acad Sci USA*. 1992;89:7674–7677. doi: 10.1073/pnas.89.16.7674
12. Foster MW, Pawloski JR, Singel DJ, Stamler JS. Role of circulating S-nitrosothiols in control of blood pressure. *Hypertension*. 2005;45:15–17. doi: 10.1161/01.HYP.0000150160.41992.71
13. Harris LK, McCormick J, Cartwright JE, Whitley GS, Dash PR. S-nitrosylation of proteins at the leading edge of migrating trophoblasts by inducible nitric oxide synthase promotes trophoblast invasion. *Exp Cell Res*. 2008;314:1765–1776. doi: 10.1016/j.yexcr.2008.02.010
14. Iyer AK, Rojanasakul Y, Azad N. Nitrosothiol signaling and protein nitrosation in cell death. *Nitric Oxide*. 2014;42:9–18. doi: 10.1016/j.niox.2014.07.002
15. Lima B, Forrester MT, Hess DT, Stamler JS. S-nitrosylation in cardiovascular signaling. *Circ Res*. 2010;106:633–646. doi: 10.1161/CIRCRESAHA.109.207381
16. Liu L, Yan Y, Zeng M, Zhang J, Hanes MA, Ahearn G, McMahon TJ, Dickfeld T, Marshall HE, Que LG, et al. Essential roles of S-nitrosothiols in vascular homeostasis and endotoxic shock. *Cell*. 2004;116:617–628. doi: 10.1016/S0092-8674(04)00131-X
17. Beigi F, Gonzalez DR, Minhas KM, Sun Q-A, Foster MW, Khan SA, Treuer AV, Dulce RA, Harrison RW, Saraiva RM, et al. Dynamic denitrosylation via S-nitrosoglutathione reductase regulates cardiovascular function. *Proc Natl Acad Sci USA*. 2012;109:4314–4319. doi: 10.1073/pnas.1113319109
18. Hatzistergos KE, Paulino EC, Dulce RA, Takeuchi LM, Bellio MA, Kulandavelu S, Cao Y, Balkan W, Kanashiro-Takeuchi RM, Hare JM. S-nitrosoglutathione reductase deficiency enhances the proliferative expansion of adult heart progenitors and myocytes post myocardial infarction. *J Am Heart Assoc*. 2015;4:e001974. doi: 10.1161/JAHA.115.001974
19. Barouch LA, Harrison RW, Skaf MW, Rosas GO, Cappola TP, Kobeissi ZA, Hobai IA, Lemmon CA, Burnett AL, O'Rourke B, et al. Nitric oxide regulates the heart by spatial confinement of nitric oxide synthase isoforms. *Nature*. 2002;416:337–339. doi: 10.1038/416337a
20. Wei W, Li B, Hanes MA, Kakar S, Chen X, Liu L. S-nitrosylation from GSNOR deficiency impairs DNA repair and promotes hepatocarcinogenesis. *Sci Transl Med*. 2010;2:19ra13.
21. Gonzalez DR, Treuer AV, Castellanos J, Dulce RA, Hare JM. Impaired S-nitrosylation of the ryanodine receptor caused by xanthine oxidase activity contributes to calcium leak in heart failure. *J Biol Chem*. 2010;285:28938–28945. doi: 10.1074/jbc.M110.154948
22. Khan SA, Skaf MW, Harrison RW, Lee K, Minhas KM, Kumar A, Fradley M, Shoukas AA, Berkowitz DE, Hare JM. Nitric oxide regulation of myocardial contractility and calcium cycling: independent impact of neuronal and endothelial nitric oxide synthases. *Circ Res*. 2003;92:1322–1329. doi: 10.1161/01.RES.0000078171.52542.9E
23. Crow JP. Dichlorodihydrofluorescein and dihydrorhodamine 123 are sensitive indicators of peroxynitrite in vitro: implications for intracellular measurement of reactive nitrogen and oxygen species. *Nitric Oxide*. 1997;1:145–157. doi: 10.1006/niox.1996.0113
24. Strijdom H, Muller C, Lochner A. Direct intracellular nitric oxide detection in isolated adult cardiomyocytes: flow cytometric analysis using the fluorescent probe, diaminofluorescein. *J Mol Cell Cardiol*. 2004;37:897–902. doi: 10.1016/j.yjmcc.2004.05.018
25. Kim H, Bae S, Kim Y, Cho CH, Kim SJ, Kim YJ, Lee SP, Kim HR, Hwang YI, Kang JS, et al. Vitamin C prevents stress-induced damage on the heart caused by the death of cardiomyocytes, through down-regulation of the excessive production of catecholamine, TNF-alpha, and ROS production in Gulo(-/-)Vit C-Insufficient mice. *Free Radic Biol Med*. 2013;65:573–583.
26. Szklarczyk D, Gable AL, Lyon D, Junge A, Wyder S, Huerta-Cepas J, Simonovic M, Doncheva NT, Morris JH, Bork P, et al. STRING v11: protein-protein association networks with increased coverage, supporting functional discovery in genome-wide experimental datasets. *Nucleic Acids Res*. 2019;47:D607–D613. doi: 10.1093/nar/gky1131
27. Stillman IE, Karumanchi SA. The glomerular injury of preeclampsia. *J Am Soc Nephrol: JASN*. 2007;18:2281–2284. doi: 10.1681/ASN.2007020255
28. Kronborg C, Vittinghus E, Allen J, Knudsen UB. Excretion patterns of large and small proteins in pre-eclamptic pregnancies. *Acta Obstet Gynecol Scand*. 2011;90:897–902. doi: 10.1111/j.1600-0412.2011.01164.x
29. Novelli GP, Valensise H, Vasapollo B, Larciprete G, Altomare F, Di Pierro G, Casalino B, Galante A, Arduini D. Left ventricular concentric geometry as a risk factor in gestational hypertension. *Hypertension*. 2003;41:469–475. doi: 10.1161/01.HYP.0000058001.67791.0A
30. Schiattarella GG, Altamirano F, Tong D, French KM, Villalobos E, Kim SY, Luo X, Jiang N, May HI, Wang ZV, et al. Nitrosative stress drives heart failure with preserved ejection fraction. *Nature*. 2019;568:351–356. doi: 10.1038/s41586-019-1100-z
31. Karsdorp VH, van Vugt JM, van Geijn HP, Kostense PJ, Arduini D, Montenegro N, Todros T. Clinical significance of absent or reversed end diastolic velocity waveforms in umbilical artery. *Lancet*. 1994;344:1664–1668. doi: 10.1016/S0140-6736(94)90457-X
32. Groten T, Gebhard N, Kreienberg R, Schleussner E, Reister F, Huppertz B. Differential expression of VE-cadherin and VEGFR2 in placental syncytiotrophoblast during preeclampsia–new perspectives to explain the pathophysiology. *Placenta*. 2010;31:339–343. doi: 10.1016/j.placenta.2010.01.014
33. Grummer MA, Sullivan JA, Magness RR, Bird IM. Vascular endothelial growth factor acts through novel, pregnancy-enhanced receptor signalling pathways to stimulate endothelial nitric oxide synthase activity in uterine artery endothelial cells. *Biochem J*. 2009;417:501–511. doi: 10.1042/BJ20081013
34. Sanchez-Aranguren LC, Prada CE, Riano-Medina CE, Lopez M. Endothelial dysfunction and preeclampsia: role of oxidative stress. *Front Physiol*. 2014;5:372. doi: 10.3389/fphys.2014.00372
35. Phipps EA, Thadhani R, Benzing T, Karumanchi SA. Pre-eclampsia: pathogenesis, novel diagnostics and therapies. *Nat Rev Nephrol*. 2019;15:275–289. doi: 10.1038/s41581-019-0119-6
36. Kohr MJ, Sun J, Aponte A, Wang G, Gucek M, Murphy E, Steenbergen C. Simultaneous measurement of protein oxidation and S-nitrosylation during preconditioning and ischemia/reperfusion injury with resin-assisted capture. *Circ Res*. 2011;108:418–426. doi: 10.1161/CIRCRESAHA.110.232173
37. Xu L, Eu JP, Meissner G, Stamler JS. Activation of the cardiac calcium release channel (ryanodine receptor) by poly-S-nitrosylation. *Science*. 1998;279:234–237. doi: 10.1126/science.279.5348.234
38. Hubel CA, Kagan VE, Kisin ER, McLaughlin MK, Roberts JM. Increased ascorbate radical formation and ascorbate depletion in plasma from women with preeclampsia: implications for oxidative stress. *Free Radic Biol Med*. 1997;23:597–609. doi: 10.1016/S0891-5849(97)00010-5

39. Xu A, Vita JA, Keaney JF Jr. Ascorbic acid and glutathione modulate the biological activity of S-nitrosoglutathione. *Hypertension*. 2000;36:291–295.
40. Chen X, Touyz RM, Park JB, Schiffrin EL. Antioxidant effects of vitamins C and E are associated with altered activation of vascular NADPH oxidase and superoxide dismutase in stroke-prone SHR. *Hypertension*. 2001;38:606–611. doi: 10.1161/hy09t1.094005
41. Groebler LK, Wang XS, Kim HB, Shanu A, Hossain F, McMahon AC, Witting PK. Cosupplementation with a synthetic, lipid-soluble polyphenol and vitamin C inhibits oxidative damage and improves vascular function yet does not inhibit acute renal injury in an animal model of rhabdomyolysis. *Free Radic Biol Med*. 2012;52:1918–1928. doi: 10.1016/j.freeradbiomed.2012.02.011
42. Chung HS, Murray CI, Van Eyk JE. A proteomics workflow for dual labeling biotin switch assay to detect and quantify protein S-nitroylation. *Methods Mol Biol*. 2018;1747:89–101. doi: 10.1007/978-1-4939-7695-9_8
43. Forrester MT, Foster MW, Stamler JS. Assessment and application of the biotin switch technique for examining protein S-nitrosylation under conditions of pharmacologically induced oxidative stress. *J Biol Chem*. 2007;282:13977–13983. doi: 10.1074/jbc.M609684200
44. Chung HS, Murray CI, Venkatraman V, Crowgey EL, Rainer PP, Cole RN, Bomgarden RD, Rogers JC, Balkan W, Hare JM, et al. Dual labeling biotin switch assay to reduce bias derived from different cysteine subpopulations: a method to maximize S-nitrosylation detection. *Circ Res*. 2015;117:846–857. doi: 10.1161/CIRCRESAHA.115.307336
45. Massy ZA, Fumeron C, Borderie D, Tuppin P, Nguyen-Khoa T, Benoit MO, Jacquot C, Buisson C, Drueke TB, Ekindjian OG, et al. Increased plasma S-nitrosothiol concentrations predict cardiovascular outcomes among patients with end-stage renal disease: a prospective study. *J Am Soc Nephrol: JASN*. 2004;15:470–476. doi: 10.1097/01.asn.0000106716.22153.bb
46. Raijmakers MT, Zusterzeel PL, Steegers EA, Hectors MP, Demacker PN, Peters WH. Plasma thiol status in preeclampsia. *Obstet Gynecol*. 2000;95:180–184.
47. Pawloski JR, Hess DT, Stamler JS. Export by red blood cells of nitric oxide bioactivity. *Nature*. 2001;409:622–626. doi: 10.1038/35054560
48. Hlaing KH, Clement MV. Formation of protein S-nitrosylation by reactive oxygen species. *Free Radical Res*. 2014;48:996–1010. doi: 10.3109/10715762.2014.942842
49. Gomes SA, Rangel EB, Premer C, Dulce RA, Cao Y, Florea V, Balkan W, Rodrigues CO, Schally AV, Hare JM. S-nitrosoglutathione reductase (GSNOR) enhances vasculogenesis by mesenchymal stem cells. *Proc Natl Acad Sci USA*. 2013;110:2834–2839. doi: 10.1073/pnas.1220185110
50. Eddy AC, Bidwell GL III, George EM. Pro-angiogenic therapeutics for preeclampsia. *Biol Sex Differ*. 2018;9:36. doi: 10.1186/s13293-018-0195-5
51. Cindrova-Davies T, Sanders DA, Burton GJ, Charnock-Jones DS. Soluble FLT1 sensitizes endothelial cells to inflammatory cytokines by antagonizing VEGF receptor-mediated signalling. *Cardiovasc Res*. 2011;89:671–679. doi: 10.1093/cvr/cvq346
52. McCance DR, Holmes VA, Maresh MJ, Patterson CC, Walker JD, Pearson DW, Young IS, Diabetes and Pre-eclampsia Intervention Trial Study G. Vitamins C and E for prevention of pre-eclampsia in women with type 1 diabetes (DAPIT): a randomised placebo-controlled trial. *Lancet*. 2010;376:259–266. doi: 10.1016/S0140-6736(10)60630-7
53. Poston L, Briley AL, Seed PT, Kelly FJ, Shennan AH, and Vitamins in Pre-eclampsia Trial C. Vitamin C and vitamin E in pregnant women at risk for pre-eclampsia (VIP trial): randomised placebo-controlled trial. *Lancet*. 2006;367:1145–1154. doi: 10.1016/S0140-6736(06)68433-X
54. Roberts JM, Myatt L, Spong CY, Thom EA, Hauth JC, Leveno KJ, Pearson GD, Wapner RJ, Varner MW, Thorp JM, et al. Vitamins C and E to prevent complications of pregnancy-associated hypertension. *New Engl J Med*. 2010;362:1282–1291. doi: 10.1056/NEJMoa0908056
55. Roberts JM. The perplexing pregnancy disorder preeclampsia: what next? *Physiol Genomics*. 2018;50:459–467. doi: 10.1152/physiolgenomics.00017.2018

Supplemental Material

Table S1. List of proteins nitrosylated in GSNOR$^{-/-}$ placentas as compared to B6 placentas determined using dual-labelling mass spectrometry analysis. All SNOylated proteins were detected in at least 2 of 5 placentas/group. The number in the observation column is the number of placentas that showed expression of that particular SNOylated protein for that particular group.

label	Uniprot Accession	SNO site	Protein name	Log2 fold change vs background GSNOR$^{-/-}$	observations
HPDP	Q99L04	C10	Dehydrogenase/reductase SDR family member 1	23.05415	2
HPDP	Q99MN1	C432	Lysine--tRNA ligase	22.7331744	2
HPDP	Q8C7R4	C298	Ubiquitin-like modifier-activating enzyme 6 (Ubiquitin-activating enzyme 6)	22.10295762	2
HPDP	Q8VC70	C217	RNA-binding motif, single-stranded-interacting	21.71700633	2
HPDP	Q9D1I5	C168	Methylmalonyl-CoA epimerase, mitochondrial	21.24558726	2
HPDP	Q9JIG4	C419	Protein phosphatase 1 regulatory subunit 3F (R3F)	20.95864848	2
HPDP	Q9EPK7	C43	Exportin-7 (Exp7) (Ran-binding protein 16)	20.94875308	2
HPDP	Q9QUI0	C164	Transforming protein RhoA	20.91330254	2
HPDP	Q64514	C967	Tripeptidyl-peptidase 2 (TPP-2)	20.80956501	2
HPDP	O70400	C73	PDZ and LIM domain protein 1 (C-terminal LIM domain protein 1) (Elfin) (LIM domain protein CLP-	20.77362179	2
HPDP	P24270	C232	Catalase	20.71680767	2
HPDP	Q8BY89	C401	Choline transporter-like protein 2 (Solute carrier family 44 member 2)	20.70444271	2
HPDP	P61982	C112	14-3-3 protein gamma [Cleaved into: 14-3-3 protein gamma, N-terminally processed]	20.6712323	2
HPDP	Q8VDD5	C740	Myosin-9 (Cellular myosin heavy chain, type A) (Myosin heavy chain 9) (Myosin heavy chain, non-muscle IIa) (Non-muscle myosin heavy chain A) (NMMHC-A) (Non-muscle myosin heavy chain IIa) (NMMHC II-a) (NMMHC-IIA)	20.40955957	2
HPDP	P23198	C177	Chromobox protein homolog 3 (Heterochromatin protein 1 homolog gamma) (HP1 gamma) (M32) (Modifier 2 protein)	20.32635422	2

HPDP	O88844	C73	Isocitrate dehydrogenase [NADP] cytoplasmic (IDH)	20.28660949	2
HPDP	Q7TSI1	C464	Pleckstrin homology domain-containing family M member 1 (PH domain-containing family M member	20.27430909	2
HPDP	Q62419	C277	Endophilin-A2 (Endophilin-2) (SH3 domain protein 2B) (SH3 domain-containing GRB2-like protein 1)	20.1597845	2
HPDP	Q9Z2W0	C411	Aspartyl aminopeptidase	20.08429446	2
HPDP	Q9JJL8	C425	Serine--tRNA ligase, mitochondrial	20.04438709	2
HPDP	P21981	C553	Protein-glutamine gamma-glutamyltransferase 2	19.98447735	2
HPDP	Q91Y97	C158	Fructose-bisphosphate aldolase B	19.87182726	2
HPDP	Q9DBN5	C405	Lon protease homolog 2, peroxisomal	19.84850213	2
HPDP	Q8VC03	C421	Echinoderm microtubule-associated protein-like 3 (EMAP-3)	19.83187399	2
HPDP	P62242	C100	40S ribosomal protein S8	19.81349615	2
HPDP	A2ASS6	C29432	Titin	19.79460004	2
HPDP	Q63ZW7	C1406	InaD-like protein (Inadl protein) (Channel-interacting PDZ domain-containing protein) (Pals1-associated tight junction protein) (Protein associated to tight	19.70935729	2
HPDP	Q9CPV4	C45	Glyoxalase domain-containing protein 4	19.70621887	2
HPDP	Q68FD5	C1266	Clathrin heavy chain 1	19.69269741	2
HPDP	P54823	C390	Probable ATP-dependent RNA helicase DDX6	19.49673091	2
HPDP	Q91YL2	C32	E3 ubiquitin-protein ligase RNF126	19.48361501	2
HPDP	A6H8H2	C1083	DENN domain-containing protein 4C	19.41978765	3
HPDP	Q01853	C69,C77	Transitional endoplasmic reticulum ATPase (TER ATPase)	19.40789288	2
HPDP	B7ZMP1	C491	Xaa-Pro aminopeptidase 3 (X-Pro aminopeptidase 3)	19.29977564	2
HPDP	A2ASS6	C21780	Titin	19.12293298	2
HPDP	Q9ES28	C427	Rho guanine nucleotide exchange factor 7 (Beta-Pix) (PAK-interacting exchange factor beta) (p85SPR)	19.12161126	2
HPDP	A2ARV4	C2518	Low-density lipoprotein receptor-related protein 2 (LRP-2) (Glycoprotein 330) (gp330) (Megalin)	19.03682762	2

HPDP	Q6ZPJ3	C365	(E3-independent) E2 ubiquitin-conjugating enzyme UBE2O	18.97268389	3
HPDP	Q61655	C392	ATP-dependent RNA helicase DDX19A	18.88880189	2
HPDP	P14824	C669	Annexin A6 (67 kDa calelectrin) (Annexin VI) (Annexin-6) (Calphobindin-II) (CPB-II) (Chromobindin-20) (Lipocortin VI) (Protein III) (p68)	18.8218629	2
HPDP	Q5HZI1	C823	Microtubule-associated tumor suppressor 1 homolog (AT2 receptor-binding protein) (Angiotensin-II type 2 receptor-interacting protein) (Coiled-coiled tumor suppressor gene 1 protein) (Mitochondrial tumor suppressor 1 homolog)	18.76396509	2
HPDP	P53996	C141,C151	Cellular nucleic acid-binding protein (CNBP) (Zinc finger protein 9)	18.75122145	2
HPDP	Q921G6	C454	Leucine-rich repeat and calponin homology domain-containing protein 4	18.56565726	4
HPDP	P82343	C250	N-acylglucosamine 2-epimerase (AGE)	16.42343934	2
HPDP	Q91W50	C129	Cold shock domain-containing protein E1	16.0168855	2
TMT	Q7TNJ0	C89	Dendritic cell-specific transmembrane protein (DC-STAMP) (mDC-STAMP) (Dendrocyte-expressed seven transmembrane protein) (Transmembrane 7 superfamily member 4)	13.72900332	4
TMT	Q8R418	C306	Endoribonuclease Dicer	13.02362462	5
TMT	Q5FW85	C8	Extracellular matrix protein 2 (Tenonectin)	13.00944639	4
TMT	Q8BV57	C6	Soluble scavenger receptor cysteine-rich domain-containing protein SSC5D (Scavenger receptor cysteine-rich domain-containing protein LOC284297	12.76398811	5
TMT	P70277	C65	Alpha-N-acetylgalactosaminide alpha-2,6-sialyltransferase 2	12.6184686	5
TMT	Q3UAW9	C362	Transcription factor IIIB 50 kDa subunit (B-related factor 2) (BRF-2)	12.585631	5
TMT	Q8BLR9	C236	Hypoxia-inducible factor 1-alpha inhibitor	12.5665622	5

TMT	Q9JMG4	C8,C14	Sodium/potassium-transporting ATPase subunit beta-1-interacting protein 4 (Na(+)/K(+)-transporting ATPase subunit beta-1-interacting protein 4) (Protein FAM77A)	12.39302865	5
TMT	A1Z198	C330	NACHT, LRR and PYD domains-containing protein 1b allele 2	12.36513178	5
TMT	Q9DB60	C44,C47	Prostamide/prostaglandin F synthase (Prostamide/PG F synthase) (Prostamide/PGF synthase)	12.33380021	5
TMT	P57110	C677	A disintegrin and metalloproteinase with thrombospondin motifs 8 (ADAM-TS 8) (ADAM-	12.30280006	5
TMT	Q571F5	C271	SPRY domain-containing SOCS box protein 3 (SSB-	12.24478409	5
TMT	O09118	C17	Netrin-1	12.21630324	5
TMT	Q8C0W1	C818	Ankyrin repeat and MYND domain-containing protein	12.20108475	5
TMT	Q9DBP5	C20	UMP-CMP kinase	12.14459788	5
TMT	O35963	C48	Ras-related protein Rab-33B	12.08737651	5
TMT	A1L0T3	C138	Scavenger receptor cysteine-rich domain-containing group B protein (Four scavenger receptor cysteine-rich domains-containing protein) (S4D-SRCRB)	11.90176048	5
TMT	Q8CGM1	C1034	Adhesion G protein-coupled receptor B2 (Brain-specific angiogenesis inhibitor 2)	11.8771311	5
TMT	Q9WTN3	C738,C753	Sterol regulatory element-binding protein 1 (SREBP-1) (Sterol regulatory element-binding transcription factor 1) [Cleaved into: Processed sterol regulatory element-binding protein 1]	11.804481	5
TMT	Q8CJ70	C5,C18	Interleukin-19 (IL-19)	11.69925873	5
TMT	Q6DFV8	C217	von Willebrand factor D and EGF domain-containing protein	11.67417859	4

TMT	Q8CGK5	C81	Interferon lambda receptor 1 (IFN-lambda R1) (Cytokine receptor class-II member 12) (Cytokine receptor family 2 member 12) (CRF2-12) (Interleukin-28 receptor subunit alpha) (IL-28 receptor subunit alpha) (IL-28R-alpha) (IL-28RA)	11.61269071	5
TMT	Q4VAE3	C31	Transmembrane protein 65	11.41109714	5
TMT	Q9JLL3	C25	Tumor necrosis factor receptor superfamily member 19 (TRADE) (Toxicity and JNK inducer)	11.35771618	5
TMT	Q8K400	C293	Syntaxin-binding protein 5 (Lethal(2) giant larvae protein homolog 3) (Tomosyn-1)	11.21114736	5
TMT	Q9DC22	C200,C211	DDB1- and CUL4-associated factor 6 (IQ motif and WD repeat-containing protein 1) (Nuclear receptor interaction protein) (NRIP)	11.00286202	5
HPDP	Q9WUM3	C25	Coronin-1B (Coronin-2)	7.079871538	2
HPDP	Q8K274	C11	Ketosamine-3-kinase	5.271225169	2
HPDP	P46471	C389	26S proteasome regulatory subunit 7 (26S proteasome AAA-ATPase subunit RPT1) (Proteasome 26S subunit ATPase 2) (Protein MSS1)	5.062936789	2
HPDP	P62754	C12	40S ribosomal protein S6 (Phosphoprotein NP33)	4.714241907	2
HPDP	Q8R5H1	C264	Ubiquitin carboxyl-terminal hydrolase 15	4.569012373	2
HPDP	Q9JJ28	C1069	Protein flightless-1 homolog	4.407051634	2
HPDP	Q60992	C196,C197	Guanine nucleotide exchange factor VAV2 (VAV-2)	4.179681175	2
HPDP	Q9D662	C425	Protein transport protein Sec23B (SEC23-related protein B)	3.985939588	2
HPDP	O70439	C28	Syntaxin-7	3.955148625	3
HPDP	Q61768	C632	Kinesin-1 heavy chain (Conventional kinesin heavy chain) (Ubiquitous kinesin heavy chain) (UKHC)	3.760958689	2
HPDP	Q99JY3	C61	GTPase IMAP family member 4 (Immunity-associated nucleotide 1 protein) (IAN-1) (Immunity-associated protein 4)	3.614276688	2
HPDP	P99029	C200	Peroxiredoxin-5, mitochondrial	3.604855607	3

HPDP	Q8BZB2	C7	Phosphopantothenoylcysteine decarboxylase (PPC-	3.603461526	2
TMT	Q80VD1	C52	Protein FAM98B	3.259995258	5
TMT	Q80XD8	C9	Proline-rich acidic protein 1 (Pregnancy-specific uterine protein) (Uterine-specific proline-rich acidic	3.172829061	5
TMT	Q9ESD6	C54	CKLF-like MARVEL transmembrane domain-containing protein 7 (Chemokine-like factor superfamily member 7) (LNV)	2.984893682	5
HPDP	Q9CYN2	C26	Signal peptidase complex subunit 2	2.967611159	2
HPDP	P14131	C25	40S ribosomal protein S16	2.96535426	2
TMT	Q9JIP3	C12	Interleukin-17 receptor B (IL-17 receptor B) (IL-17RB) (IL-17 receptor homolog 1) (IL-17ER) (IL-17Rh1) (IL17Rh1) (Interleukin-17B receptor) (IL-17B receptor)	2.927411041	5
TMT	Q8BKK5	C263	Zinc finger protein 689	2.920765805	5
HPDP	Q99LG0	C24	Ubiquitin carboxyl-terminal hydrolase 16	2.800809396	2
HPDP	Q9Z1Z0	C802	General vesicular transport factor p115 (Protein USO1 homolog) (Transcytosis-associated protein) (TAP) (Vesicle-docking protein)	2.748838009	2
TMT	O08738	C259	Caspase-6 (CASP-6)	2.742606331	5
TMT	O88282	C381,C384	B-cell CLL/lymphoma 6 member B protein (Bcl6-associated zinc finger protein)	2.722924669	5
TMT	Q9Z0L3	C371	Otoconin-90 (Oc90) (Otoconin-95) (Oc95)	2.71298463	5
TMT	E9PZZ1	C653	PR domain zinc finger protein 13	2.547554782	4
HPDP	Q8VHX6	C2661	Filamin-C (FLN-C) (ABP-280-like protein) (ABP-L) (Actin-binding-like protein) (Filamin-2) (Gamma-	2.489804487	2
TMT	Q8BYA0	C665	Tubulin-specific chaperone D (Beta-tubulin cofactor D) (Tubulin-folding cofactor D)	2.48712789	5
HPDP	P53996	C120	Cellular nucleic acid-binding protein (CNBP) (Zinc finger protein 9)	2.455112234	2
HPDP	Q8CGB6	C548	Tensin-2	2.399443288	3
HPDP	P15105	C183	Glutamine synthetase (GS)	2.388341937	2

HPDP	Q9CQ58	C101	Prolactin-8A9 (Placental prolactin-like protein C2) (PLP-C2) (PRL-like protein C2) (Prolactin-like protein C-beta) (PLP C-beta)	2.373532499	3
TMT	Q60676	C221	Serine/threonine-protein phosphatase 5 (PP5)	2.35208233	5
HPDP	Q80XN0	C209	D-beta-hydroxybutyrate dehydrogenase, mitochondrial	2.33471439	3
HPDP	Q93092	C250	Transaldolase	2.325417107	2
TMT	Q5F2L2	C13	Alpha-(1,3)-fucosyltransferase 10	2.317276958	5
TMT	O09008	C18	Beta-1,3-N-acetylglucosaminyltransferase manic fringe	2.305226515	4
HPDP	P17742	C67	Peptidyl-prolyl cis-trans isomerase A (PPIase A)	2.291684824	2
HPDP	A2ASS6	C21834	Titin	2.248744617	2
HPDP	O08573	C258	Galectin-9 (Gal-9)	2.210136624	2
HPDP	Q9D1Q6	C92	Endoplasmic reticulum resident protein 44 (ER protein 44) (ERp44) (Thioredoxin domain-containing	2.147055114	2
HPDP	P53995	C988	Anaphase-promoting complex subunit 1 (APC1) (Cyclosome subunit 1) (Mitotic checkpoint regulator) (Testis-specific gene 24 protein)	2.039981245	2
HPDP	P70441	C201	Na(+)/H(+) exchange regulatory cofactor NHE-RF1 (NHERF-1) (Ezrin-radixin-moesin-binding phosphoprotein 50) (EBP50) (Regulatory cofactor of Na(+)/H(+) exchanger) (Sodium-hydrogen exchanger regulatory factor 1) (Solute carrier family 9 isoform A3 regulatory factor 1)	1.988263764	2
TMT	Q9QXW9	C209	Large neutral amino acids transporter small subunit 2 (L-type amino acid transporter 2) (mLAT2) (Solute carrier family 7 member 8)	1.963679629	5
HPDP	P60766	C157	Cell division control protein 42 homolog (G25K GTP-binding protein)	1.950445964	2
TMT	Q66X22	C891,C907,C908	NACHT, LRR and PYD domains-containing protein 9B (NALP-delta)	1.935676951	4

HPDP	P01027	C559	Complement C3 (HSE-MSF) [Cleaved into: Complement C3 beta chain; C3-beta-c (C3bc); Complement C3 alpha chain; C3a anaphylatoxin; Acylation stimulating protein (ASP) (C3adesArg); Complement C3b alpha' chain; Complement C3c alpha' chain fragment 1; Complement C3dg fragment; Complement C3g fragment; Complement C3d fragment; Complement C3f fragment; Complement C3c alpha' chain fragment 2]	1.93095258	2
HPDP	O88986	C26	2-amino-3-ketobutyrate coenzyme A ligase, mitochondrial (AKB ligase)	1.921218785	2
HPDP	P35979	C141	60S ribosomal protein L12	1.912774567	2
HPDP	P63017	C603	Heat shock cognate 71 kDa protein (Heat shock 70 kDa protein 8)	1.900311126	2
TMT	Q8BLY7	C180	Hermansky-Pudlak syndrome 6 protein homolog (Ruby-eye protein) (Ru)	1.878707928	5
HPDP	Q7TMW6	C270	Cytosolic iron-sulfur assembly component 3 (Cytosolic Fe-S cluster assembly factor NARFL) (Iron-only hydrogenase-like protein 1) (IOP1) (Nuclear prelamin A recognition factor-like protein)	1.847995032	2
HPDP	Q60864	C461	Stress-induced-phosphoprotein 1 (STI1) (mSTI1) (Hsc70/Hsp90-organizing protein) (Hop)	1.832341765	2
HPDP	A2ASS6	C13473	Titin	1.794763146	2
TMT	Q8K4G1	C1393,C1403	Latent-transforming growth factor beta-binding protein 4 (LTBP-4)	1.71923574	5
HPDP	O89053	C24	Coronin-1A (Coronin-like protein A) (Clipin-A) (Coronin-like protein p57) (Tryptophan aspartate-containing coat protein) (TACO)	1.710727777	2
TMT	Q7TPG7	C107	Protein FAM19A2 (Chemokine-like protein TAFA-2)	1.706388912	5
HPDP	Q9QUM9	C167	Proteasome subunit alpha type-6	1.696998107	2
HPDP	Q80X90	C1434	Filamin-B (FLN-B) (ABP-280-like protein) (Actin-binding-like protein) (Beta-filamin)	1.668503957	2

HPDP	A2ASS6	C33458	Titin	1.640392354	2
HPDP	Q61553	C481	Fascin (Singed-like protein)	1.636609875	2
HPDP	P61514	C48	60S ribosomal protein L37a	1.593487828	2
HPDP	P61161	C221	Actin-related protein 2 (Actin-like protein 2)	1.554988721	2
TMT	P46097	C91	Synaptotagmin-2 (Inositol polyphosphate-binding protein) (IP4-binding protein) (IP4BP) (Synaptotagmin II) (SytII)	1.554328226	5
HPDP	Q8VDF3	C347	Death-associated protein kinase 2 (DAP kinase 2)	1.52416734	2
HPDP	Q78PY7	C152	Staphylococcal nuclease domain-containing protein 1	1.520546542	2
HPDP	Q8BTM8	C2582	Filamin-A (FLN-A) (Actin-binding protein 280) (ABP-280) (Alpha-filamin) (Endothelial actin-binding protein) (Filamin-1) (Non-muscle filamin)	1.416572906	2
HPDP	Q64514	C150	Tripeptidyl-peptidase 2 (TPP-2)	1.399757173	2
HPDP	Q09324	C100	Beta-1,3-galactosyl-O-glycosyl-glycoprotein beta-1,6-N-acetylglucosaminyltransferase	1.397345074	2
HPDP	Q9CY97	C12	RNA polymerase II subunit A C-terminal domain phosphatase SSU72 (CTD phosphatase SSU72)	1.39424147	2
HPDP	P39054	C607	Dynamin-2	1.374247771	2
HPDP	P68040	C153	Receptor of activated protein C kinase 1 (12-3) (Guanine nucleotide-binding protein subunit beta-2-like 1) (Receptor for activated C kinase) (Receptor of activated protein kinase C 1) (p205) [Cleaved into: Receptor of activated protein C kinase 1, N-terminally processed (Guanine nucleotide-binding protein subunit beta-2-like 1, N-terminally processed)]	1.359971038	3
HPDP	P26039	C956	Talin-1	1.354647422	2
HPDP	O70133	C440	ATP-dependent RNA helicase A	1.344512262	2
HPDP	Q80X90	C991	Filamin-B (FLN-B) (ABP-280-like protein) (Actin-binding-like protein) (Beta-filamin)	1.337916373	2

HPDP	Q99K30	C546	Epidermal growth factor receptor kinase substrate 8-like protein 2 (EPS8-like protein 2) (Epidermal growth factor receptor pathway substrate 8-related protein 2) (EPS8-related protein 2)	1.332404247	2
HPDP	P62908	C134	40S ribosomal protein S3	1.319576402	2
HPDP	E9Q394	C609	A-kinase anchor protein 13 (AKAP-13) (AKAP-Lbc)	1.277028431	3
TMT	P02798	C33	Metallothionein-2 (MT-2) (Metallothionein-II) (MT-	1.266697299	4
HPDP	P62908	C119	40S ribosomal protein S3	1.254357417	2
HPDP	Q99LR1	C40	Monoacylglycerol lipase ABHD12	1.23650774	2
HPDP	P46471	C377	26S proteasome regulatory subunit 7 (26S proteasome AAA-ATPase subunit RPT1) (Proteasome 26S subunit ATPase 2) (Protein MSS1)	1.228249064	2
HPDP	P28653	C77	Biglycan (Bone/cartilage proteoglycan I) (PG-S1)	1.222294589	2
HPDP	O35075	C243	Down syndrome critical region protein 3 homolog (Down syndrome critical region protein A homolog)	1.212332349	2
HPDP	P61161	C11	Actin-related protein 2 (Actin-like protein 2)	1.199108066	2
HPDP	P01837	C106	Immunoglobulin kappa constant (Ig kappa chain C region MOPC 21)	1.19005698	2
TMT	Q61554	C1099	Fibrillin-1 [Cleaved into: Asprosin]	1.179059728	3
HPDP	Q80X90	C1280	Filamin-B (FLN-B) (ABP-280-like protein) (Actin-binding-like protein) (Beta-filamin)	1.169029965	2
HPDP	D3YYU8	C149	Obscurin-like protein 1	1.102544141	2
HPDP	P53996	C159	Cellular nucleic acid-binding protein (CNBP) (Zinc finger protein 9)	1.087825704	2
TMT	P56546	C18	C-terminal-binding protein 2 (CtBP2)	1.074827722	3
HPDP	Q9JJ28	C576	Protein flightless-1 homolog	1.067369682	2
HPDP	Q80X90	C604	Filamin-B (FLN-B) (ABP-280-like protein) (Actin-binding-like protein) (Beta-filamin)	1.066918314	2
TMT	Q811Q4	C430	Disintegrin and metalloproteinase domain-containing protein 29 (ADAM 29)	1.066068555	3
HPDP	A2ASS6	C20340	Titin	1.062863942	2

HPDP	Q9DBF1	C522	Alpha-aminoadipic semialdehyde dehydrogenase (Alpha-AASA dehydrogenase)	1.062682493	2
HPDP	P52480	C49	Pyruvate kinase PKM	1.060038804	2
HPDP	Q9D1A2	C300	Cytosolic non-specific dipeptidase	1.044536941	2
TMT	Q6R5P0	C743	Toll-like receptor 11 (Toll-like receptor 12)	1.020796529	4
HPDP	Q8K4I3	C563	Rho guanine nucleotide exchange factor 6 (Alpha-PIX) (Rac/Cdc42 guanine nucleotide exchange factor	1.015633881	2
HPDP	P31230	C159	Aminoacyl tRNA synthase complex-interacting multifunctional protein 1 (Multisynthase complex auxiliary component p43) [Cleaved into: Endothelial monocyte-activating polypeptide 2 (EMAP-2) (Endothelial monocyte-activating polypeptide II) (EMAP-II) (Small inducible cytokine subfamily E	0.995152319	2
HPDP	Q8VD04	C104	GRIP1-associated protein 1 (GRASP-1) (HCMV-interacting protein) [Cleaved into: GRASP-1 C-terminal chain (30kDa C-terminus form)]	0.963548687	3
HPDP	Q8R146	C309	Acylamino-acid-releasing enzyme (AARE)	0.921391689	2
TMT	P15920	C315	V-type proton ATPase 116 kDa subunit a isoform 2 (V-ATPase 116 kDa isoform a2) (Immune suppressor factor J6B7) (ISF) (Lysosomal H(+)-transporting ATPase V0 subunit a2) (ShIF) (Vacuolar proton translocating ATPase 116 kDa subunit a isoform 2)	0.912327311	2
HPDP	P12399	C103	Protein CTLA-2-alpha (Cytotoxic T-lymphocyte-associated protein 2-alpha)	0.908725648	2
HPDP	P41105	C13	60S ribosomal protein L28	0.866404857	2
HPDP	Q8BGF6	C98	ELMO domain-containing protein 2	0.863404858	2
HPDP	Q9DCM0	C34	Persulfide dioxygenase ETHE1, mitochondrial	0.859102687	2
HPDP	O54988	C1136	STE20-like serine/threonine-protein kinase (STE20-like kinase) (mSLK)	0.854916117	2
HPDP	D3Z6Q9	C425	Bridging integrator 2	0.828034499	2

HPDP	P11983	C357	T-complex protein 1 subunit alpha (TCP-1-alpha) (CCT-alpha) (Tailless complex polypeptide 1A) (TCP-1-A) (Tailless complex polypeptide 1B) (TCP-1-B)	0.815170441	2
HPDP	P62874	C25	Guanine nucleotide-binding protein G(I)/G(S)/G(T) subunit beta-1 (Transducin beta chain 1)	0.777801095	2
HPDP	Q9JHW9	C164	Aldehyde dehydrogenase family 1 member A3	0.775764306	2
HPDP	Q64213	C279	Splicing factor 1 (CW17) (Mammalian branch point-binding protein) (BBP) (mBBP) (Transcription factor ZFM1) (mZFM) (Zinc finger gene in MEN1 locus) (Zinc finger protein 162)	0.727433087	2
HPDP	Q80X90	C450,C455	Filamin-B (FLN-B) (ABP-280-like protein) (Actin-binding-like protein) (Beta-filamin)	0.723299502	2
HPDP	P21981	C370	Protein-glutamine gamma-glutamyltransferase 2	0.702284056	2
HPDP	P62983	C144,C155	Ubiquitin-40S ribosomal protein S27a (Ubiquitin carboxyl extension protein 80) [Cleaved into: Ubiquitin; 40S ribosomal protein S27a]	0.697668035	2
HPDP	Q8VDP3	C82	[F-actin]-monooxygenase MICAL1	0.684887184	2
HPDP	Q91W34	C12	RUS1 family protein C16orf58 homolog	0.643663222	2

Table S2. List of proteins nitrosylated in GSNOR$^{-/-}$ placentas as compared to B6 placentas and B6- and GSNOR$^{-/-}$ placentas treated with ascorbate. All SNOylated proteins were detected in at least 2 of 5 placentas/group. The number in the observation column is the number of placentas that showed expression of that particular SNOylated protein for that

label	Uniprot Accession	SNO site	Protein name	Log2 fold change vs background GSNOR$^{-/-}$	observations
TMT	Q8R418	C306	Endoribonuclease Dicer	13.0236246	5
TMT	Q5FW85	C8	Extracellular matrix protein 2 (Tenonectin)	13.0094464	4
TMT	Q8BV57	C6	Soluble scavenger receptor cysteine-rich domain-containing protein SSC5D (Scavenger receptor cysteine-rich domain-containing protein LOC284297 homolog)	12.7639881	5
TMT	P70277	C65	Alpha-N-acetylgalactosaminide alpha-2,6-sialyltransferase 2	12.6184686	5
TMT	Q9JMG4	C8,C14	Sodium/potassium-transporting ATPase subunit beta-1-interacting protein 4 (Na(+)/K(+)-transporting ATPase subunit beta-1-interacting protein 4) (Protein FAM77A)	12.3930287	5
TMT	A1Z198	C330	NACHT, LRR and PYD domains-containing protein 1b allele 2	12.3651318	5
TMT	Q9DB60	C44,C47	Prostamide/prostaglandin F synthase (Prostamide/PG F synthase) (Prostamide/PGF synthase)	12.3338002	5
TMT	P57110	C677	A disintegrin and metalloproteinase with thrombospondin motifs 8 (ADAM-TS 8) (ADAM-TS8) (ADAMTS-8)	12.3028001	5
TMT	Q571F5	C271	SPRY domain-containing SOCS box protein 3 (SSB-3)	12.2447841	5
TMT	O09118	C17	Netrin-1	12.2163032	5
TMT	Q8C0W1	C818	Ankyrin repeat and MYND domain-containing protein 1	12.2010848	5
TMT	Q9DBP5	C20	UMP-CMP kinase	12.1445979	5
TMT	O35963	C48	Ras-related protein Rab-33B	12.0873765	5
TMT	A1L0T3	C138	Scavenger receptor cysteine-rich domain-containing group B protein (Four scavenger receptor cysteine-rich domains-containing protein) (S4D-SRCRB)	11.9017605	5

TMT	Q8CGM1	C1034	Adhesion G protein-coupled receptor B2 (Brain-specific angiogenesis inhibitor 2)	11.8771311	5
TMT	Q9WTN3	C738,C753	Sterol regulatory element-binding protein 1 (SREBP-1) (Sterol regulatory element-binding transcription factor 1) [Cleaved into: Processed sterol regulatory element-binding protein 1]	11.804481	5
TMT	Q8CJ70	C5,C18	Interleukin-19 (IL-19)	11.6992587	5
TMT	Q6DFV8	C217	von Willebrand factor D and EGF domain-containing protein	11.6741786	4
TMT	Q8CGK5	C81	Interferon lambda receptor 1 (IFN-lambda R1) (Cytokine receptor class-II member 12) (Cytokine receptor family 2 member 12) (CRF2-12) (Interleukin-28 receptor subunit alpha) (IL-28 receptor subunit alpha) (IL-28R-alpha) (IL-28RA)	11.6126907	5
TMT	Q4VAE3	C31	Transmembrane protein 65	11.4110971	5
TMT	Q9JLL3	C25	Tumor necrosis factor receptor superfamily member 19 (TRADE) (Toxicity and JNK inducer)	11.3577162	5
TMT	Q8K400	C293	Syntaxin-binding protein 5 (Lethal(2) giant larvae protein homolog 3) (Tomosyn-1)	11.2111474	5
TMT	Q9DC22	C200,C211	DDB1- and CUL4-associated factor 6 (IQ motif and WD repeat-containing protein 1) (Nuclear receptor interaction protein) (NRIP)	11.002862	5
TMT	Q80VD1	C52	Protein FAM98B	3.25999526	5
TMT	Q80XD8	C9	Proline-rich acidic protein 1 (Pregnancy-specific uterine protein) (Uterine-specific proline-rich acidic protein)	3.17282906	5
TMT	Q9ESD6	C54	CKLF-like MARVEL transmembrane domain-containing protein 7 (Chemokine-like factor superfamily member 7) (LNV)	2.98489368	5
TMT	Q9JIP3	C12	Interleukin-17 receptor B (IL-17 receptor B) (IL-17RB) (IL-17 receptor homolog 1) (IL-17ER) (IL-17Rh1) (IL17Rh1) (Interleukin-17B receptor) (IL-17B receptor)	2.92741104	5
TMT	Q8BKK5	C263	Zinc finger protein 689	2.9207658	5
TMT	O08738	C259	Caspase-6 (CASP-6)	2.74260633	5
TMT	O88282	C381,C384	B-cell CLL/lymphoma 6 member B protein (Bcl6-associated zinc finger protein)	2.72292467	5

TMT	Q9Z0L3	C371	Otoconin-90 (Oc90) (Otoconin-95) (Oc95)	2.71298463	5
TMT	E9PZZ1	C653	PR domain zinc finger protein 13	2.54755478	4
TMT	Q8BYA0	C665	Tubulin-specific chaperone D (Beta-tubulin cofactor D) (Tubulin-folding cofactor D)	2.48712789	5
TMT	Q60676	C221	Serine/threonine-protein phosphatase 5 (PP5)	2.35208233	5
TMT	Q5F2L2	C13	Alpha-(1,3)-fucosyltransferase 10	2.31727696	5
TMT	O09008	C18	Beta-1,3-N-acetylglucosaminyltransferase manic fringe	2.30522651	4
HPDP	A2ASS6	C21834	Titin	2.24874462	2
TMT	Q9QXW9	C209	Large neutral amino acids transporter small subunit 2 (L-type amino acid transporter 2) (mLAT2) (Solute carrier family 7	1.96367963	5
TMT	Q66X22	C891,C907,C908	NACHT, LRR and PYD domains-containing protein 9B (NALP-delta)	1.93567695	4
TMT	Q8BLY7	C180	Hermansky-Pudlak syndrome 6 protein homolog (Ruby-eye protein) (Ru)	1.87870793	5
TMT	Q8K4G1	C1393,C1403	Latent-transforming growth factor beta-binding protein 4 (LTBP-4)	1.71923574	5
TMT	Q7TPG7	C107	Protein FAM19A2 (Chemokine-like protein TAFA-2)	1.70638891	5
TMT	P46097	C91	Synaptotagmin-2 (Inositol polyphosphate-binding protein) (IP4-binding protein) (IP4BP) (Synaptotagmin II) (SytII)	1.55432823	5
TMT	P02798	C33	Metallothionein-2 (MT-2) (Metallothionein-II) (MT-II)	1.2666973	4
HPDP	P01837	C106	Immunoglobulin kappa constant (Ig kappa chain C region MOPC 21)	1.19005698	2
TMT	Q61554	C1099	Fibrillin-1 [Cleaved into: Asprosin]	1.17905973	3
TMT	P56546	C18	C-terminal-binding protein 2 (CtBP2)	1.07482772	3
TMT	Q811Q4	C430	Disintegrin and metalloproteinase domain-containing protein 29 (ADAM 29)	1.06606856	3
TMT	Q6R5P0	C743	Toll-like receptor 11 (Toll-like receptor 12)	1.02079653	4

TMT	P15920	C315	V-type proton ATPase 116 kDa subunit a isoform 2 (V-ATPase 116 kDa isoform a2) (Immune suppressor factor J6B7) (ISF) (Lysosomal H(+)-transporting ATPase V0 subunit a2) (ShIF) (Vacuolar proton translocating ATPase 116 kDa subunit a isoform 2)	0.91232731	2

Table S3. List of peptides identified using mass spectrometry analysis.				
Gene	Protein	SNO site	Peptide Modified Sequence	orginal label
1433G_MOUSE	P61982	C112	NC[+57]SETQYESK	HPDP
A16A1_MOUSE	Q571I9	C249	VAFC[+57]GAVEEGR	HPDP
AAK1_MOUSE	Q3UHJ0	C319	EC[+57]PVPNVQNSPIPAK	HPDP
AATM_MOUSE	P05202	C295	VGAFTVVC[+329]K	IodoTMT6
ABD12_MOUSE	Q99LR1	C40	C[+125]AASGSSSSGSAAAALDADC[+57]SLK	HPDP
ABI1_MOUSE	Q8CBW3	C33	VADYC[+57]ENNYIQATDK	HPDP
ABLM1_MOUSE	Q8K4G5	C146	NGDYLC[+57]TLDYQR	HPDP
ACINU_MOUSE	Q9JIX8	C513	SSLPEC[+57]STQK	HPDP
ACOC_MOUSE	P28271	C392	DFESC[+57]LGAK	HPDP
ACTG_MOUSE	P63260	C17	EEEIAALVIDNGSGMC[+329]K	IodoTMT6
ACTN1_MOUSE	Q7TPR4	C480	IC[+57]DQWDNLGALTQK	HPDP
ACTN4_MOUSE	Q7TPR4	C860	ELPPDQAEYC[+329]IAR	IodoTMT6
ADA29_MOUSE	Q811Q4	C430	EQC[+125]DC[+125]GSLRNC[+125]TNDLC[+329]CMSNCTLST	IodoTMT6
AEDO_MOUSE	Q6PDY2	C225	EASGSAC[+57]DLPR	HPDP
AGK_MOUSE	Q9ESW4	C72	ATVFLNPAAC[+57]K	HPDP
AGM1_MOUSE	Q9CYR6	C200	AFVDLTNQVSC[+57]SGDVK	HPDP
AGM1_MOUSE	Q9CYR6	C348	VPVYC[+57]TK	HPDP
AGRB2_MOUSE	Q8CGM1	C1034	FLC[+329]LGWGLPALVVAVSVGFTRTK	IodoTMT6
AGRG4_MOUSE	B7ZCC9	C2279,C2281	GQGM[+16]DAIFHVPYSC[+329]AC[+329]WVIIKAKSSLESVEL	IodoTMT6
AHDC1_MOUSE	Q6PAL7	C788	NC[+57]GFQGTEAR	HPDP
AIFM1_MOUSE	Q9Z0X1	C440	SNIWVAGDAAC[+57]FYDIK	HPDP
AIMP1_MOUSE	P31230	C159	IGC[+57]IVTAK	HPDP
AIMP2_MOUSE	Q8R010	C168	C[+57]FGEQAR	HPDP
AKA10_MOUSE	O88845	C110	SC[+57]LDYQTQETK	HPDP
AKA12_MOUSE	Q9WTQ5	C1113	ATTC[+57]QVIK	HPDP
AKP13_MOUSE	E9Q394	C1644	QQGFNYC[+57]TSAISSPLTK	HPDP
AKP13_MOUSE	E9Q394	C417	EGLPSC[+57]GNR	HPDP
AKP13_MOUSE	E9Q394	C609	VLGGQEPDTSIAGFC[+57]K	HPDP
AL1A3_MOUSE	Q9JHW9	C164	TIPTDDNVVC[+57]FTR	HPDP
AL3A2_MOUSE	P47739	C229	DC[+125]DLDVAC[+329]R	IodoTMT6

AL7A1_MOUSE	Q9DBF1	C522	STC[+57]TINYSTSLPLAQGIK	HPDP
ALBU_MOUSE	P07724	C289	YMC[+57]ENQATISSK	HPDP
ALBU_MOUSE	P07724	C294	YM[+16]C[+57]ENQATISSK	HPDP
ALBU_MOUSE	P07724	C416	TNC[+57]DLYEK	HPDP
ALBU_MOUSE	P07724	C58	C[+57]SYDEHAK	HPDP
ALBU_MOUSE	P07724	C591	DTC[+57]FSTEGPNLVTR	HPDP
ALBU_MOUSE	P07724	C77, C86	TC[+57]VADESAANC[+57]DK	HPDP
ALBU_MOUSE	P07724	C289	YMC[+329]ENQATISSK	IodoTMT6
ALBU_MOUSE	P07724	C591	AADKDTC[+329]FSTEGPNLVTR	IodoTMT6
ALBU_MOUSE	P07724	C77,C86	TC[+329]VADESAANC[+329]DK	IodoTMT6
ALDH2_MOUSE	P47738	C68	TFPTVNPSTGEVIC[+57]QVAEGNK	HPDP
ALDOA_MOUSE	P05064	C339	ALANSLAC[+57]QGK	HPDP
ALDOA_MOUSE	P05064	C339	RALANSLAC[+57]QGK	HPDP
ALDOB_MOUSE	Q91Y97	C158	IADQC[+57]PSSLAIQENANALAR	HPDP
ALDOB_MOUSE	Q91Y97	C269	TVPAAVPGIC[+57]FLSGGMSEEDATLNLNAINR	HPDP
AMPL_MOUSE	Q9CPY7	C445	QVIDC[+57]QLADVNNLGK	HPDP
ANKL2_MOUSE	Q6P1H6	C462	TPEEVIC[+57]ER	HPDP
ANMY1_MOUSE	Q8C0W1	C818	ALYLSKRAELAPC[+329]HR	IodoTMT6
ANR17_MOUSE	Q99NH0	C2059	NSPLDC[+57]GSASPNK	HPDP
ANX11_MOUSE	P97384	C224	GFGTDEQAIIDC[+57]LGSR	HPDP
ANXA4_MOUSE	P97429	C141	SLEEDIC[+329]SDTSFMFQR	IodoTMT6
ANXA6_MOUSE	P14824	C669	ALLALC[+57]GGED	HPDP
AP1B1_MOUSE	O35643	C863	DC[+57]PLNTEAASNK	HPDP
AP1G1_MOUSE	P22892	C400	ADC[+57]ASGIFLAAEK	HPDP
AP2A2_MOUSE	P17427	C902	TTQIGC[+57]LLR	HPDP
APC1_MOUSE	P53995	C988	QAC[+57]EGNLPR	HPDP
APEH_MOUSE	Q8R146	C309	C[+125]ELLSDESLAVC[+57]SPR	HPDP
AQP1_MOUSE	Q02013	C189	DLGGSAPLAIGLSVALGHLLAIDYTGC[+329]GINPAR	IodoTMT6
ARAF_MOUSE	P04627	C595	TQADELPAC[+57]LLSAAR	HPDP
ARFG1_MOUSE	Q9EPJ9	C350	SPSSDSWTC[+57]ADASTGR	HPDP
ARHG6_MOUSE	Q8K4I3	C25	TVC[+57]DPEEFLK	HPDP
ARHG6_MOUSE	Q8K4I3	C563	TSSSSC[+57]STHSSFSSTGQPR	HPDP

ARHG7_MOUSE	Q9ES28	C427	NLSAQC[+57]QEVR	HPDP
ARHG7_MOUSE	Q9ES28	C700	VIEAYC[+57]TSAK	HPDP
ARHGC_MOUSE	Q8R4H2	C1325	TGTGDIATC[+57]DSPR	HPDP
ARP2_MOUSE	P61161	C11	VVVC[+57]DNGTGFVK	HPDP
ARP2_MOUSE	P61161	C11	KVVVC[+57]DNGTGFVK	HPDP
ARP2_MOUSE	P61161	C221	LC[+57]YVGYNIEQEQK	HPDP
ARP3_MOUSE	Q99JY9	C408	DYEEIGPSIC[+57]R	HPDP
ARP3_MOUSE	Q99JY9	C408	KDYEEIGPSIC[+57]R	HPDP
ARP3_MOUSE	Q99JY9	C8, C12	LPAC[+57]VVDC[+57]GTGYTK	HPDP
ARP3_MOUSE	Q99JY9	C408	KDYEEIGPSIC[+329]R	IodoTMT6
ARP3_MOUSE	Q99JY9	C408	DYEEIGPSIC[+329]R	IodoTMT6
ARRB1_MOUSE	Q8BWG8	C150	AFC[+57]AENLEEK	HPDP
AS3MT_MOUSE	Q91WU5	C33	TSADLQTNAC[+329]VTR	IodoTMT6
ASAH1_MOUSE	Q9WV54	C291	SGEGC[+57]VITR	HPDP
AT131_MOUSE	Q9EPE9	C333	SPQENLVPC[+57]DVLLLR	HPDP
AT1A1_MOUSE	Q8VDN2	C211	IISANGC[+57]K	HPDP
AT2A2_MOUSE	O55143	C377	VEGDTC[+57]SLNEFSITGSTYAPIGEVQK	HPDP
AT2A2_MOUSE	O55143	C669	DAC[+57]LNAR	HPDP
ATS8_MOUSE	P57110	C677	GQC[+329]VKAGCDHVVNSPKK	IodoTMT6
BAG3_MOUSE	Q9JLV1	C185	SQSPAASDC[+57]SSSSSSASLPSSGR	HPDP
BAG3_MOUSE	Q9JLV1	C154	QC[+329]GQMPATATTAAAQPPTAHGPER	IodoTMT6
BCL6B_MOUSE	O88282	C381,C384	IHSGEKPYKC[+329]ETC[+329]GSRFVQVAHLR	IodoTMT6
BDH_MOUSE	Q80XN0	C209	SPYC[+57]ITK	HPDP
BIN2_MOUSE	D3Z6Q9	C425	ASGSGSC[+57]NAPGSPEGSSQLC[+125]SPR	HPDP
BOLA1_MOUSE	Q9D8S9	C126	ENPQLDISPPC[+57]LGGSK	HPDP
BRF2_MOUSE	Q3UAW9	C362	RASPTPLLPPC[+329]MLKPPKR	IodoTMT6
CA123_MOUSE	Q8BHG2	C102	TIVEFEC[+57]R	HPDP
CACL1_MOUSE	Q8R0X2	C370	AGDELAYNSPSAC[+57]ASSR	HPDP
CALR_MOUSE	P14211	C105	HEQNIDC[+57]GGGYVK	HPDP
CALR_MOUSE	P14211	C137	DMHGDSEYNIMFGPDIC[+329]GPGTKK	IodoTMT6
CALR_MOUSE	P14211	C137	DMHGDSEYNIMFGPDIC[+329]GPGTK	IodoTMT6
CAND2_MOUSE	Q6ZQ73	C1138	LATLC[+329]PAPVLQRVDRLIEPLR	IodoTMT6

CAP1_MOUSE	P40124	C426	NSLDC[+57]EIVSAK	HPDP
CAPZB_MOUSE	P47757	C62	DYLLC[+57]DYNR	HPDP
CARL1_MOUSE	Q6EDY6	C712	AC[+57]GGDAIQEDLK	HPDP
CASP6_MOUSE	O08738	C259	QVPC[+329]FASM[+16]LTKKLHFCPKPSK	IodoTMT6
CATA_MOUSE	P24270	C232	LVNADGEAVYC[+57]K	HPDP
CATA_MOUSE	P24270	C425	SALEHSVQC[+57]AVDVK	HPDP
CATA_MOUSE	P24270	C393	DGPMC[+329]MHDNQGGAPNYYPNSFSAPEQQR	IodoTMT6
CATB_MOUSE	P10605	C211	SC[+57]EAGYSPSYK	HPDP
CATB_MOUSE	P10605	C211	SC[+329]EAGYSPSYKEDK	IodoTMT6
CATB_MOUSE	P10605	C211	SC[+329]EAGYSPSYK	IodoTMT6
CATZ_MOUSE	Q9WUU7	C156	HGIPDETC[+329]NNYQAK	IodoTMT6
CBX3_MOUSE	P23198	C177	LTWHSC[+57]PEDEAQ	HPDP
CDC23_MOUSE	Q8BGZ4	C532	LWDEASTC[+57]AQK	HPDP
CDC42_MOUSE	P60766	C157	YVEC[+57]SALTQK	HPDP
CEAM5_MOUSE	Q3UKK2	C909	C[+57]QLSIDPVWR	HPDP
CERU_MOUSE	Q61147	C239	TFC[+57]SEPEK	HPDP
CERU_MOUSE	Q61147	C694	GTFDVEC[+57]LTTDHYTGGM[+16]K	HPDP
CERU_MOUSE	Q61147	C694	GTFDVEC[+57]LTTDHYTGGMK	HPDP
CERU_MOUSE	Q61147	C713	YTVNQC[+57]QR	HPDP
CERU_MOUSE	Q61147	C173	ADDKVLPGQQYVYVLHANEPSPGEGDSNC[+329]VTR	IodoTMT6
CERU_MOUSE	Q61147	C173	VLPGQQYVYVLHANEPSPGEGDSNC[+329]VTR	IodoTMT6
CERU_MOUSE	Q61147	C239	TFC[+329]SEPEK	IodoTMT6
CERU_MOUSE	Q61147	C239	TFC[+329]SEPEKVDKDNEDFQESNR	IodoTMT6
CERU_MOUSE	Q61147	C694	GTFDVEC[+329]LTTDHYTGGMK	IodoTMT6
CERU_MOUSE	Q61147	C713	YTVNQC[+329]QR	IodoTMT6
CH082_MOUSE	Q8VE95	C132	LSYC[+57]GGGEALAIPFEPAR	HPDP
CHPT1_MOUSE	Q8C025	C386	TSC[+57]QQAPEQVYK	HPDP
CHRD1_MOUSE	Q9D1P4	C211	RKTSDFNTFLAQEGC[+329]TR	IodoTMT6
CHRD1_MOUSE	Q9D1P4	C211	KTSDFNTFLAQEGC[+329]TR	IodoTMT6
CHRD1_MOUSE	Q9D1P4	C211	TSDFNTFLAQEGC[+329]TR	IodoTMT6
CK5P3_MOUSE	Q99LM2	C136	C[+57]QQLQQEYSR	HPDP
CKAP4_MOUSE	Q8BMK4	C79	SSAATANASSASC[+57]SR	HPDP

CKAP4_MOUSE	Q8BMK4	C79	SSAATANASSASC[+329]SR	IodoTMT6
CKLF7_MOUSE	Q9ESD6	C54	VAQMVTLLIAFIC[+329]VR	IodoTMT6
CLCB_MOUSE	Q6IRU5	C199	VAQLC[+57]DFNPK	HPDP
CLH1_MOUSE	Q68FD5	C1266	EVC[+125]FAC[+57]VDGK	HPDP
CLH1_MOUSE	Q68FD5	C1102	C[+329]NEPAVWSQLAK	IodoTMT6
CLIC1_MOUSE	Q9Z1Q5	C223	EEFASTC[+57]PDDEEIELAYEQVAR	HPDP
CMTR1_MOUSE	Q9DBC3	C503	SNESYC[+57]SLQIK	HPDP
CMTR1_MOUSE	Q9DBC3	C534	EC[+57]LQLWK	HPDP
CNBP_MOUSE	P53996	C120	C[+57]YSC[+125]GEFGHIQK	HPDP
CNBP_MOUSE	P53996	C141	C[+57]GETGHVAINC[+125]SK	HPDP
CNBP_MOUSE	P53996	C141, C151	C[+57]GETGHVAINC[+57]SK	HPDP
CNBP_MOUSE	P53996	C157	C[+125]GETGHVAINC[+57]SK	HPDP
CNBP_MOUSE	P53996	C159	TSEVNC[+57]YR	HPDP
CNBP_MOUSE	P53996	C162	C[+57]GESGHLAR	HPDP
CNDP2_MOUSE	Q9D1A2	C300	DVGAETLLHSC[+57]K	HPDP
CNDP2_MOUSE	Q9D1A2	C300	DVGAETLLHSC[+57]KK	HPDP
CNN2_MOUSE	Q08093	C164	AGQC[+57]VIGLQM[+16]GTNK	HPDP
CNN2_MOUSE	Q08093	C164	AGQC[+57]VIGLQMGTNK	HPDP
CNN2_MOUSE	Q08093	C215	C[+57]ASQVGM[+16]TAPGTR	HPDP
CO3_MOUSE	P01027	C559	DSC[+57]IGTLVVK	HPDP
CO4A1_MOUSE	P02463	C1460	HSQTTDDPLC[+329]PPGTK	IodoTMT6
CO4A1_MOUSE	P02463	C1493	AHGQDLGTAGSC[+329]LR	IodoTMT6
CO4A2_MOUSE	P08122	C1532	AHNQDLGLAGSC[+329]LAR	IodoTMT6
COAC_MOUSE	Q8BZB2	C7	APC[+57]PAAVPSEER	HPDP
COF1_MOUSE	P18760	C39	AVLFC[+57]LSEDK	HPDP
COF1_MOUSE	P18760	C39	AVLFC[+57]LSEDKK	HPDP
COPB2_MOUSE	O55029	C56	TFEVC[+57]DLPVR	HPDP
COPB2_MOUSE	O55029	C351	DMGSC[+329]EIYPQTIQHNPNGR	IodoTMT6
COR1A_MOUSE	O89053	C24	ADQC[+57]YEDVR	HPDP
COR1B_MOUSE	Q9WUM3	C25	NDQC[+57]YEDIR	HPDP
COR1C_MOUSE	Q9WUM4	C190	NGSLIC[+57]TASK	HPDP
COR1C_MOUSE	Q9WUM4	C424	KSELSC[+57]APK	HPDP

CPNE1_MOUSE	Q8C166	C52	NC[+57]SSPEFSK	HPDP
CPNS1_MOUSE	O88456	C145	TDGFGIDTC[+57]R	HPDP
CPSF1_MOUSE	Q9EPU4	C1042	VYAVATSTNTPC[+57]TR	HPDP
CPSM_MOUSE	Q8C196	C225	VVAVDC[+57]GIK	HPDP
CPZIP_MOUSE	Q3UZA1	C244	NTC[+57]NSTEKPEELVR	HPDP
CRIP2_MOUSE	Q9DCT8	C126	ASSVTTFTGEPNMC[+329]PR	IodoTMT6
CSDE1_MOUSE	Q91W50	C129	SPAAPGQSPTGSVC[+57]YER	HPDP
CSK22_MOUSE	O54833	C336	EQSQPC[+57]AENTVLSSGLTAAR	HPDP
CSRP1_MOUSE	P97315	C122	C[+57]SQAVYAAEK	HPDP
CSRP1_MOUSE	P97315	C167	GLESTTLADKDGEIYC[+329]K	IodoTMT6
CSRP1_MOUSE	P97315	C167	C[+125]GKGLESTTLADKDGEIYC[+329]K	IodoTMT6
CSRP1_MOUSE	P97315	C58	KNLDSTTVAVHGEEIYC[+329]K	IodoTMT6
CSRP1_MOUSE	P97315	C58	NLDSTTVAVHGEEIYC[+329]K	IodoTMT6
CSRP2_MOUSE	P97314	C167	EGEIYC[+57]K	HPDP
CSRP2_MOUSE	P97314	C167	SLESTTLTEKEGEIYC[+57]K	HPDP
CSRP2_MOUSE	P97314	C167	SLESTTLTEKEGEIYC[+329]K	IodoTMT6
CSRP2_MOUSE	P97314	C58	NLDSTTVAIHDEEIYC[+329]K	IodoTMT6
CTBP2_MOUSE	P56546	C18	LDRIC[+329]EGIRPQIM[+16]NGPLHPRPLVALLDGRDC[+125]T	IodoTMT6
CTCF_MOUSE	Q61164	C472	YC[+329]DAVFHER	IodoTMT6
CTL2_MOUSE	Q8BY89	C401	VVDDTAC[+57]PLLR	HPDP
CTL2A_MOUSE	P12399	C103	TNC[+57]YGNSLNR	HPDP
CTNA1_MOUSE	P26231	C116	SAAGEFADDPC[+57]SSVK	HPDP
CTNA1_MOUSE	P26231	C116	SAAGEFADDPC[+329]SSVK	IodoTMT6
CTNA1_MOUSE	P26231	C116	SAAGEFADDPC[+329]SSVKR	IodoTMT6
CUBN_MOUSE	Q9JLB4	C1466	IAQLC[+57]SR	HPDP
CUBN_MOUSE	Q9JLB4	C1510	AVPGGC[+57]GGIFQVSR	HPDP
CUBN_MOUSE	Q9JLB4	C1927	LIGTYC[+57]GTQR	HPDP
CUBN_MOUSE	Q9JLB4	C2054	LSQQLAVLC[+57]GR	HPDP
CUBN_MOUSE	Q9JLB4	C817	ADYQVAC[+57]GGELR	HPDP
CUL4B_MOUSE	A2A432	C74	SVC[+57]PGTSGFSSPNPSAASAAAQEVR	HPDP
CXA1_MOUSE	P23242	C260	SDPYHATTGPLSPSKDC[+329]GSPK	IodoTMT6
CY24B_MOUSE	Q61093	C126	NLTFHKM[+16]VAWMIALHTAIHTIAHLFNVEWC[+329]VNAR	IodoTMT6

CYFP1_MOUSE	Q7TMB8	C428	DC[+57]PDNAEEYER	HPDP
D19L4_MOUSE	A2AJQ3	C355	VFEFYLLC[+329]TLPVTLNLIVK	IodoTMT6
DAPK2_MOUSE	Q8VDF3	C347	NC[+57]ESDTEENIAR	HPDP
DCAF6_MOUSE	Q9DC22	C200,C211	DDILINC[+125]RRAATSVAIC[+329]PPVPYYLAVGC[+329]SDS	IodoTMT6
DCSTP_MOUSE	Q7TNJ0	C89	RARC[+57]FILLAVLSC[+329]GLR	IodoTMT6
DD19A_MOUSE	Q61655	C392	VLVTTNVC[+57]AR	HPDP
DDX1_MOUSE	Q91VR5	C571	FLIC[+57]TDVAAR	HPDP
DDX6_MOUSE	P54823	C390	NLVC[+57]TDLFTR	HPDP
DEN4C_MOUSE	A6H8H2	C1083	ILTAALTC[+57]PK	HPDP
DESM_MOUSE	P31001	C332	HQIQSYTC[+329]EIDALK	IodoTMT6
DESM_MOUSE	P31001	C332	HQIQSYTC[+329]EIDALKGTNDSLMR	IodoTMT6
DHE3_MOUSE	P26443	C327	C[+329]VGVGESDGSIWNPDGIDPK	IodoTMT6
DHPR_MOUSE	Q8BVI4	C82	VDAILC[+57]VAGGWAGGNAK	HPDP
DHRS1_MOUSE	Q99L04	C10	GQVC[+57]VVTGASR	HPDP
DHSO_MOUSE	Q64442	C106	EVDEYC[+57]K	HPDP
DHX36_MOUSE	Q8VHK9	C277	AESC[+57]GNGNSTGYQIR	HPDP
DHX9_MOUSE	O70133	C440	AAEC[+57]NIVVTQPR	HPDP
DI3L2_MOUSE	Q8CI75	C376	DC[+57]IFTIDPSTAR	HPDP
DIAC_MOUSE	Q8R242	C342	GIGMWNANC[+329]LDYSDDALAR	IodoTMT6
DIAP1_MOUSE	O08808	C1210	AGC[+57]AVTSLLASELTK	HPDP
DICER_MOUSE	Q8R418	C306	QILSDC[+329]RAVLVVLGPWC[+57]ADKVAGM[+16]M[+16]V	IodoTMT6
DLGP4_MOUSE	B1AZP2	C726	DTDSDTQDANDSSC[+329]K	IodoTMT6
DNJA2_MOUSE	Q9QYJ0	C308	VIEPGC[+57]VR	HPDP
DNJB6_MOUSE	O54946	C243	SLTINGVADENALAEEC[+329]QR	IodoTMT6
DNPEP_MOUSE	Q9Z2W0	C411	NDSPC[+57]GTTIGPILASR	HPDP
DOPD_MOUSE	O35215	C57	STEPC[+329]AHLLVSSIGVVGTAEQNR	IodoTMT6
DP13A_MOUSE	Q8K3H0	C615	IC[+57]DSVGLAK	HPDP
DPM3_MOUSE	Q9D1Q4	C67	VATFHDC[+57]EDAAR	HPDP
DPYL2_MOUSE	O08553	C248	SITIANQTNC[+57]PLYVTK	HPDP
DPYL2_MOUSE	O08553	C248	SITIANQTNC[+329]PLYVTK	IodoTMT6
DPYL2_MOUSE	O08553	C248	SITIANQTNC[+329]PLYVTKVMSK	IodoTMT6
DPYL2_MOUSE	O08553	C439	THNSALEYNIFEGM[+16]EC[+329]R	IodoTMT6

DPYL2_MOUSE	O08553	C439	THNSALEYNIFEGMEC[+329]R	IodoTMT6
DSCR3_MOUSE	O35075	C243	DATEIQNIQIADGDIC[+57]R	HPDP
DYHC1_MOUSE	Q9JHU4	C631	VQYPQSQAC[+57]K	HPDP
DYN2_MOUSE	P39054	C607	QIELAC[+57]DSQEDVDSWK	HPDP
ECM2_MOUSE	Q5FW85	C8	LAVLFC[+329]FILLIVLQTDC[+125]ERGTR	IodoTMT6
EDC3_MOUSE	Q8K2D3	C137	SQDVAISPQQQQC[+57]SK	HPDP
EF1D_MOUSE	P57776	C217	SSILLDVKPWDDETDMAQLETC[+329]VR	IodoTMT6
EF2_MOUSE	P58252	C369	C[+57]ELLYEGPPDDEAAMGIK	HPDP
EF2_MOUSE	P58252	C591	ETVSEESNVLC[+57]LSK	HPDP
EF2_MOUSE	P58252	C693	EGALC[+57]EENMR	HPDP
EF2_MOUSE	P58252	C693	EGALC[+57]EENM[+16]R	HPDP
EF2_MOUSE	P58252	C591	ETVSEESNVLC[+329]LSK	IodoTMT6
EF2_MOUSE	P58252	C728	C[+329]LYASVLTAQPR	IodoTMT6
EFTU_MOUSE	Q8BFR5	C290	KGDEC[+57]ELLGHNK	HPDP
EIF3A_MOUSE	P23116	C478	HC[+57]DLQVR	HPDP
EIF3F_MOUSE	Q9DCH4	C260	TC[+57]FSPNR	HPDP
ELMD2_MOUSE	Q8BGF6	C98	TC[+57]LLQITGYK	HPDP
EMAL3_MOUSE	Q8VC03	C421	DSSC[+57]IVTSGK	HPDP
ENOA_MOUSE	P17182	C337, C339	SC[+57]NC[+57]LLLK	HPDP
ENOA_MOUSE	P17182	C357	VNQIGSVTESLQAC[+57]K	HPDP
EPN3_MOUSE	Q91W69	C461	SPSTVELDPFGDSSPSC[+329]K	IodoTMT6
ERP44_MOUSE	Q9D1Q6	C92	VDC[+57]DQHSDIAQR	HPDP
ES8L2_MOUSE	Q99K30	C546	SGQAGYVPC[+57]NILAEAR	HPDP
ESTD_MOUSE	Q9R0P3	C206	AYDATC[+57]LVK	HPDP
ETHE1_MOUSE	Q9DCM0	C170	TDFQQGC[+57]AK	HPDP
ETHE1_MOUSE	Q9DCM0	C34	SC[+57]TYTYLLGDR	HPDP
EVI5_MOUSE	P97366	C479	LSEAESQC[+57]ALK	HPDP
EXOC8_MOUSE	Q6PGF7	C419	AC[+57]ELFLR	HPDP
F16P1_MOUSE	Q9QXD6	C93	SSYATC[+57]VLVSEENTNAIIIEPEK	HPDP
F19A2_MOUSE	Q7TPG7	C107	WWCHMQPC[+57]LEGEEC[+329]KVLPDR	IodoTMT6
F19A2_MOUSE	Q7TPG7	C96	WWC[+329]HMQPC[+57]LEGEECKVLPDR	IodoTMT6
FA98B_MOUSE	Q80VD1	C52	AAEGGLSSPEFSELC[+329]IWLGSQIK	IodoTMT6

FABP4_MOUSE	P04117	C118	LVVEC[+57]VMK	HPDP
FABP4_MOUSE	P04117	C118	LVVEC[+57]VM[+16]K	HPDP
FABP4_MOUSE	P04117	C118	DGDKLVVEC[+57]VMK	HPDP
FABP4_MOUSE	P04117	C118	DGDKLVVEC[+329]VMK	IodoTMT6
FABP4_MOUSE	P04117	C118	LVVEC[+329]VMK	IodoTMT6
FABPL_MOUSE	P12710	C69	NEFTLGEEC[+57]ELETMTGEK	HPDP
FABPL_MOUSE	P12710	C69	NEFTLGEEC[+57]ELETM[+16]TGEK	HPDP
FAK1_MOUSE	P34152	C597	NVLVSSNDC[+57]VK	HPDP
FARP1_MOUSE	F8VPU2	C524	QASPLISPLLNDQAC[+57]PR	HPDP
FAS_MOUSE	P19096	C1181	LLAAAC[+57]QLQLNGNLQLELGEALAQER	HPDP
FAS_MOUSE	P19096	C223	SFDDSGSGYC[+57]R	HPDP
FBN1_MOUSE	Q61554	C1960	C[+57]NEGYEVAPDGR	HPDP
FBN1_MOUSE	Q61554	C1099	GQCVNTPGDFEC[+57]KC[+329]DEGYESGFMM[+16]M[+16]KI	IodoTMT6
FBN1_MOUSE	Q61554	C1960	C[+329]NEGYEVAPDGR	IodoTMT6
FERM2_MOUSE	Q8CIB5	C426	GC[+57]EVTPDVNISGQK	HPDP
FETA_MOUSE	P02772	C144	TAPASVPPFQFPEPAESC[+329]K	IodoTMT6
FETUA_MOUSE	P29699	C336	VGQPGAAGPVSPMC[+329]PGR	IodoTMT6
FGF5_MOUSE	P15656	C200	GC[+329]SPRVKPQHVSTHFLPR	IodoTMT6
FHL1_MOUSE	P97447	C255	C[+57]SVNLANKR	HPDP
FHL2_MOUSE	O70433	C71	C[+57]GSSLVDKPFAAK	HPDP
FHL5_MOUSE	Q9WTX7	C222,C225	KC[+329]AAC[+329]TKPITGLRGAK	IodoTMT6
FHOD1_MOUSE	Q6P9Q4	C539	AEPIQEPPTC[+57]VPK	HPDP
FINC_MOUSE	P11276	C136	ISC[+57]TIANR	HPDP
FINC_MOUSE	P11276	C232	C[+57]NDQDTR	HPDP
FKBP5_MOUSE	Q64378	C215	EEQC[+57]ILYLGPR	HPDP
FLII_MOUSE	Q9JJ28	C1069	TNGSALC[+57]TR	HPDP
FLII_MOUSE	Q9JJ28	C560	AC[+57]SAIHAVNLR	HPDP
FLII_MOUSE	Q9JJ28	C576	NYLGAEC[+57]R	HPDP
FLNA_MOUSE	Q8BTM8	C1157	AHVAPC[+57]FDASK	HPDP
FLNA_MOUSE	Q8BTM8	C1453	C[+57]SGPGLSPGMVR	HPDP
FLNA_MOUSE	Q8BTM8	C2102	VDINTEDLEDGTC[+57]R	HPDP
FLNA_MOUSE	Q8BTM8	C2582	SNFTVDC[+57]SK	HPDP

FLNA_MOUSE	Q8BTM8	C2601	TPC[+57]EEILVK	HPDP
FLNA_MOUSE	Q8BTM8	C8	C[+57]GQSAAVASPGGSIDSR	HPDP
FLNA_MOUSE	Q8BTM8	C1312	VANPSGNLTDTYVQDC[+329]GDGTYK	IodoTMT6
FLNA_MOUSE	Q8BTM8	C2102	VDINTEDLEDGTC[+329]R	IodoTMT6
FLNA_MOUSE	Q8BTM8	C2102	DAGYGGLSLSIEGPSKVDINTEDLEDGTC[+329]R	IodoTMT6
FLNA_MOUSE	Q8BTM8	C2293	DGSC[+329]GVAYVVQEPGDYEVSVK	IodoTMT6
FLNA_MOUSE	Q8BTM8	C2476	MDC[+329]QEC[+125]PEGYR	IodoTMT6
FLNA_MOUSE	Q8BTM8	C8	C[+329]GQSAAVASPGGSIDSR	IodoTMT6
FLNB_MOUSE	Q80X90	C1280	AQITNPSGASTEC[+57]FVK	HPDP
FLNB_MOUSE	Q80X90	C1326	VAVTEGC[+57]QPSR	HPDP
FLNB_MOUSE	Q80X90	C1434	IAGPGLSSC[+57]VR	HPDP
FLNB_MOUSE	Q80X90	C1868	AEISC[+57]IDNK	HPDP
FLNB_MOUSE	Q80X90	C1876	DGTC[+57]TVTYLPTLPGDYSILVK	HPDP
FLNB_MOUSE	Q80X90	C2057	VDIQTEDLEDGTC[+57]K	HPDP
FLNB_MOUSE	Q80X90	C2537	SSFLVDC[+57]SK	HPDP
FLNB_MOUSE	Q80X90	C450, C455	SPFGVQIGEAC[+57]NPNAC[+57]R	HPDP
FLNB_MOUSE	Q80X90	C604	IEYDDQNDGSC[+57]DVK	HPDP
FLNB_MOUSE	Q80X90	C660	SGC[+57]TINNPAEFIVDPK	HPDP
FLNB_MOUSE	Q80X90	C991	VVPC[+57]LVAPVAGR	HPDP
FLNB_MOUSE	Q80X90	C991	KVVPC[+57]LVAPVAGR	HPDP
FLNB_MOUSE	Q80X90	C2057	VDIQTEDLEDGTC[+329]K	IodoTMT6
FLNB_MOUSE	Q80X90	C2057	DAGYGGISLAVEGPSKVDIQTEDLEDGTC[+329]K	IodoTMT6
FLNB_MOUSE	Q80X90	C2248	NGSC[+329]GVSYIAQEPGNYEVSIK	IodoTMT6
FLNB_MOUSE	Q80X90	C2333	VHSPSGAVEEC[+329]HVSELEPDKYAVR	IodoTMT6
FLNB_MOUSE	Q80X90	C2431	MDC[+329]QEIPEGYK	IodoTMT6
FLNB_MOUSE	Q80X90	C2537	SSFLVDC[+329]SK	IodoTMT6
FLNB_MOUSE	Q80X90	C450	SPFGVQIGEAC[+329]NPNAC[+125]R	IodoTMT6
FLNB_MOUSE	Q80X90	C455	SPFGVQIGEAC[+125]NPNAC[+329]R	IodoTMT6
FLNB_MOUSE	Q80X90	C660	SGC[+329]TINNPAEFIVDPK	IodoTMT6
FLNB_MOUSE	Q80X90	C769	ANEPTHFTVDC[+329]TEAGEGDVSVGIK	IodoTMT6
FLNB_MOUSE	Q80X90	C769	SGLKANEPTHFTVDC[+329]TEAGEGDVSVGIK	IodoTMT6
FLNB_MOUSE	Q8VHX6	C1104	GAGTGGLGLTVEGPC[+329]EAK	IodoTMT6

FLNC_MOUSE	Q8VHX6	C2661	NSFTVDC[+57]SK	HPDP
FLNC_MOUSE	Q8VHX6	C2680	TPC[+329]EEVYVK	IodoTMT6
FN3C1_MOUSE	Q6DFV6	C1112	TKPLPPEPPQLNC[+329]VVYGHQSLR	IodoTMT6
FRPD1_MOUSE	A2AKB4	C1360	AYSC[+57]TTPLSR	HPDP
FSCN1_MOUSE	Q61553	C481	AC[+57]AETIDPASLWEY	HPDP
FSCN1_MOUSE	Q61553	C89	EVPDGDC[+57]R	HPDP
FUMH_MOUSE	P97807	C431	LLGDASVSFTDNC[+57]VVGIQANTER	HPDP
FUT10_MOUSE	Q5F2L2	C13	LLASC[+329]LCVTATVFLM[+16]VTLQVVVELGKFER	IodoTMT6
FXL20_MOUSE	Q9CZV8	C283	C[+57]SQLTDVGFTTLAR	HPDP
FXR1_MOUSE	Q61584	C77	ANDQEPC[+57]GWWLAK	HPDP
FXR2_MOUSE	Q9WVR4	C282	IYGETPEAC[+57]R	HPDP
G3P_MOUSE	P16858	C150	IVSNASC[+57]TTNC[+125]LAPLAK	HPDP
G3P_MOUSE	P16858	C150, C154	IVSNASC[+57]TTNC[+57]LAPLAK	HPDP
G3P_MOUSE	P16858	C160	IVSNASC[+125]TTNC[+57]LAPLAK	HPDP
GAB1_MOUSE	Q9QYY0	C406	DASSQDC[+57]YDIPR	HPDP
GALK1_MOUSE	Q9R0N0	C243	QC[+57]EEVAQALGK	HPDP
GALT_MOUSE	Q03249	C75	HDPLNPLC[+57]PGATR	HPDP
GATM_MOUSE	Q9D964	C87	AENAC[+57]VPPFTVEVK	HPDP
GATM_MOUSE	Q9D964	C64	DC[+329]PVSSYNEWDPLEEVIVGR	IodoTMT6
GATM_MOUSE	Q9D964	C87	AENAC[+329]VPPFTVEVK	IodoTMT6
GBB1_MOUSE	P62874	C25	AC[+57]ADATLSQITNNIDPVGR	HPDP
GBB1_MOUSE	P62874	C25	KAC[+57]ADATLSQITNNIDPVGR	HPDP
GCNT1_MOUSE	Q09324	C100	DC[+57]ASFIR	HPDP
GFPT1_MOUSE	P47856	C262	VDSTTC[+57]LFPVEEK	HPDP
GFPT1_MOUSE	Q9Z2Z9	C461	ETDC[+329]GVHINAGPEIGVASTK	IodoTMT6
GIMA4_MOUSE	Q99JY3	C61	VFNSGIC[+57]AK	HPDP
GLNA_MOUSE	P15105	C183	AC[+57]LYAGVK	HPDP
GLNA_MOUSE	P15105	C49	TLDC[+57]EPK	HPDP
GLOD4_MOUSE	Q9CPV4	C45	AAC[+57]NGPYDGK	HPDP
GMPR1_MOUSE	Q9DCZ1	C186	VGVGPGSVC[+57]TTR	HPDP
GON7_MOUSE	P0C8B4	C21	VSC[+57]EASGDADPLQSLSAGVVR	HPDP
GORS2_MOUSE	Q99JX3	C434	VSDC[+57]TPAVEKPVSDADASEPS	HPDP

GP126_MOUSE	Q6F3F9	C38	C[+125]C[+57]PWRLKPSALLFLFVLC[+57]VTCVPLSVC[+125]C	IodoTMT6
GP142_MOUSE	Q7TQN9	C233	LLKWAHCLIVYFIPC[+329]NVFLVTNSAIILR	IodoTMT6
GPD1L_MOUSE	Q3ULJ0	C216	NIVAVGAGFC[+57]DGLR	HPDP
GPX41_MOUSE	O70325	C195	YGPMEEPQVIEKDLPC[+329]YL	IodoTMT6
GRAP1_MOUSE	Q8VD04	C104	LC[+57]SQLEQLELENR	HPDP
GRB10_MOUSE	Q60760	C173	NQC[+329]PTDTVNPVAR	IodoTMT6
GRM1B_MOUSE	Q80TI0	C20	STPAC[+57]SPILR	HPDP
GRP75_MOUSE	P38647	C66	GAVVGIDLGTTNSC[+57]VAVMEGK	HPDP
GRP78_MOUSE	P20029	C42	KEDVGTVVGIDLGTTYSC[+57]VGVFK	HPDP
GRP78_MOUSE	P20029	C42	EDVGTVVGIDLGTTYSC[+57]VGVFK	HPDP
GSHR_MOUSE	P47791	C256	NFDSLISSNC[+57]TEELENAGVEVLK	HPDP
GSHR_MOUSE	P47791	C85	AAVVESHKLGGTC[+125]VNVGC[+329]VPK	IodoTMT6
GSHR_MOUSE	P47791	C85	LGGTC[+125]VNVGC[+329]VPK	IodoTMT6
GSTK1_MOUSE	Q9DCM2	C176	LIENTDAAC[+57]K	HPDP
HA1K_MOUSE	P14428	C317	GGDYALAPGSQTSDLSLPDC[+329]K	IodoTMT6
HDAC1_MOUSE	O09106	C408	ISIC[+57]SSDKR	HPDP
HEMO_MOUSE	Q91X72	C458	SLPQPQKVNSILGC[+57]SQ	HPDP
HEMO_MOUSE	Q91X72	C458	VNSILGC[+57]SQ	HPDP
HEMO_MOUSE	Q91X72	C364	ELGSPPGISLETIDAAFSC[+329]PGSSR	IodoTMT6
HEMO_MOUSE	Q91X72	C458	SLPQPQKVNSILGC[+329]SQ	IodoTMT6
HEMO_MOUSE	Q91X72	C458	VNSILGC[+329]SQ	IodoTMT6
HIF1N_MOUSE	Q8BLR9	C236	RC[+125]ILFPPDQFEC[+57]LYPYPVHHPC[+329]DR	IodoTMT6
HIF1N_MOUSE	Q8BLR9	C236	RC[+125]ILFPPDQFEC[+57]LYPYPVHHPC[+329]DR	IodoTMT6
HMCS2_MOUSE	P54869	C96, C106	MGFC[+57]SVQEDINSLC[+57]LTVVQR	HPDP
HNRL1_MOUSE	Q8VDM6	C533	KAIVIC[+329]PTDEDLKDR	IodoTMT6
HNRL1_MOUSE	Q8VDM6	C533	AIVIC[+329]PTDEDLKDR	IodoTMT6
HNRPD_MOUSE	Q60668	C126	FGEVVDC[+57]TLK	HPDP
HNRPL_MOUSE	Q8R081	C578	LC[+57]FSTAQHAS	HPDP
HNRPQ_MOUSE	Q7TMK9	C289	GFC[+57]FLEYEDHK	HPDP
HNRPU_MOUSE	Q8VEK3	C583	KAVVVC[+57]PK	HPDP
HNRPU_MOUSE	Q8VEK3	C583	AVVVC[+57]PKDEDYK	HPDP
HPRT_MOUSE	P00493	C106	SYC[+57]NDQSTGDIK	HPDP

HPRT_MOUSE	P00493	C206	DLNHVC[+57]VISETGK	HPDP
HPS6_MOUSE	Q8BLY7	C180	TLETSGEAGTKLGC[+329]THILLHHCPLFGLIASR	IodoTMT6
HPS6_MOUSE	Q8BLY7	C692	LLLAEFAQHRRLDAHLPLLC[+329]R	IodoTMT6
HSP72_MOUSE	P17156	C606	VC[+57]NPIISK	HPDP
HSP74_MOUSE	Q61316	C167	SVMDATQIAGLNC[+329]LR	IodoTMT6
HSP7C_MOUSE	P63017	C17	GPAVGIDLGTTYSC[+57]VGVFQHGK	HPDP
HSP7C_MOUSE	P63017	C603	VC[+57]NPIITK	HPDP
HXK2_MOUSE	O08528	C375	IC[+57]QIVSTR	HPDP
I17RB_MOUSE	Q9JIP3	C12	MLLVLLILAASC[+329]RSALPR	IodoTMT6
ICAL_MOUSE	P51125	C408	C[+329]GEDEDTVPAEYR	IodoTMT6
IDHC_MOUSE	O88844	C73	C[+57]ATITPDEK	HPDP
IF2G_MOUSE	Q9Z0N1	C105	SC[+57]GSSTPDEFPTDIPGTK	HPDP
IF2G_MOUSE	Q9Z0N1	C105	SC[+329]GSSTPDEFPTDIPGTK	IodoTMT6
IF4B_MOUSE	Q8BGD9	C543	VDVVGATQGQAGSC[+57]SR	HPDP
IF4B_MOUSE	Q8BGD9	C543	DGNKVDVVGATQGQAGSC[+57]SR	HPDP
IF5_MOUSE	P59325	C122	KQTIGNSC[+329]K	IodoTMT6
IGHM_MOUSE	P01872	C453	STGKPTLYNVSLIM[+16]SDTGGTC[+329]Y	IodoTMT6
IGHM_MOUSE	P01872	C453	STGKPTLYNVSLIMSDTGGTC[+329]Y	IodoTMT6
IGHM_MOUSE	P01872	C88	SILEGSDEYLVC[+329]K	IodoTMT6
IGKC_MOUSE	P01837	C106	SFNRNEC[+57]	HPDP
IGKC_MOUSE	P01837	C86	HNSYTC[+57]EATHK	HPDP
IL19_MOUSE	Q8CJ70	C5,C18	KTQC[+329]ASTWLLGM[+16]TLILC[+329]SVHIYSLRR	IodoTMT6
INADL_MOUSE	Q63ZW7	C1406	ESESPDSAAC[+57]QIK	HPDP
INLR1_MOUSE	Q8CGK5	C81	TGWRPVEHCAGIKALVC[+329]PLMCLKK	IodoTMT6
INSM1_MOUSE	Q63ZV0	C482	GAQERHLRLLHAAQVFPC[+329]K	IodoTMT6
IRGQ_MOUSE	Q8VIM9	C370	AGIGDSGC[+57]TAAR	HPDP
KBL_MOUSE	O88986	C26	C[+57]ILDSELEGIR	HPDP
KBTBD_MOUSE	Q8C828	C337	GRLFVCLWRPADITAVVEYVVQMDKWLPVAELC[+329]R	IodoTMT6
KCY_MOUSE	Q9DBP5	C20	KPLVVFVLGGPGAGKGTQC[+329]AR	IodoTMT6
KINH_MOUSE	Q61768	C632	ELAAC[+57]QLR	HPDP
KNG1_MOUSE	O08677	C339	ESNTELAEDC[+57]EIK	HPDP
KNG1_MOUSE	O08677	C125	ENEFFIVTQTC[+329]K	IodoTMT6

KNG1_MOUSE	O08677	C369	C[+329]QALDMTEMAR	IodoTMT6
KPCI_MOUSE	Q62074	C190	LVTIEC[+57]GR	HPDP
KPYM_MOUSE	P52480	C423, C424	C[+57]C[+57]SGAIIVLTK	HPDP
KPYM_MOUSE	P52480	C49	NTGIIC[+57]TIGPASR	HPDP
KPYM_MOUSE	P52480	C423	C[+329]C[+125]SGAIIVLTK	IodoTMT6
KPYM_MOUSE	P52480	C423	C[+329]C[+125]SGAIIVLTKSGR	IodoTMT6
KPYM_MOUSE	P52480	C424	C[+125]C[+329]SGAIIVLTK	IodoTMT6
KPYM_MOUSE	P52480	C49	NTGIIC[+329]TIGPASR	IodoTMT6
KPYR_MOUSE	P53657	C360,C369	VFLAQKMMIGRC[+329]NLAGKPVVC[+329]ATQMLESMITK	IodoTMT6
KT3K_MOUSE	Q8K274	C11	ELGC[+57]SSVK	HPDP
LAC3_MOUSE	P01844	C103	SLSPAEC[+329]L	IodoTMT6
LAMA5_MOUSE	Q61001	C69	ITASATC[+57]GEEAPTR	HPDP
LAMA5_MOUSE	Q61001	C69	ITASATC[+329]GEEAPTR	IodoTMT6
LAMB1_MOUSE	P02469	C643	C[+329]GNTVPDDDNQVVSLSPGSR	IodoTMT6
LAMC1_MOUSE	P02468	C349	SQEC[+329]YFDPELYR	IodoTMT6
LAS1L_MOUSE	A2BE28	C488	VC[+57]SIYTQNGENGLAK	HPDP
LAT2_MOUSE	Q9QXW9	C209	LLALALIIIM[+16]GIVQIC[+329]K	IodoTMT6
LAT4_MOUSE	Q8CGA3	C295	LC[+57]LSTVDLEVK	HPDP
LCAP_MOUSE	Q8C129	C305	SAFPC[+57]FDEPAFK	HPDP
LDHA_MOUSE	P06151	C35	ITVVGVGAVGMAC[+57]AISILMK	HPDP
LDHB_MOUSE	P16125	C36	ITVVGVGQVGMAC[+57]AISILGK	HPDP
LEG2_MOUSE	Q9CQW5	C57	FDESTIVC[+57]NTSEGGR	HPDP
LEG9_MOUSE	O08573	C258	C[+57]GGDIAFHLNPR	HPDP
LIPB2_MOUSE	O35711	C398	C[+57]VDGNQLSPVGEPK	HPDP
LKHA4_MOUSE	P24527	C147	AILPC[+57]QDTPSVK	HPDP
LKHA4_MOUSE	P24527	C147	AILPC[+329]QDTPSVK	IodoTMT6
LKHA4_MOUSE	P24527	C17	PEVADTC[+125]SLASPASVC[+329]R	IodoTMT6
LMCD1_MOUSE	Q8VEE1	C246	EVEYVC[+125]ELC[+329]K	IodoTMT6
LMNA_MOUSE	P48678	C522	AQNTWGC[+57]GSSLR	HPDP
LMNA_MOUSE	P48678	C590, C593	TVLC[+57]GTC[+57]GQPADK	HPDP
LMNB2_MOUSE	P21619	C190	C[+57]QSLQEELAFSK	HPDP
LONP2_MOUSE	Q9DBN5	C405	IALGGVC[+57]DQSDIR	HPDP

LR16A_MOUSE	Q6EDY6	C1360	C[+329]SDSGEEAEKEFIFV	IodoTMT6
LRC47_MOUSE	Q505F5	C544	DGQC[+57]PLVVEQVR	HPDP
LRC59_MOUSE	Q922Q8	C131	VAGDC[+57]LDEK	HPDP
LRCH4_MOUSE	Q921G6	C454	AAGAGASAPSTQATC[+57]NGPPK	HPDP
LRP1B_MOUSE	Q9JI18	C1540	GPC[+329]SHLCLINHNRSAACAC[+125]PHLM[+16]KLSSDK	IodoTMT6
LRP2_MOUSE	A2ARV4	C2518	AIVLDPC[+57]R	HPDP
LRP2_MOUSE	A2ARV4	C2713	C[+57]ISQDWK	HPDP
LRP2_MOUSE	A2ARV4	C2830	C[+329]QTTNIC[+57]VPR	IodoTMT6
LSM7_MOUSE	Q9CQQ8	C76	QLGLVVC[+329]R	IodoTMT6
LSM7_MOUSE	Q9CQQ8	C76	LTEDTRQLGLVVC[+329]R	IodoTMT6
LTBP4_MOUSE	Q8K4G1	C1393,C1403	RC[+125]VSNESQSLDDNLGVC[+329]WQEVGPDLVC[+329]SR	IodoTMT6
LY6C2_MOUSE	P0CW02	C53	ASDGFC[+329]IAQNIELIEDSQR	IodoTMT6
MA7D1_MOUSE	A2AJI0	C363	THPSAAVPVC[+57]PR	HPDP
MAGI3_MOUSE	Q9EQJ9	C1439	AGC[+57]TPQSSSLVK	HPDP
MAOX_MOUSE	P06801	C415	AEC[+57]SAEQC[+125]YK	HPDP
MAOX_MOUSE	P06801	C415, C420	AEC[+57]SAEQC[+57]YK	HPDP
MAOX_MOUSE	P06801	C415	AEC[+329]SAEQC[+125]YK	IodoTMT6
MAP1B_MOUSE	P14873	C1913	SPC[+329]DSGYSYETIEK	IodoTMT6
MAP2_MOUSE	O08663	C121	VQTDPPSVPIC[+57]DLYPNGVFPK	HPDP
MAP4_MOUSE	P27546	C636	ETPGSQPSEPC[+57]SGVSR	HPDP
MAP4_MOUSE	P27546	C636	ETPGSQPSEPC[+329]SGVSR	IodoTMT6
MARC2_MOUSE	Q922Q1	C301	LC[+57]DPSVK	HPDP
MCEE_MOUSE	Q9D1I5	C168	DC[+57]GGVLVELEQA	HPDP
MD1L1_MOUSE	Q9WTX8	C233	LC[+57]LQEQDAAVVK	HPDP
MDHC_MOUSE	P14152	C137	KSVKVIVVGNPANTNC[+329]LTASK	IodoTMT6
MDHC_MOUSE	P14152	C137	SVKVIVVGNPANTNC[+329]LTASK	IodoTMT6
MDHC_MOUSE	P14152	C137	VIVVGNPANTNC[+329]LTASK	IodoTMT6
MDHC_MOUSE	P14152	C154	SAPSIPKENFSC[+329]LTR	IodoTMT6
MDR1A_MOUSE	P21447	C638	LVMTQTAGNEIELGNEAC[+329]K	IodoTMT6
MET7B_MOUSE	Q9DD20	C96	VTC[+57]VDPNPNFEK	HPDP
MFAP3_MOUSE	Q922T2	C241	SVPLPPLILNC[+329]RAFVEEMFEAVR	IodoTMT6
MFN1_MOUSE	Q811U4	C681	LC[+57]QQVDVTQK	HPDP

MFNG_MOUSE	O09008	C18	HC[+57]RLFRGM[+16]AGALFTLLC[+329]VGLLSLR	IodoTMT6
MICA1_MOUSE	Q8VDP3	C82	ASQPVYQQGQAC[+57]TNTK	HPDP
MPRI_MOUSE	Q07113	C1910	SYDEC[+329]VLEGR	IodoTMT6
MPRIP_MOUSE	P97434	C723	EGYVLQATC[+57]ER	HPDP
MT1_MOUSE	P02802	C44	C[+329]AQGC[+125]VC[+125]K	IodoTMT6
MT1_MOUSE	P02802	C44	C[+329]AQGC[+57]VC[+57]K	IodoTMT6
MT1_MOUSE	P02802	C50	C[+125]AQGC[+125]VC[+329]K	IodoTMT6
MT1_MOUSE	P02802	C50	C[+125]AQGC[+57]VC[+329]K	IodoTMT6
MT2_MOUSE	P02798	C44, C48, C50	C[+57]SQGC[+57]IC[+57]K	HPDP
MT2_MOUSE	P02798	C54, C56	C[+125]SQGC[+57]IC[+57]K	HPDP
MT2_MOUSE	P02798	C33	SC[+329]C[+57]SC[+125]C[+57]PVGC[+57]AK	IodoTMT6
MT2_MOUSE	P02798	C33,C41	SC[+329]C[+57]SC[+125]C[+57]PVGC[+329]AK	IodoTMT6
MT2_MOUSE	P02798	C33,C41	SC[+329]C[+125]SC[+125]C[+57]PVGC[+329]AK	IodoTMT6
MT2_MOUSE	P02798	C34,C41	SC[+125]C[+329]SC[+125]C[+125]PVGC[+329]AK	IodoTMT6
MT2_MOUSE	P02798	C36,C41	SC[+57]C[+125]SC[+329]C[+57]PVGC[+329]AK	IodoTMT6
MT2_MOUSE	P02798	C37,C41	SC[+57]C[+57]SC[+125]C[+329]PVGC[+329]AK	IodoTMT6
MT2_MOUSE	P02798	C41	SC[+57]C[+57]SC[+125]C[+57]PVGC[+329]AK	IodoTMT6
MT2_MOUSE	P02798	C41	SC[+57]C[+125]SC[+57]C[+57]PVGC[+329]AK	IodoTMT6
MT2_MOUSE	P02798	C41	SC[+125]C[+57]SC[+125]C[+57]PVGC[+329]AK	IodoTMT6
MT2_MOUSE	P02798	C41	SC[+57]C[+57]SC[+125]C[+125]PVGC[+329]AK	IodoTMT6
MT2_MOUSE	P02798	C41	SC[+125]C[+125]SC[+57]C[+57]PVGC[+329]AK	IodoTMT6
MT2_MOUSE	P02798	C41	SC[+125]C[+125]SC[+125]C[+57]PVGC[+329]AK	IodoTMT6
MT2_MOUSE	P02798	C44	C[+329]SQGC[+125]IC[+125]K	IodoTMT6
MT2_MOUSE	P02798	C44	C[+329]SQGC[+57]IC[+125]K	IodoTMT6
MT2_MOUSE	P02798	C50	C[+125]SQGC[+125]IC[+329]K	IodoTMT6
MT2_MOUSE	P02798	C50	C[+125]SQGC[+57]IC[+329]K	IodoTMT6
MTCH2_MOUSE	Q791V5	C79	LC[+57]SGVLGTVVHGK	HPDP
MTMR2_MOUSE	Q9Z2D1	C95	DVTYIC[+57]PFTGAVR	HPDP
MTMR7_MOUSE	Q9Z2C9	C158	VC[+57]DSYPTELYVPR	HPDP
MTMR7_MOUSE	Q9Z2C9	C68	QATTATGC[+57]PLLIR	HPDP
MTMR9_MOUSE	Q9Z2D0	C392	C[+125]AQSAYC[+57]SSK	HPDP
MTMRA_MOUSE	Q7TPM9	C703	SGPLEAC[+57]YAELDQSR	HPDP

MTNB_MOUSE	Q9WVQ5	C187	MAHAMNEYPDSC[+329]AVLVRR	IodoTMT6
MTNB_MOUSE	Q9WVQ5	C187	MAHAMNEYPDSC[+329]AVLVR	IodoTMT6
MTR1L_MOUSE	O88495	C363	AC[+57]VAVEGTPR	HPDP
MTUS1_MOUSE	Q5HZI1	C823	SLC[+57]IQTQTAPDVLSSER	HPDP
MYG_MOUSE	P04247	C67	HGC[+57]TVLTALGTILK	HPDP
MYH9_MOUSE	Q8VDD5	C740	QAC[+57]VLMIK	HPDP
MYH9_MOUSE	Q8VDD5	C816	NC[+57]AAYLR	HPDP
MYH9_MOUSE	Q8VDD5	C896	LQLQEQLQAETELC[+57]AEAEELR	HPDP
MYH9_MOUSE	Q8VDD5	C988	KLEEDQIIM[+16]EDQNC[+329]K	IodoTMT6
MYH9_MOUSE	Q8VDD5	C988	LKKLEEDQIIMEDQNC[+329]K	IodoTMT6
MYH9_MOUSE	Q8VDD5	C988	KLEEDQIIMEDQNC[+329]K	IodoTMT6
MYH9_MOUSE	Q8VDD5	C988	LEEDQIIM[+16]EDQNC[+329]K	IodoTMT6
MYH9_MOUSE	Q8VDD5	C988	LEEDQIIMEDQNC[+329]K	IodoTMT6
MYL3_MOUSE	P09542	C191	LMAGQEDSNGC[+57]INYEAFVK	HPDP
MYL6_MOUSE	Q60605	C32	ILYSQC[+57]GDVM[+16]R	HPDP
MYL6_MOUSE	Q60605	C32	ILYSQC[+57]GDVMR	HPDP
MYO1E_MOUSE	E9Q634	C960	AAPAPPGC[+57]HQNGVIR	HPDP
MYOF_MOUSE	Q69ZN7	C1540	ELPDSVPQEC[+57]TVR	HPDP
MYOF_MOUSE	Q69ZN7	C409	VC[+57]TNIIER	HPDP
MYOF_MOUSE	Q69ZN7	C409	KVC[+57]TNIIER	HPDP
MYOM1_MOUSE	Q62234	C656	C[+57]DVGAENWQR	HPDP
MYOTI_MOUSE	Q9JIF9	C321	ASDAGPYAC[+57]VAR	HPDP
MYPC3_MOUSE	O70468	C1204	SIIAGYNAILC[+125]C[+57]AVR	HPDP
NAL9B_MOUSE	Q66X22	C891,C907,C90	QLC[+57]EALSHPNC[+329]NLEC[+57]LGLDLCEFTSDC[+329]C	IodoTMT6
NARFL_MOUSE	Q7TMW6	C270	DVDC[+57]VLTTGEVFR	HPDP
NDKA_MOUSE	P15532	C145	SC[+329]AQNWIYE	IodoTMT6
NDKB_MOUSE	Q01768	C145	SC[+329]AHDWVYE	IodoTMT6
NDUV1_MOUSE	Q91YT0	C125	YLVVNADEGEPGTC[+329]K	IodoTMT6
NET1_MOUSE	O09118	C17	M[+16]MRAVWEALAALAAVAC[+329]LVGAVR	IodoTMT6
NEXN_MOUSE	Q7TPW1	C585	GETYC[+125]LYLPETFPEDGGEYMC[+329]K	IodoTMT6
NHRF1_MOUSE	P70441	C201	IVEVNGVC[+57]M[+16]EGK	HPDP
NHRF1_MOUSE	P70441	C201	IVEVNGVC[+57]MEGK	HPDP

NID1_MOUSE	P10493	C1232	C[+329]PDNTLGVDC[+57]IER	IodoTMT6
NIPA_MOUSE	Q80YV2	C405	LC[+57]SSSSSDTSPR	HPDP
NIT1_MOUSE	Q8VDK1	C247, C255	AIESQC[+57]YVIAAAQC[+57]GR	HPDP
NKAI4_MOUSE	Q9JMG4	C8,C14	C[+329]TLLALC[+329]ALQLVTALER	IodoTMT6
NL1B2_MOUSE	A1Z198	C330	QIFGIKALMMVESNPVLLTLCEVPWVCWLVC[+329]NC[+125]I	IodoTMT6
NMDZ1_MOUSE	P35438	C459	KVIC[+125]TGPNDTSPGSPRHTVPQC[+125]C[+125]YGFC[+32	IodoTMT6
NOP58_MOUSE	Q6DFW4	C439	TYDPSGDSTLPTC[+57]SK	HPDP
NPAS4_MOUSE	Q8BGD7	C149	QQLTM[+16]PSALDADRLFRC[+329]R	IodoTMT6
NRDC_MOUSE	Q8BHG1	C685	AFDC[+57]PETEYPAK	HPDP
NSF_MOUSE	P46460	C11	C[+57]PTDELSLSNC[+125]AVVNEK	HPDP
NSF_MOUSE	P46460	C11, C21	C[+57]PTDELSLSNC[+57]AVVNEK	HPDP
NTKL_MOUSE	Q9EQC5	C241	SLVTHYC[+329]ELVGANPKVRPNPARFLQNCR	IodoTMT6
NUMA1_MOUSE	E9Q7G0	C728	AADALKEQQC[+57]R	HPDP
NUMB_MOUSE	Q9QZS3	C176	EC[+57]GVTATFDASR	HPDP
OBSCN_MOUSE	A2AAJ9	C3100	GTLTLQC[+57]EVSDPEAR	HPDP
OBSCN_MOUSE	A2AAJ9	C3864	SLTIADAGEYLC[+57]TC[+125]GQEK	HPDP
OBSCN_MOUSE	A2AAJ9	C4816	DLTVEDTGEYSC[+57]TC[+125]GQER	HPDP
OBSL1_MOUSE	D3YYU8	C149	GEEVVLTC[+57]QVGGLPEPK	HPDP
OC90_MOUSE	Q9Z0L3	C371	QVGC[+329]LHGRRSQSSVVCEDHMAK	IodoTMT6
OSBL1_MOUSE	Q91XL9	C520	DC[+57]GGGDALSNGIK	HPDP
OSBP1_MOUSE	Q3B7Z2	C222	VEDLSTC[+57]NDLIAK	HPDP
OXSM_MOUSE	Q9D404	C86	NIPC[+57]SVAAYVPR	HPDP
P3H1_MOUSE	Q3V1T4	C648	TVTAEVQPQC[+57]GR	HPDP
PA2G4_MOUSE	P50580	C49	SLVEASSSGVSVLSLC[+57]EK	HPDP
PACN2_MOUSE	Q9WVE8	C465	IEDEDEQGWC[+329]K	IodoTMT6
PACN2_MOUSE	Q9WVE8	C465	AGDELTKIEDEDEQGWC[+329]K	IodoTMT6
PAFA_MOUSE	Q60963	C290	C[+329]GVALDPWMYPVNEELYSR	IodoTMT6
PAFA_MOUSE	Q60963	C290	C[+329]GVALDPWM[+16]YPVNEELYSR	IodoTMT6
PAFA_MOUSE	Q60963	C290	C[+329]GVALDPWMYPVNEELYSR	IodoTMT6
PARK7_MOUSE	Q99LX0	C53	DVMIC[+57]PDTSLEDAK	HPDP
PARK7_MOUSE	Q99LX0	C58	DVM[+16]IC[+57]PDTSLEDAK	HPDP
PARK7_MOUSE	Q99LX0	C53	DVMIC[+329]PDTSLEDAK	IodoTMT6

PAXI_MOUSE	Q8VI36	C108	NSSASNTQDGVGSLC[+329]SR	IodoTMT6
PCBP1_MOUSE	P60335	C109	LVVPATQC[+57]GSLIGK	HPDP
PCCB_MOUSE	Q99MN9	C271	AFDNDVDALC[+57]NLR	HPDP
PDC6I_MOUSE	Q9WU78	C40	FIQQTYPSGGEEQAQYC[+57]R	HPDP
PDIA5_MOUSE	Q921X9	C449, C454	IAC[+57]AAVDC[+57]VK	HPDP
PDIA5_MOUSE	Q921X9	C449, C454	KIAC[+57]AAVDC[+57]VK	HPDP
PDIA5_MOUSE	Q921X9	C463	DKNQDLC[+57]QQEAVK	HPDP
PDLI1_MOUSE	O70400	C73	GC[+57]ADNM[+16]TLTVSR	HPDP
PDLI1_MOUSE	O70400	C73	GC[+57]ADNMTLTVSR	HPDP
PDLI5_MOUSE	Q8CI51	C73	AC[+57]TGSLNMTLQR	HPDP
PDLI5_MOUSE	Q8CI51	C73	AC[+57]TGSLNM[+16]TLQR	HPDP
PEA15_MOUSE	Q62048	C27	SAC[+57]KEDIPSEK	HPDP
PEG10_MOUSE	Q7TN75	C521	SIVFNSDYC[+57]R	HPDP
PEG10_MOUSE	Q7TN75	C521	SIVFNSDYC[+329]R	IodoTMT6
PEG3_MOUSE	Q3URU2	C383	EC[+57]GETFSR	HPDP
PELP1_MOUSE	Q9DBD5	C202	AC[+57]VTYFPR	HPDP
PELP1_MOUSE	Q9DBD5	C523	NANSDVC[+57]AAALR	HPDP
PEPD_MOUSE	Q11136	C183	FNVNNTILHPEIVEC[+329]R	IodoTMT6
PEPD_MOUSE	Q11136	C183	EASFEGISKFNVNNTILHPEIVEC[+329]R	IodoTMT6
PEPD_MOUSE	Q11136	C482	TVEEIEAC[+125]MAGC[+329]DK	IodoTMT6
PEPD_MOUSE	Q11136	C58	YC[+329]TDTSIIFR	IodoTMT6
PEPL1_MOUSE	Q6NSR8	C357	LVLADGVSYAC[+57]K	HPDP
PFD3_MOUSE	P61759	C8	DGC[+57]GLETAAGNGR	HPDP
PFKAP_MOUSE	Q9WUA3	C410	SNC[+57]NVAVINVGAPAAGMNAAVR	HPDP
PFKAP_MOUSE	Q9WUA3	C410	SNC[+329]NVAVINVGAPAAGMNAAVR	IodoTMT6
PGBM_MOUSE	Q05793	C1628	TC[+57]ESLGAGGYR	HPDP
PGBM_MOUSE	Q05793	C2456	DITLEC[+57]ISSGEPR	HPDP
PGBM_MOUSE	Q05793	C1530	ALEVEEC[+329]R	IodoTMT6
PGBM_MOUSE	Q05793	C2456	DITLEC[+329]ISSGEPR	IodoTMT6
PGBM_MOUSE	Q05793	C479	EADQGAYTC[+329]EAMNSR	IodoTMT6
PGBM_MOUSE	Q05793	C892	GSLGTSGETC[+329]R	IodoTMT6
PGFS_MOUSE	Q9DB60	C44,C47	AC[+57]VVAGLRRFGC[+329]MVC[+329]R	IodoTMT6

PGS1_MOUSE	P28653	C77	VVQC[+57]SDLGLK	HPDP
PHAG1_MOUSE	Q3U1F9	C423	ESDYESIGDLQQC[+57]R	HPDP
PHAG1_MOUSE	Q3U1F9	C423	ESDYESIGDLQQC[+329]R	IodoTMT6
PIPNB_MOUSE	P53811	C187	ELANTPDC[+57]PR	HPDP
PKHA7_MOUSE	Q3UIL6	C969	DREQGQC[+57]VNGDLK	HPDP
PKHM1_MOUSE	Q7TSI1	C464	SAAGLC[+57]TSPVQDTPESR	HPDP
PKP3_MOUSE	Q9QY23	C129	SAVDLTC[+57]SR	HPDP
PLEC_MOUSE	Q9QXS1	C1386	QEQIQAVPIANC[+57]QAAR	HPDP
PLEC_MOUSE	Q9QXS1	C4267	C[+125]ITDPQTGLC[+57]LLPLKEK	HPDP
PLEC_MOUSE	Q9QXS1	C4267	C[+125]ITDPQTGLC[+57]LLPLK	HPDP
PLRG1_MOUSE	Q922V4	C208	C[+57]IAVEPGNQWFVTGSADR	HPDP
PLRG1_MOUSE	Q922V4	C263	SPYLFSC[+329]GEDK	IodoTMT6
PLRG1_MOUSE	Q922V4	C337	C[+329]QAAEPQIITGSHDTTIRLWDLVAGKTR	IodoTMT6
PLRG1_MOUSE	Q922V4	C337	C[+329]QAAEPQIITGSHDTTIR	IodoTMT6
PMGE_MOUSE	P15327	C145	VC[+57]DVPLDQLPR	HPDP
PP2AB_MOUSE	P63330	C269	C[+329]GNQAAIMELDDTLK	IodoTMT6
PP4P1_MOUSE	Q3TWL2	C94	VC[+57]QSPINVEGK	HPDP
PP4R1_MOUSE	Q8K2V1	C385	LESLEGC[+57]AAK	HPDP
PP6R3_MOUSE	Q922D4	C815	C[+329]TAPLTPSSSPEQR	IodoTMT6
PPBT_MOUSE	P09242	C119	TYNTNAQVPDSAGTATAYLC[+329]GVK	IodoTMT6
PPIA_MOUSE	P17742	C161	KITISDC[+57]GQL	HPDP
PPIA_MOUSE	P17742	C161	ITISDC[+57]GQL	HPDP
PPIA_MOUSE	P17742	C161	TSKKITISDC[+57]GQL	HPDP
PPIA_MOUSE	P17742	C67	IIPGFM[+16]C[+57]QGGDFTR	HPDP
PPIA_MOUSE	P17742	C161	KITISDC[+329]GQL	IodoTMT6
PPIA_MOUSE	P17742	C62	IIPGFMC[+329]QGGDFTR	IodoTMT6
PPIG_MOUSE	A2AR02	C174	ILSC[+57]GELIPK	HPDP
PPIG_MOUSE	A2AR02	C308	EC[+57]NPPNSQPASYQR	HPDP
PPME1_MOUSE	Q8BVQ5	C238	QC[+57]EGITSPEGSK	HPDP
PPP5_MOUSE	Q60676	C404	GVSC[+57]QFGPDVTK	HPDP
PPP5_MOUSE	Q60676	C221	EVLC[+329]KLSTLVETTLK	IodoTMT6
PPR3F_MOUSE	Q9JIG4	C419	ILPATC[+57]GLGGPPR	HPDP

PR8A9_MOUSE	Q9CQ58	C101	AGTYC[+57]HSTLSNPPDR	HPDP
PRAP1_MOUSE	Q80XD8	C9	RFLLATC[+329]LVAALLWEAGAAPAHQVPVK	IodoTMT6
PRD13_MOUSE	E9PZZ1	C653	THTGYKPLKC[+125]KVC[+329]LRPFGDPSNLNK	IodoTMT6
PRDX4_MOUSE	O08807	C54	ENEC[+329]HFYAGGQVYPGEASR	IodoTMT6
PRDX5_MOUSE	P99029	C200	ALNVEPDGTGLTC[+57]SLAPNILSQL	HPDP
PRDX5_MOUSE	P99029	C96	GVLFGVPGAFTPGC[+57]SK	HPDP
PRDX6_MOUSE	O08709	C47	DFTPVC[+57]TTELGR	HPDP
PRDX6_MOUSE	O08709	C47	DFTPVC[+329]TTELGR	IodoTMT6
PRP19_MOUSE	Q99KP6	C298	IWSVPNTSC[+57]VQVVR	HPDP
PRS40_MOUSE	A6H6T1	C60	STLSLSEVC[+57]GK	HPDP
PRS6A_MOUSE	O88685	C399	C[+125]TDDFNGAQC[+329]K	IodoTMT6
PRS7_MOUSE	P46471	C377	LC[+57]PNSTGAEIR	HPDP
PRS7_MOUSE	P46471	C389	SVC[+57]TEAGMFAIR	HPDP
PRS7_MOUSE	P46471	C389	SVC[+57]TEAGM[+16]FAIR	HPDP
PSA6_MOUSE	Q9QUM9	C154, C161	C[+57]DPAGYYC[+57]GFK	HPDP
PSA6_MOUSE	Q9QUM9	C167	C[+125]DPAGYYC[+57]GFK	HPDP
PSA6_MOUSE	Q9QUM9	C161	C[+125]DPAGYYC[+329]GFK	IodoTMT6
PSD13_MOUSE	Q9WVJ2	C114	SSDEAVILC[+329]KTAIGALK	IodoTMT6
PTGR1_MOUSE	Q91YR9	C251	TGPC[+57]PQGPAPEVVIYQQLR	HPDP
PTN1_MOUSE	P35821	C32	HEASDFPC[+57]K	HPDP
PUR2_MOUSE	Q64737	C41	QVLVAPGNAGTAC[+57]AGK	HPDP
PUR4_MOUSE	Q5SUR0	C270	FC[+57]DNSSAIQGK	HPDP
PUR9_MOUSE	Q9CWJ9	C434	YTQSNSVC[+57]YAK	HPDP
PURA2_MOUSE	P46664	C58	VVDLLAQDADIVC[+57]R	HPDP
PZP_MOUSE	Q61838	C933	EQTYNTLLC[+329]PQDTELQDNWSLELPPNVVEGSAR	IodoTMT6
QCR1_MOUSE	Q9CZ13	C268	VYEEDAVPGLTPC[+329]R	IodoTMT6
RABL6_MOUSE	Q5U3K5	C501	VAPQQC[+57]SEPETK	HPDP
RACK1_MOUSE	P68040	C153	YTVQDESHSEWVSC[+57]VR	HPDP
RAE1L_MOUSE	Q8C570	C106	VFTASC[+57]DK	HPDP
RB33B_MOUSE	O35963	C48	IIVIGDSNVGKTC[+329]LTYRFCAGR	IodoTMT6
RB6I2_MOUSE	Q99MI1	C258	TGEPC[+57]VAELTEENFQR	HPDP
RBMS2_MOUSE	Q8VC70	C217	TPPGVAAPSDPLLC[+57]K	HPDP

RBX1_MOUSE	P62878	C94	QVC[+57]PLDNR	HPDP
RENBP_MOUSE	P82343	C250	DGQVVLENVSEDGKELPGC[+57]LGR	HPDP
RFLB_MOUSE	Q5SVD0	C88	LC[+57]PLSFGEGVEFDPLPPK	HPDP
RHG01_MOUSE	Q5FWK3	C91	IIVFSAC[+57]R	HPDP
RHG10_MOUSE	Q6Y5D8	C587	TSPDTTFAEPTC[+57]LSASPPNAPPR	HPDP
RHG29_MOUSE	Q8CGF1	C1152	SSDSC[+57]PATAVR	HPDP
RHOA_MOUSE	Q9QUI0	C164	IGAFGYM[+16]EC[+57]SAK	HPDP
RL12_MOUSE	P35979	C141	EILGTAQSVGC[+57]NVDGR	HPDP
RL12_MOUSE	P35979	C17	C[+57]TGGEVGATSALAPK	HPDP
RL12_MOUSE	P35979	C17	C[+329]TGGEVGATSALAPK	IodoTMT6
RL13A_MOUSE	P19253	C38	C[+57]EGINISGNFYR	HPDP
RL18A_MOUSE	P62717	C64	SSGEIVYC[+57]GQVFEK	HPDP
RL18A_MOUSE	P62717	C64	SSGEIVYC[+329]GQVFEKSPLR	IodoTMT6
RL18A_MOUSE	P62717	C64	SSGEIVYC[+329]GQVFEK	IodoTMT6
RL23_MOUSE	P62830	C125	EC[+57]ADLWPR	HPDP
RL27A_MOUSE	P14115	C144	GVGGAC[+57]VLVA	HPDP
RL28_MOUSE	P41105	C13	NC[+57]SSFLIK	HPDP
RL28_MOUSE	P41105	C13	NC[+57]SSFLIKR	HPDP
RL30_MOUSE	P62889	C92	VC[+57]TLAIIDPGDSDIIR	HPDP
RL30_MOUSE	P62889	C52	LVILANNC[+329]PALR	IodoTMT6
RL30_MOUSE	P62889	C92	VC[+329]TLAIIDPGDSDIIR	IodoTMT6
RL36_MOUSE	P47964	C48	EVC[+57]GFAPYER	HPDP
RL36A_MOUSE	P83882	C72, C77	LEC[+57]VEPNC[+57]R	HPDP
RL37A_MOUSE	P61514	C48	YTC[+125]SFC[+57]GK	HPDP
RL37A_MOUSE	P61514	C42	YTC[+125]SFC[+329]GK	IodoTMT6
RL4_MOUSE	Q9D8E6	C101	SGQGAFGNM[+16]C[+57]R	HPDP
RL4_MOUSE	Q9D8E6	C208	GPC[+57]IIYNEDNGIIK	HPDP
RL7A_MOUSE	P12970	C182	MGVPYC[+57]IIK	HPDP
RL9_MOUSE	P51410	C134	TGVAC[+57]SVSQAQK	HPDP
RLA0_MOUSE	P14869	C119	AGAIAPC[+57]EVTVPAQNTGLGPEK	HPDP
RLA0_MOUSE	P14869	C119	AGAIAPC[+329]EVTVPAQNTGLGPEK	IodoTMT6
RLA0_MOUSE	P14869	C119	AGAIAPC[+329]EVTVPAQNTGLGPEKTSFFQALGITTKISR	IodoTMT6

RLA0_MOUSE	P14869	C119	AGAIAPC[+329]EVTVPAQNTGLGPEKTSFFQALGITTK	IodoTMT6
RN126_MOUSE	Q91YL2	C32	C[+57]ESGFIEELPEETR	HPDP
RPAP3_MOUSE	Q9D706	C341	DC[+57]TQAIVLDGSYSK	HPDP
RPB2_MOUSE	Q8CFI7	C221	YAYTGEC[+57]R	HPDP
RPB2_MOUSE	Q8CFI7	C892	DC[+57]STFLR	HPDP
RRAGC_MOUSE	Q99K70	C376	SC[+57]SHQTSAPSLK	HPDP
RRAS2_MOUSE	P62071	C55	QC[+57]VIDDR	HPDP
RRBP1_MOUSE	Q99PL5	C1327	EAEETQNSLQAEC[+57]DQYR	HPDP
RRBP1_MOUSE	Q99PL5	C1327	LREAEETQNSLQAEC[+57]DQYR	HPDP
RRBP1_MOUSE	Q99PL5	C1198	LKELESQVSC[+329]LEK	IodoTMT6
RRBP1_MOUSE	Q99PL5	C1327	LREAEETQNSLQAEC[+329]DQYR	IodoTMT6
RRBP1_MOUSE	Q99PL5	C1327	EAEETQNSLQAEC[+329]DQYR	IodoTMT6
RS11_MOUSE	P62281	C131	DVQIGDIVTVGEC[+57]RPLSK	HPDP
RS11_MOUSE	P62281	C60	C[+329]PFTGNVSIR	IodoTMT6
RS16_MOUSE	P14131	C25	TATAVAHC[+57]K	HPDP
RS17_MOUSE	P63276	C35	VC[+57]EEIAIIPSK	HPDP
RS17_MOUSE	P63276	C35	VC[+57]EEIAIIPSKK	HPDP
RS27A_MOUSE	P62983	C144, C155	C[+57]C[+125]LTYC[+57]FNKPEDK	HPDP
RS3_MOUSE	P62908	C119	AC[+57]YGVLR	HPDP
RS3_MOUSE	P62908	C134	GC[+57]EVVVSGK	HPDP
RS5_MOUSE	P97461	C66	AQC[+57]PIVER	HPDP
RS6_MOUSE	P62754	C12	LNISFPATGC[+57]QK	HPDP
RS8_MOUSE	P62242	C100	NC[+57]IVLIDSTPYR	HPDP
RSSA_MOUSE	P14206	C163	YVDIAIPC[+57]NNK	HPDP
RTCB_MOUSE	Q99LF4	C193	EGYAWAEDKEHC[+329]EEYGR	IodoTMT6
RUS1_MOUSE	Q91W34	C12	APLC[+57]TEQFGSGAPR	HPDP
RUVB2_MOUSE	Q9WTM5	C227	FVQC[+57]PDGELQK	HPDP
RUXF_MOUSE	P62307	C66	C[+329]NNVLYIR	IodoTMT6
S2533_MOUSE	Q3TZX3	C30	ATGTQQKENTLLHLFAGGC[+125]GGTVGAIFTC[+329]PLEVI	IodoTMT6
S27A1_MOUSE	Q60714	C80	AGDTIPC[+57]IFQAVAR	HPDP
S7A6O_MOUSE	Q7TPE5	C27	NAEPAEALVLAC[+57]K	HPDP
SAC1_MOUSE	Q9EP69	C445	NAWADNANAC[+57]AK	HPDP

SAFB1_MOUSE	Q80YR5	C219	ILDILGETC[+329]K	IodoTMT6
SAHH_MOUSE	P50247	C278	EGNIFVTTTGC[+57]VDIILGR	HPDP
SAHH_MOUSE	P50247	C297	DDAIVC[+57]NIGHFDVEIDVK	HPDP
SAHH3_MOUSE	Q68FL4	C189	GSSDFC[+57]VK	HPDP
SAMH1_MOUSE	Q60710	C342	IC[+57]EVEYK	HPDP
SAMH1_MOUSE	Q60710	C614	TSSC[+57]LQEVSK	HPDP
SBP1_MOUSE	P17563	C31	C[+125]GPGYSTPLEAMKGPREEIVYLPC[+329]IYR	IodoTMT6
SBP1_MOUSE	Q63836	C31	GPREEIVYLPC[+329]IYR	IodoTMT6
SBP1_MOUSE	Q63836	C31	EEIVYLPC[+329]IYR	IodoTMT6
SC23A_MOUSE	Q01405	C74	AVLNPLC[+57]QVDYR	HPDP
SC23B_MOUSE	Q9D662	C425	IAGAIGPC[+57]VSLNVK	HPDP
SC23B_MOUSE	Q9D662	C434	GPC[+57]VSENELGVGGTSQWK	HPDP
SC23B_MOUSE	Q9D662	C74	AILNPLC[+57]QVDYR	HPDP
SC31A_MOUSE	Q3UPL0	C173	TQPPEDISC[+57]IAWNR	HPDP
SC31A_MOUSE	Q3UPL0	C60	SC[+57]ATFSSSHR	HPDP
SEC62_MOUSE	Q8BU14	C82	ESVVDYC[+57]NR	HPDP
SF01_MOUSE	Q64213	C279	SITNTTVC[+57]TK	HPDP
SGT1_MOUSE	Q9CX34	C79	SLELNPNNC[+57]TALLR	HPDP
SH3G1_MOUSE	Q62419	C277	EPFELGELEQPNGGFPC[+57]APAPK	HPDP
SH3G1_MOUSE	Q62419	C311	SMPPLDQPSC[+329]K	IodoTMT6
SHRM2_MOUSE	A2ALU4	C886	SLATSC[+57]GEILSDR	HPDP
SI1L1_MOUSE	Q8C0T5	C585	HSTARGLPLKEVLEHVIPELNVQC[+329]LR	IodoTMT6
SIA7B_MOUSE	P70277	C65	KSRLC[+329]QHSLSLAIQK	IodoTMT6
SIDT2_MOUSE	Q8CIF6	C430	QYLC[+57]VADLAR	HPDP
SLK_MOUSE	O54988	C1136	DLQLQC[+57]EANVR	HPDP
SMD2_MOUSE	P62317	C46	NNTQVLINC[+329]R	IodoTMT6
SMD2_MOUSE	P62317	C46	EEEEFNTGPLSVLTQSVKNNTQVLINC[+329]R	IodoTMT6
SMD2_MOUSE	P62317	C46	REEEEFNTGPLSVLTQSVKNNTQVLINC[+329]R	IodoTMT6
SMD3_MOUSE	P62320	C20	VLHEAEGHIVTC[+329]ETNTGEVYR	IodoTMT6
SMU1_MOUSE	Q3UKJ7	C383	TTEC[+57]SNTFK	HPDP
SND1_MOUSE	Q78PY7	C152	LSEC[+57]EEQAK	HPDP
SODC_MOUSE	P08228	C147	LAC[+57]GVIGIAQ	HPDP

SODC_MOUSE	P08228	C147	TGNAGSRLAC[+57]GVIGIAQ	HPDP
SODC_MOUSE	P08228	C7	AVC[+329]VLKGDGPVQGTIHFEQK	IodoTMT6
SPAS2_MOUSE	Q8K1N4	C356	FTC[+57]DVETLK	HPDP
SPCS2_MOUSE	Q9CYN2	C26	SGGGGGSSGAGGGPSC[+57]GTSSSR	HPDP
SPEG_MOUSE	Q62407	C2710	APC[+57]TYTLER	HPDP
SPNS1_MOUSE	Q8R0G7	C44	SGELEVPDC[+57]EGLQR	HPDP
SPSB3_MOUSE	Q571F5	C271	VIRSC[+329]ASSTSLQYLCCYRLR	IodoTMT6
SPTN1_MOUSE	P16546	C1930	VNDVC[+57]TNGQDLIK	HPDP
SRB4D_MOUSE	A1L0T3	C138	QLGCGLALPVPRPLAFGQGRGPIFLDNVEC[+329]R	IodoTMT6
SRBP1_MOUSE	Q9WTN3	C738,C753	QAC[+329]LAQSGSVPLAMQWLC[+329]HPVGHR	IodoTMT6
SRC_MOUSE	P05480	C408	AANILVGENLVC[+329]K	IodoTMT6
SRCRL_MOUSE	Q8BV57	C6	MRGLAC[+329]LLAM[+16]LVGIQAIER	IodoTMT6
SRP09_MOUSE	P49962	C48	VTDDLVC[+57]LVYR	HPDP
SRRT_MOUSE	Q99MR6	C489	EC[+57]ELSPGVNR	HPDP
SRSF1_MOUSE	Q6PDM2	C148	EAGDVC[+57]YADVYR	HPDP
SRSF3_MOUSE	P84104	C6, C10	DSC[+57]PLDC[+57]K	HPDP
SSU72_MOUSE	Q9CY97	C12	VAVVC[+57]SSNQNR	HPDP
STA5B_MOUSE	P42232	C688	YYTPVPC[+57]EPATAK	HPDP
STIM1_MOUSE	P70302	C49	NTGASSGATSEESTEAEFC[+329]R	IodoTMT6
STIP1_MOUSE	Q60864	C461	ALDLDSSC[+57]K	HPDP
STIP1_MOUSE	Q60864	C461	ALDLDSSC[+57]KEAADGYQR	HPDP
STK39_MOUSE	Q9Z1W9	C461	EGPC[+57]AVNLVLR	HPDP
STRN4_MOUSE	P58404	C569	LASC[+57]SADGTVR	HPDP
STX7_MOUSE	O70439	C28	ITQC[+57]SVEIQR	HPDP
STXB5_MOUSE	Q8K400	C293	KPEPC[+329]KPILKVELKTTR	IodoTMT6
SUCB1_MOUSE	Q9Z2I9	C164	IC[+125]NQVLVC[+57]ER	HPDP
SUCB1_MOUSE	Q9Z2I9	C430	ILAC[+57]DDLDEAAK	HPDP
SYDC_MOUSE	Q922B2	C76	QC[+57]FLVLR	HPDP
SYEP_MOUSE	Q8CGC7	C697	EAPC[+57]ILIYIPDGHTK	HPDP
SYEP_MOUSE	Q8CGC7	C910	VAC[+57]QGEVVR	HPDP
SYK_MOUSE	Q99MN1	C432	AVEC[+57]PPPR	HPDP
SYNPO_MOUSE	Q8CC35	C686	ASPAAAEEAVPEWASC[+57]LK	HPDP

SYSM_MOUSE	Q9JJL8	C425	YGEVTSASNC[+57]TDFQSR	HPDP
SYT2_MOUSE	P46097	C91	IPLPPWALIAM[+16]AVVAGLLLLTCC[+57]FCIC[+57]KKCC[+3	IodoTMT6
SYTC_MOUSE	Q9D0R2	C266	C[+125]GPLIDLC[+57]R	HPDP
TALDO_MOUSE	Q93092	C250	ALAGC[+57]DFLTISPK	HPDP
TARA_MOUSE	Q99KW3	C1491	SC[+57]TDVTEYAVQR	HPDP
TARA_MOUSE	Q99KW3	C1921	SFIASQGTGNSC[+57]GR	HPDP
TARA_MOUSE	Q99KW3	C1930	SSC[+57]ELEVLLR	HPDP
TARA_MOUSE	Q99KW3	C1491	SC[+329]TDVTEYAVQR	IodoTMT6
TB182_MOUSE	P58871	C259	LAC[+57]SEAPTDVSK	HPDP
TBA1B_MOUSE	P68368	C295	AYHEQLSVAEITNAC[+329]FEPANQM[+16]VK	IodoTMT6
TBA1B_MOUSE	P68368	C295	AYHEQLSVAEITNAC[+329]FEPANQMVK	IodoTMT6
TBCD_MOUSE	Q8BYA0	C665	AVQSLKQIHQQLC[+329]DRHLYR	IodoTMT6
TBPL1_MOUSE	P62340	C68	IIC[+57]TGATSEEEAK	HPDP
TCPA_MOUSE	P11983	C147	DC[+57]LINAAK	HPDP
TCPA_MOUSE	P11983	C357	IC[+57]DDELILIK	HPDP
TCPA_MOUSE	P11983	C357	IC[+57]DDELILIKNTK	HPDP
TCPD_MOUSE	P80315	C295	TGC[+57]NVLLIQK	HPDP
TCPG_MOUSE	P80318	C403	NLQDAM[+16]QVC[+57]R	HPDP
TCPH_MOUSE	P80313	C370	TC[+57]TIILR	HPDP
TERA_MOUSE	Q01853	C105	LGDVISIQPC[+57]PDVK	HPDP
TERA_MOUSE	Q01853	C69, C77	EAVC[+57]IVLSDDTC[+57]SDEK	HPDP
TERA_MOUSE	Q01853	C184	VVETDPSPYC[+125]IVAPDTVIHC[+329]EGEPIKR	IodoTMT6
TERA_MOUSE	Q01853	C69	EAVC[+329]IVLSDDTC[+125]SDEKIR	IodoTMT6
TERA_MOUSE	Q01853	C69	EAVC[+329]IVLSDDTC[+125]SDEK	IodoTMT6
TERA_MOUSE	Q01853	C77	EAVC[+125]IVLSDDTC[+329]SDEK	IodoTMT6
TERA_MOUSE	Q01853	C77	EAVC[+125]IVLSDDTC[+329]SDEKIR	IodoTMT6
TGM2_MOUSE	P21981	C27	DHHTADLC[+57]QEK	HPDP
TGM2_MOUSE	P21981	C370	SEGTYC[+57]C[+125]GPVSVR	HPDP
TGM2_MOUSE	P21981	C370, C371	SEGTYC[+57]C[+57]GPVSVR	HPDP
TGM2_MOUSE	P21981	C553	YSGC[+57]LTESNLIK	HPDP
TGM2_MOUSE	P21981	C10	C[+329]DLEIQANGR	IodoTMT6
THIM_MOUSE	Q8BWT1	C382	YAVGSAC[+57]IGGGQGIALIIQNTA	HPDP

THIM_MOUSE	Q8BWT1	C92, C103, C10	LC[+57]GSGFQSIVSGC[+57]QEIC[+57]SK	HPDP
TIF1B_MOUSE	Q62318	C628	LASPSGSTSSGLEVVAPEVTSAPVSGPGILDDSATIC[+329]R	IodoTMT6
TINAL_MOUSE	Q99JR5	C445	GTNEC[+57]DIETFVLGVWGR	HPDP
TINAL_MOUSE	Q99JR5	C326	C[+329]PNGQVDSNDIYQVTPAYR	IodoTMT6
TIPRL_MOUSE	Q8BH58	C87	VAC[+57]AEEWQESR	HPDP
TITIN_MOUSE	A2ASS6	C13473	C[+57]EVSKDVPVK	HPDP
TITIN_MOUSE	A2ASS6	C14323	ILIIQNAQLEDAGSYNC[+57]R	HPDP
TITIN_MOUSE	A2ASS6	C16418	C[+57]NEHLVPVLTYTAK	HPDP
TITIN_MOUSE	A2ASS6	C18063	EC[+57]MYTIPK	HPDP
TITIN_MOUSE	A2ASS6	C18869	VPDLLEGC[+57]QYEFR	HPDP
TITIN_MOUSE	A2ASS6	C20340	C[+57]NAAAQLIR	HPDP
TITIN_MOUSE	A2ASS6	C2115	VVGKPDPEC[+57]EWYK	HPDP
TITIN_MOUSE	A2ASS6	C21280	C[+57]DPPVISNITK	HPDP
TITIN_MOUSE	A2ASS6	C21561	YILTLENSC[+57]GK	HPDP
TITIN_MOUSE	A2ASS6	C21561	YILTLENSC[+57]GKK	HPDP
TITIN_MOUSE	A2ASS6	C21780	DLPDLC[+57]YLAK	HPDP
TITIN_MOUSE	A2ASS6	C21834	VSVESTAVNTTLVVYDC[+57]QK	HPDP
TITIN_MOUSE	A2ASS6	C24876	SYAAVVTNC[+57]HK	HPDP
TITIN_MOUSE	A2ASS6	C24969	NTDKWSEC[+57]AR	HPDP
TITIN_MOUSE	A2ASS6	C26841	AAADEWTTC[+57]TPPSGLQGK	HPDP
TITIN_MOUSE	A2ASS6	C28709	ELQTNALVC[+57]VENSTDLASILIK	HPDP
TITIN_MOUSE	A2ASS6	C29432	YTVILDNAVC[+57]R	HPDP
TITIN_MOUSE	A2ASS6	C33458	EVYDYYC[+57]R	HPDP
TITIN_MOUSE	A2ASS6	C34371	FSC[+57]DTDGEPVPTVTWLR	HPDP
TITIN_MOUSE	A2ASS6	C6675	SSC[+57]TAVVDVSDR	HPDP
TITIN_MOUSE	A2ASS6	C9704	AEDQGQYTC[+57]K	HPDP
TJAP1_MOUSE	Q9DCD5	C335	NSPLPNC[+57]TYATR	HPDP
TKT_MOUSE	P40142	C468	AVELAANTKGIC[+329]FIR	IodoTMT6
TLN1_MOUSE	P26039	C1087	C[+57]TQDLGNSTK	HPDP
TLN1_MOUSE	P26039	C956	ASAGPQPLLVQSC[+57]K	HPDP
TLR11_MOUSE	Q6R5P0	C743	TLLFSFLATNCPHGTEFWGFLTSFILLLLLIILPLISC[+329]PK	IodoTMT6
TMM65_MOUSE	Q4VAE3	C31	SLRPGPAAAPRLPSWCC[+329]CGRGLLALGVPGGPR	IodoTMT6

TNNC1_MOUSE	P19123	C35	AAFDIFVLGAEDGC[+57]ISTK	HPDP
TNR19_MOUSE	Q9JLL3	C189	DTALAAVICSALATVLLALLILC[+329]VIYCK	IodoTMT6
TNR19_MOUSE	Q9JLL3	C25	MALKVLPLHRTVLFAAILFLLHLAC[+329]K	IodoTMT6
TNS2_MOUSE	Q8CGB6	C548	LLGGC[+57]GVASAGR	HPDP
TOM34_MOUSE	Q9CYG7	C222	YSESLLC[+57]SSLESATYSNR	HPDP
TPIS_MOUSE	P17751	C177	VSHALAEGLGVIAC[+57]IGEK	HPDP
TPIS_MOUSE	P17751	C268	IIYGGSVTGATC[+57]K	HPDP
TPIS_MOUSE	P17751	C268	SNVNDGVAQSTRIIYGGSVTGATC[+57]K	HPDP
TPIS_MOUSE	P17751	C268	IIYGGSVTGATC[+329]K	IodoTMT6
TPM1_MOUSE	P58771	C190	C[+329]AELEEELK	IodoTMT6
TPM1_MOUSE	P58771	C190	C[+329]AELEEELKTVTNNLK	IodoTMT6
TPM2_MOUSE	P58774	C190	C[+329]GDLEEELKIVTNNLK	IodoTMT6
TPM4_MOUSE	P58774	C190	C[+329]GDLEEELK	IodoTMT6
TPM4_MOUSE	Q6IRU2	C247	EENVGLHQTLDQTLNELNC[+329]I	IodoTMT6
TPP2_MOUSE	Q64514	C150	VALAEAC[+57]R	HPDP
TPP2_MOUSE	Q64514	C209	AC[+57]VDSNENGDLSK	HPDP
TPP2_MOUSE	Q64514	C967	GAGPGC[+57]YLAGSLTLSK	HPDP
TPSN_MOUSE	Q9R233	C118	SLSPEQNC[+57]PR	HPDP
TRFE_MOUSE	Q921I1	C373	TKC[+57]DEWSIISEGK	HPDP
TRFE_MOUSE	Q921I1	C260	KPVDQYEDC[+329]YLAR	IodoTMT6
TRFE_MOUSE	Q921I1	C350	NQQEGVC[+329]PEGSIDNSPVK	IodoTMT6
TRFE_MOUSE	Q921I1	C373	TKC[+329]DEWSIISEGK	IodoTMT6
TRFE_MOUSE	Q921I1	C373	C[+329]DEWSIISEGK	IodoTMT6
TRFE_MOUSE	Q921I1	C386,C395	IEC[+329]ESAETTEDC[+329]IEK	IodoTMT6
TRFE_MOUSE	Q921I1	C395	IEC[+57]ESAETTEDC[+329]IEK	IodoTMT6
TRFE_MOUSE	Q921I1	C395	TKC[+57]DEWSIISEGKIEC[+57]ESAETTEDC[+329]IEK	IodoTMT6
TRFE_MOUSE	Q921I1	C472	SC[+329]HTGVDR	IodoTMT6
TRFE_MOUSE	Q921I1	C67	KTSYPDC[+329]IK	IodoTMT6
TRFE_MOUSE	Q921I1	C67	TSYPDC[+329]IK	IodoTMT6
TRI42_MOUSE	Q9D2H5	C18,C27	ETAMCVC[+57]SPCC[+57]TWQRC[+125]C[+329]PRLFSCLCC[	IodoTMT6
TXND5_MOUSE	Q91W90	C107,C114	VDC[+329]TADSDVC[+329]SAQGVR	IodoTMT6
TXND5_MOUSE	Q91W90	C114	VDC[+57]TADSDVC[+329]SAQGVR	IodoTMT6

U3IP2_MOUSE	Q91WM3	C460	NSVC[+57]IIPLR	HPDP
UBA6_MOUSE	Q8C7R4	C298	TFC[+57]FEPLESQIK	HPDP
UBA6_MOUSE	Q8C7R4	C347	C[+57]QQDSDELLK	HPDP
UBA6_MOUSE	Q8C7R4	C546	VC[+57]PATESIYSDEFYTK	HPDP
UBAC1_MOUSE	Q8VDI7	C134	ATANLPAC[+57]STDR	HPDP
UBE2O_MOUSE	Q6ZPJ3	C309	SFC[+57]PGGTDSVSPPPSIITQENLGR	HPDP
UBE2O_MOUSE	Q6ZPJ3	C365	IAWEC[+57]PEK	HPDP
UBP15_MOUSE	Q8R5H1	C264	NSNYC[+57]LPSYTAYK	HPDP
UBP16_MOUSE	Q99LG0	C24	SAPDTVASESAEPVC[+57]R	HPDP
UBP4_MOUSE	P35123	C758	SLYFDEQESEAC[+329]EK	IodoTMT6
UBP47_MOUSE	Q8BY87	C856	AGGDSGNVDDDC[+57]ER	HPDP
UBR1_MOUSE	O70481	C279	AGVYATC[+57]QEAK	HPDP
UBR1_MOUSE	O70481	C996	SC[+57]LVVATTSGLEC[+125]VK	HPDP
UBR2_MOUSE	Q6WKZ8	C112	VGEPTYSC[+57]R	HPDP
UPP1_MOUSE	P52624	C132	C[+57]SNITIIR	HPDP
USO1_MOUSE	Q9Z1Z0	C802	SQLC[+57]SQSLEITR	HPDP
UTP20_MOUSE	Q5XG71	C2058	KPAAPVPDARLPPQSC[+329]LLLPATPVRGGPK	IodoTMT6
VAT1_MOUSE	Q62465	C99	AC[+57]GLNFADLM[+16]GR	HPDP
VATG1_MOUSE	Q9CR51	C69	EAAALGSHGSC[+57]SSEVEK	HPDP
VAV2_MOUSE	Q60992	C196, C197	SC[+57]C[+57]LLEIQETEAK	HPDP
VDAC1_MOUSE	Q60932	C245	YQVDPDAC[+329]FSAK	IodoTMT6
VDAC2_MOUSE	Q60930	C48	SC[+329]SGVEFSTSGSSNTDTGK	IodoTMT6
VDAC3_MOUSE	Q60931	C36	SC[+329]SGVEFSTSGHAYTDTGK	IodoTMT6
VIGLN_MOUSE	Q8VDJ3	C53	AAC[+57]LESAQEPAGAWSNK	HPDP
VIME_MOUSE	P20152	C328	QVQSLTC[+329]EVDALK	IodoTMT6
VIME_MOUSE	P20152	C328	QVQSLTC[+329]EVDALKGTNESLER	IodoTMT6
VPP2_MOUSE	P15920	C315	KMKAIYHMLNMC[+329]SFDVTNK	IodoTMT6
VPS8_MOUSE	Q0P5W1	C1293	EC[+57]TLEVEGQTR	HPDP
VTNC_MOUSE	P29788	C179	GQYC[+329]YELDETAVRPGYPK	IodoTMT6
VTNC_MOUSE	P29788	C473	SIAQYWLGC[+329]PTSEK	IodoTMT6
VWDE_MOUSE	Q6DFV8	C217	ISVELLGSLVFC[+125]RC[+329]TFDVSPTNTSVGFLIAWSR	IodoTMT6
WASF2_MOUSE	Q8BH43	C27	QTLPSDTSELEC[+329]R	IodoTMT6

WDR1_MOUSE	O88342	C225	VC[+57]ALGESK	HPDP
WDR1_MOUSE	O88342	C382	M[+16]TVNESEQLVSC[+329]SMDDTVR	IodoTMT6
WDR1_MOUSE	O88342	C382	MTVNESEQLVSC[+329]SMDDTVR	IodoTMT6
WDR5_MOUSE	P61965	C195	DGSLIVSSSYDGLC[+57]R	HPDP
WDR5_MOUSE	P61965	C195	DGSLIVSSSYDGLC[+329]R	IodoTMT6
WFD11_MOUSE	A2A5H7	C8	KPSWFPC[+329]LVFLC[+125]M[+16]LLLSALGGRK	IodoTMT6
XDH_MOUSE	Q00519	C970, C974	C[+57]WDEC[+57]IASSQYQAR	HPDP
XIRP1_MOUSE	O70373	C997	ISGSTPC[+57]PPPSR	HPDP
XPO7_MOUSE	Q9EPK7	C43	ALVEFTNSPDC[+57]LSK	HPDP
XPP3_MOUSE	B7ZMP1	C491	IEDDVVVTQDSPLILSADC[+57]PK	HPDP
XRN2_MOUSE	Q9DBR1	C276	DC[+57]EGLPR	HPDP
YAP1_MOUSE	P46938	C328	C[+57]QELALR	HPDP
YIPF5_MOUSE	Q9EQQ2	C42	QYAGC[+57]DYSQQGR	HPDP
Z354C_MOUSE	Q571J5	C248	LHTGEKPYKC[+329]SECGKSFSHR	IodoTMT6
ZFPL1_MOUSE	Q9DB43	C56	LC[+57]NTPLASR	HPDP
ZN106_MOUSE	O88466	C7,C10	KC[+329]ILC[+329]HIVYGSK	IodoTMT6
ZN363_MOUSE	Q9CR50	C243	LC[+57]DSYNTAQAGGR	HPDP
ZN689_MOUSE	Q8BKK5	C263	TTHTGEKPHQC[+329]PSCGRRFAYPSLLAIHQR	IodoTMT6
ZYX_MOUSE	Q62523	C376	QSVAVNESC[+57]GK	HPDP
ZYX_MOUSE	Q62523	C379	C[+57]NQPLAR	HPDP

Figure S1. (A) Systolic, (B) diastolic and (C) mean arterial blood pressure were determined in non-pregnant and at 17.5 days (d) of gestation (N=5-8 mothers per group) in C57Bl/6J (B6), GSNOR−/− (KO), and in mice treated with ascorbate (Asc).

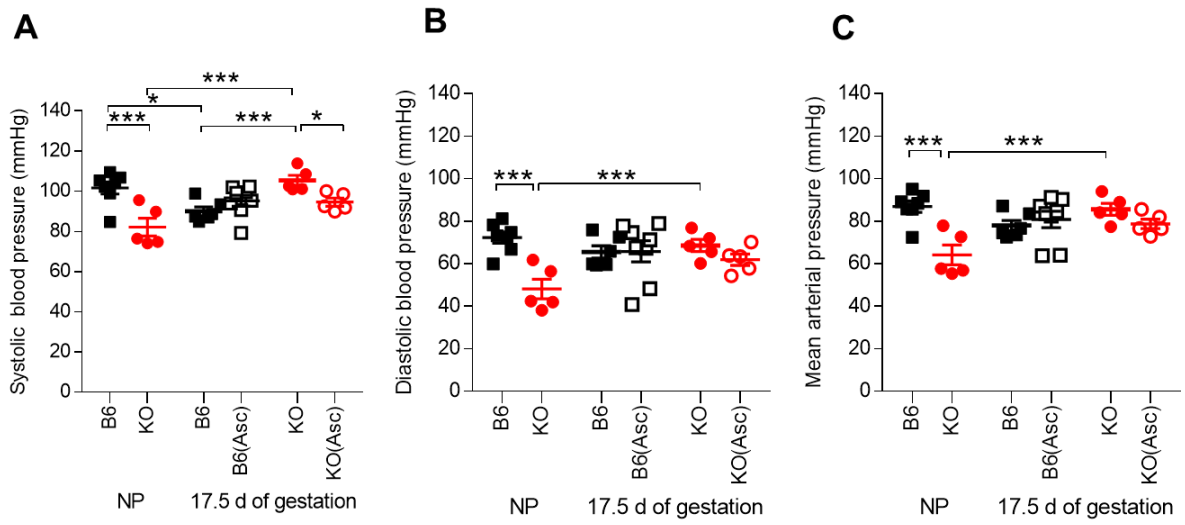

Systolic, diastolic and mean arterial pressure were significantly lower in KO mice prior to pregnancy. During pregnancy, blood pressure increased in KO mice. Ascorbate treatment prevented the onset of systolic blood pressure in KO mice at 17.5 d of gestation. Results are shown as mean ± SEM. *P<0.05, ***P<0.001. Two-way ANOVA with Newman-Keuls for post hoc analysis.

Figure S2. Umbilical arterial and venous blood flow (A, C) and blood flow normalized to fetal weight (B, D) were determined using micro-ultrasound in isoflurane-anesthetized embryos on day 17.5 of gestation in C57Bl/6J (B6), GSNOR−/− (KO), and in mice treated with ascorbate (Asc).

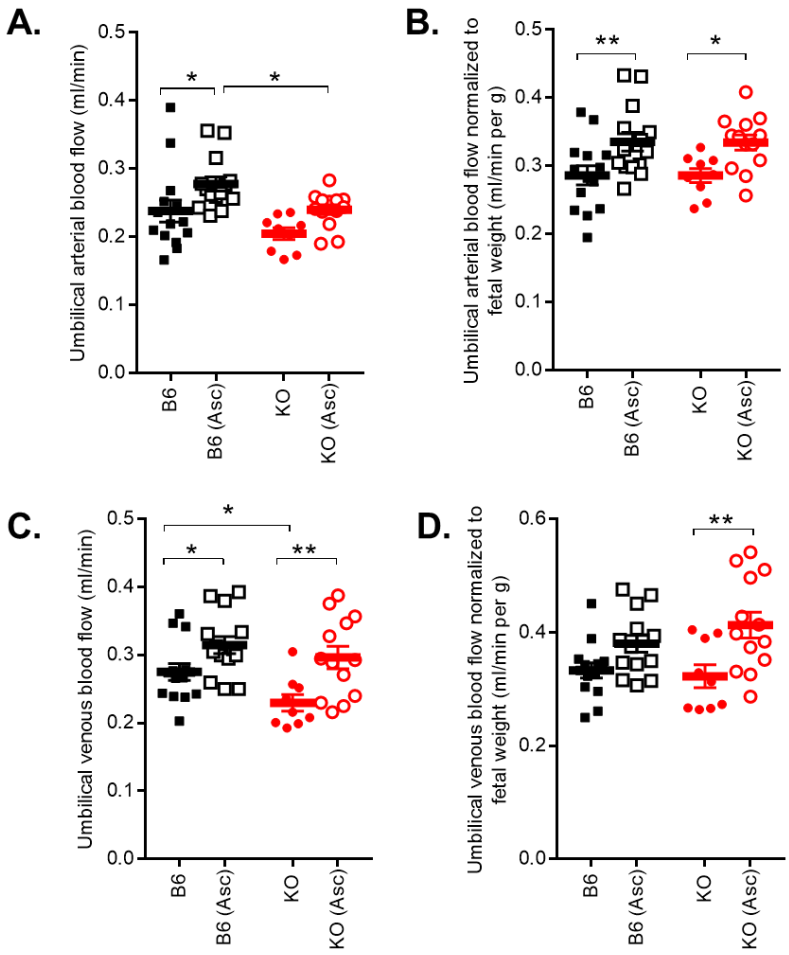

Umbilical venous blood flow was significantly lower in KO fetuses at 17.5 d of gestation and was rescued with Asc treatment. Results are shown as mean ± SEM. *P<0.05, **P<0.01. Two-way ANOVA with Newman-Keuls for post hoc analysis.

Figure S3. Pathway analysis of list of proteins nitrosylated in GSNOR−/− placentas as compared to B6 placentas determined using dual-labelling mass spectrometry analysis was created using String-DB.

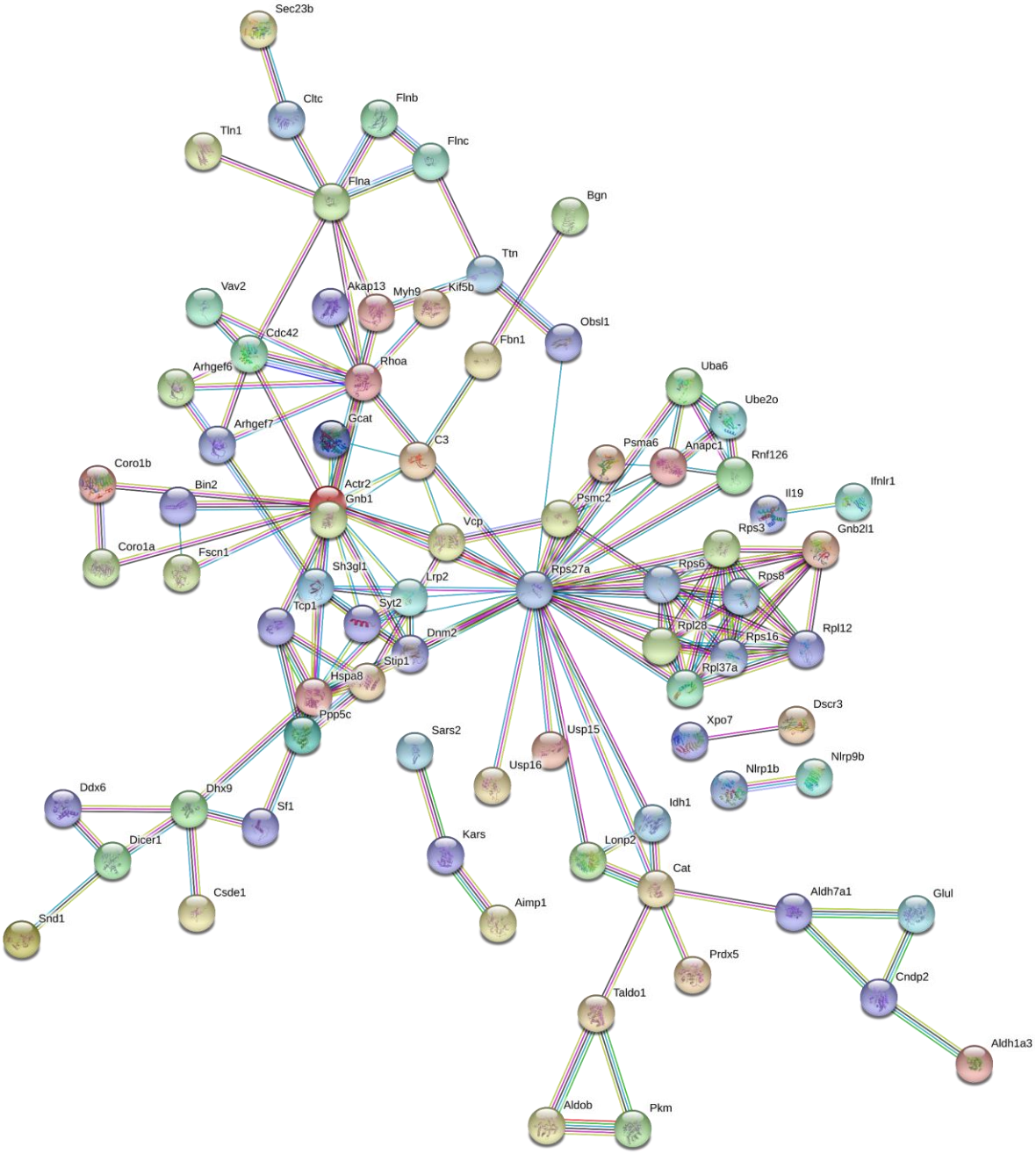

All SNO-proteins were detected in at least 2 of 5 placentas/group. The number in the observation column is the number of placentas that showed expression of that particular SNO-protein for that group. These proteins correlate to data shown in Table S2.